MODELING PLANKTON DYNAMICS DURING A *Prymnesium parvum* BLOOM: THE IMPORTANCE OF INFLOWS AND ALLELOPATHIC RELATIONSHIPS ON BLOOM DYNAMICS

A Thesis

by

NATALIE CASE HEWITT

Submitted to the Office of Graduate Studies of
Texas A&M University
in partial fulfillment of the requirements for the degree of

MASTER OF SCIENCE

May 2011

Major Subject: Water Management and Hydrological Science

MODELING PLANKTON DYNAMICS DURING A *Prymnesium parvum* BLOOM: THE IMPORTANCE OF INFLOWS AND ALLELOPATHIC RELATIONSHIPS ON BLOOM DYNAMICS

A Thesis

by

NATALIE CASE HEWITT

Submitted to the Office of Graduate Studies of
Texas A&M University
in partial fulfillment of the requirements for the degree of

MASTER OF SCIENCE

Approved by:

Chair of Committee,	Daniel Roelke
Committee Members,	James Grover
	Patricia Smith
	Ralph Wurbs
Intercollegiate Faculty Chair,	Ronald Kaiser

May 2011

Major Subject: Water Management and Hydrological Science

ABSTRACT

Modeling Plankton Dynamics During a *Prymnesium parvum* Bloom: The Importance of Inflows and Allelopathic Relationships on Bloom Dynamics. (May 2011)

Natalie Case Hewitt, B.S., Brown University

Chair of Advisory Committee: Dr. Daniel L Roelke

Harmful algal blooms' global amplification has driven research on growth characteristics and instigating mechanisms. These blooms prosper under diverse environmental conditions, creating challenges identifying bloom initiation. The haptophyte, *Prymnesium parvum*, plagues the southwestern United States with massive system disruptions and huge fish kills caused by its toxin. Despite many abiotic factors' association with *P. parvum* blooms, low nutrient levels stress the alga increasing toxin production, eliminating nutrient competition, and alleviating grazing pressures. This model examines the relationship between nutrient availability and *P. parvum* toxin production against another phytoplankton and a single grazing zooplankton, using a Monod function relating population growth rate with limiting nutrient concentrations. Sensitivity analyses emphasize plankton biological parameters most influential in accumulating biomass. The impact of toxin production on zooplankton grazing rates underscores *P. parvum*'s need for top-down control suppression. The toxin production equation increases production when *P. parvum* experiences low specific growth rates from nutrient availability and low biomass. This equation is analyzed against previously published allelopathic relationships, comparing plankton reactions and bloom endurance.

The model's toxin production equation proves more ecologically feasible, incorporating competing phytoplankton species' mortality and variables easily verified through laboratory experiments. Though not intended for management strategy development, the model explores and supports the proposed strategy of incorporating hydraulic flushing, pulsed and continuous inflows, to eliminate biomass accumulation. Inflows relieve stressful nutrient-limiting conditions, introducing resources affecting bloom stability and plankton community dynamics. The faster-growing competing phytoplankton gains survival advantages when inflow rates fall lower than its maximum specific growth rate, but greater than *P. Parvum*'s, emphasizing the accurate measuring of competitors' maximum specific growth rates and identifying a dilution rate range where *P. parvum* loses at nutrient intake. Inflows with various nutrient levels representing different source waters from freshwater lakes were tested for impacts on plankton dynamics. Adding any hydrological effect reduced *P. parvum* biomass. Disruptions create disturbance, removing *P. parvum*'s system-dominating position, allowing the phytoplankton to exceed *P. parvum*'s density. The model highlights the importance of *P. parvum*'s toxin's presence to maintain dominance and emphasizes flushing agitation as potential and feasible management schemes to deter bloom continuation and increase species diversity.

ACKNOWLEDGEMENTS

I would like to thank my committee chair, Dr. Roelke, for all the support throughout the course of this research. I would also like to thank my committee members, Dr. Grover, Dr. Smith, and Dr. Wurbs for all their support and guidance through this research as well.

To my family, this one's for all of us. It took everyone to get this finished. It is finally done. Thanks for all the support and faked enthusiasm and understanding.

Thank you also to all my friends for putting up with my "Super Science Nerd" weekends and for always being there for a much-needed cold refreshment whenever we all could get away.

TABLE OF CONTENTS

Page

LIST OF FIGURES

FIGURE Page

FIGURE Page

LIST OF TABLES

1. INTRODUCTION

Harmful algal blooms (HABs) are occurring more frequently and with more intensity, increasing in size and impact, in both freshwater and marine systems globally (Smayda, 1990; Hallegraeff, 1993; Smith, 2003). Processes leading to blooms are diverse (Roelke and Buyukates, 2001); many marine blooms are linked to nutrient availability allowing similar conclusions to be drawn for freshwater systems as well (Paerl, 1997). Increased nutrient loadings into aquatic systems affect planktonic communities, impacting the growth and development of the first tier of the food chain (Smith, 2003; Anderson, 2009). The excess nutrient load promotes growth and accumulation of algal biomass, at times leading to conditions prompting the development of an HAB (Anderson et al., 2002).

Many species that develop into an HAB harness mechanisms to increase their chances of survival either through enhanced nutrient uptake strategies or defense tactics against competitors or grazing populations. Smayda (1997) notes major adaptations associated with many harmful algae that facilitate nutrient acquisition and minimize cell losses: mixotrophy, grazer inhibition, and allelopathy. The latter two mechanisms involve the production of chemicals targeting competitors through allelopathy and the inhibition of grazing (Gross, 2003; Graneli and Salomon, 2010). Multiple factors drive toxin production including nutrient limitation, biomass density, pH, temperature,

---

This thesis follows the style of Ecological Modelling.

and light (Fistarol et al., 2003; Legrand et al., 2003; Baker et al. 2007, 2009; Graneli and Salomon, 2010). The lysing, growth inhibition, and death of the targeted cells caused by the toxic chemicals decreases competition over nutrients and allows the toxin-producing alga an advantage in nutrient sequestration (Fistarol et al., 2003; Legrand et al., 2003).

The impact on higher trophic levels from the production of these toxins results in huge economic losses worldwide from fish mortalities; contamination and closure of fisheries; and decreased tourism (Shumway et al., 2003; Anderson, 2009). In addition to lower levels of available prey sources when an HAB eliminates competing phytoplankton, some toxins irritate or impair fish gill tissue or create hypoxic conditions, suffocating fish populations and devastating fish hatcheries nearby (Burkholder, 1998).

The detriment of HABs on water systems drives research for management practices and ecological manipulations intended to reduce the frequency of blooms. Ideal strategies would prevent future blooms while mitigating and controlling existing blooms. The array of conditions associated with bloom initiations increases the difficulty in accurately identifying the start of a bloom. Often linked with the beginning stages of blooms, attempts to control external nutrient loads entering lakes, rivers and streams has been suggested to impact algal biomass and tested as management strategies (Roelke, 2000; Smith, 2003). Many monitoring programs establish early detection signs of a bloom often including early impacts on aquatic life historically associated with an HAB (Heil and Steidinger, 2009).

Flushing and inflows into some water bodies appear to be viable strategies to combat HABs. Natural pulsing and flushing regenerates the system, introducing

nutrients and sediments beneficial to planktonic growth (Verspagen et al., 2006). Without replenishing nutrient supplies, nutrient-limited conditions increase competition among phytoplankton, and better adapted species, those with lower nutrient requirements for growth or with mechanisms to combat competition, tend to persist. Some HABs respond to the increased competition from nutrient limitations by producing toxins targeting competing phytoplankton for the uptake of nutrients (Fehling and Davidson, 2004). With lower levels of competition resulting from the death of competitors and increased availability of resources, these nutrient-limited systems paradoxically enable bloom conditions (Chicharo et al., 2006; Roelke et al., 2007). Renewing the system's nutrient supply through inflows regenerates nutrient supply, circumventing toxin production.

The timing and intensity of discharges and inflows to the system present an opportunity to impact the development of plankton growth. Different growth strategies are successful in pulsed versus continuous flows (Chicharo et al., 2006). Slower growing species experience greater success in continuous flows whereas pulsed flows alleviate nutrient stress and lead to an increase in species diversity favoring faster-growing species (Miller et al., 2008; Roelke et al., 1999). Shifts in phytoplankton influence the presence or absence of grazing zooplankton populations (Roelke 2000; Buyukates and Roelke, 2005). Though a potentially impractical application, releasing water from reservoirs at a quicker rate than algae can replicate could prevent biomass accumulation regardless of nutrient concentration since the regeneration of systems has the potential to disrupt succession favoring HABs (Hilton et al., 2006). Small water

fluctuations create disturbances in foodweb dynamics generating cascading effects. Low flow rates produce changes in the delivery of nutrients to the system inducing reactionary changes in phytoplankton competition (Sommer, 1984). Phytoplankton diversity alters higher level dynamics as grazing zooplankton respond to shifts in prey availability (Reynolds, 1984). The regeneration of systems via opportunely timed inflow and flushing events has the potential to disrupt succession associated with HABs.

This research focuses on a particularly effective toxic chemical-producing HAB, *Prymnesium parvum*, found only recently in the southwestern United States. The haptophyte, *P. parvum*, also known as golden algae, was first spotted in Texas after fish kills were documented along the Pecos River in 1985 (James and De La Cruz, 1989). Since then the alga, easily spotted by its characteristic golden hue, has caused massive fish kills in over 30 reservoirs on 6 Texas river systems amounting to an estimated loss of $13 million (Southard et al., 2010).

High biomass golden algae blooms, defined as over 10^7 cells liter^{-1}, are frequently seen in nutrient limited systems (Lindholm et al., 1999; Roelke et al., 2007; Southard et al., 2010), though a variety of abiotic and biotic tendencies are associated with *P. parvum* blooms (Baker et al 2009; Graneli and Salomon, 2010). The alga's optimal growing conditions have been narrowed down to eutrophic waters, a salinity of 22 practical salinity units (psu), and a temperature of 27^{o}C (Baker et al., 2009), however the alga has formed blooms in systems that are nutrient depleted, in salinities as low as 2-4 psu, and temperatures ranging from 5-30^{o}C (Baker et al., 2007 and 2009; Roelke et

al 2010b). The wide range of values the alga occurs in makes bloom predictions difficult.

When stressed by environmental conditions or lack of resources, *P. parvum* produces and releases allelopathic chemicals to eliminate resource competitors and deter grazing (Graneli and Hansen, 2006). The multiple functioning toxins, called prymnesins, prevent grazing and inhibit the growth of other phytoplankton competitors (Graneli and Johansson, 2003). Without a measuring standard, toxin concentrations are unknown. Higher trophic levels endure hemorrhaging of gills and a loss of food when in contact with the toxin (Barkoh et al., 2010). Though known to produce toxins irrespective of its nutrient state, Graneli et al (2008) found that chemical production increases by several magnitudes when the alga is under duress from reduced resource supplies. Blooms of *P. parvum* in Texas are typically found in the winter months during which the alga experiences decreased maximum specific growth rates. The alga's growth is already typically lower than other phytoplankton typically found in the same Texas lake systems as itself, giving the competing phytoplankton species a survival advantage. The resulting increased competition for resources leads to potential increases in toxic chemical production by *P. parvum* as it combats the competing phytoplankton's superior intake abilities.

Water flowing into Lake Granbury from the Brazos River brings replenishing nutrients into the reservoir. These supplemental nutrients alleviate aspects of the stress induced by the competition between phytoplankton species. Nutrient influxes disturb already highly competitive system by reducing resource competition. The system

disruptions brought about by nutrient additions, in this case a reduced competition over nutrients, are supported by previous research conducted at Lake Possum Kingdom and emphasize the importance of nutrient availability in attempting to control *P. parvum* and the production of its toxic chemicals (Roelke et al., 2007). Combining the use of hydrological events to relieve high concentrations of *P. parvum* (Roelke et al., 2010a; Schwierzke et al., 2010) with different nutrient concentrations found in the studied lake systems may lead to promising potential management strategies.

The primary goal of this research was to construct a simple numerical model during a *P. parvum* bloom and use the model to investigate plankton dynamics three ways: a sensitivity analysis of the model investigating influential parameters, the implementation of different toxin production equations, and the introduction of hydrology to the system. Without a standard to measure prymnesin toxin concentrations, little is known about the prymnesin toxins' capacity to increase *P. parvum*'s competitive advantage and dominate communities through the removal of resource competitors. Other toxin production equations exist that model *P. parvum*'s

toxin production but without measurable standards, these relationships are based on observational data. This research seeks to develop a production equation that represents toxin production based on nutrient limitation. Comparison of this model's toxin production rate with previously published equations provides the opportunity to contrast the toxin production methods and display plankton reactions to the presence of the toxin. Lastly, incorporating hydrology to the system creates disruptions similar to those thought to be associated with bloom dissolution (Roelke et al., 2010a). These three modes of model manipulation strengthen current knowledge of *P. parvum* and aid in prioritizing further research.

2. METHODS

2.1 Model Design

The model is constructed of ordinary differential equations, solved using Matlab^{TM}'s fourth-order Runge-Kutta methods(The Math Works, 2009) and uses a carbon currency to depict two phytoplankton groups (A_i, μmol carbon L^{-1}) competing for two nutrients (R_j, μmol nutrient L^{-1}), nitrogen (N) and phosphorus (P), and consumed by a grazing zooplankton group (G, individuals L^{-1}), feeding without preference on the phytoplankton. One of the phytoplankton groups, A_1, represents *P. parvum* and produces a toxic chemical (T, μg toxin L^{-1}) targeting the competing phytoplankton and

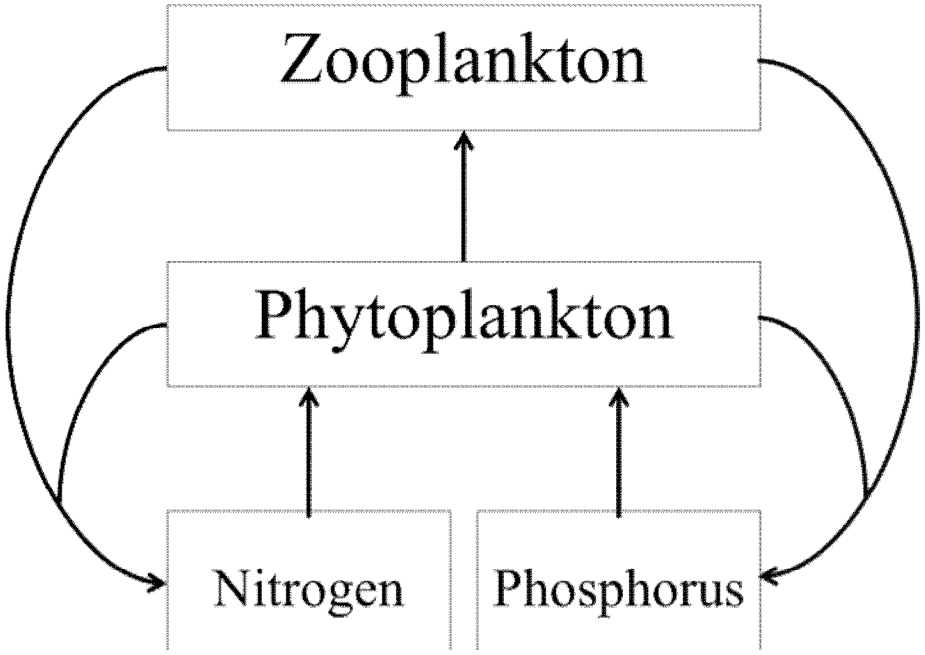

Figure 1. Generalized diagram illustrating the interactions between the components of the model

grazer populations. The competing algae, A_2, is modeled after freshwater diatoms and the grazer group after rotifers, both species common in two lakes where *P. parvum* is known to bloom and much research has been conducted, Lakes Granbury and Possum Kingdom. The mixotrophic ability of *P. parvum* was not incorporated into this model. The simplicity of the model also disregards the inclusion of other abiotic variables important in *P. parvum* blooms (Graneli and Hansen, 2006; Baker et al., 2009).

In all of the following equations, the subscript *i* refers to a phytoplankton species and *j* to a resource. Figure 1 shows a graphical representation of the interactions of the model.

2.2 Differential Equations

Phytoplankton concentration (i = 1, 2)

$$\frac{dA_i}{dt} = growth_{A_i} - grazing_{A_i} - mortality_{A_i} - flushing \tag{1}$$

Zooplankton concentration

$$\frac{dG}{dt} = assimilation_G - respiration_G - mortality_G - flushing \tag{2}$$

Nitrogen Concentration

$$\frac{dN}{dt} = mortality_{A_i|N} + mortality_{G|N} + respired_{G|N} + egestion_{G|N} - uptake_{A_i|N} - flushing + inflow_N \tag{3}$$

Phosphorus Concentration

$$\frac{dP}{dt} = mortality_{A_i|P} + mortality_{G|P} + respired_{G|P} + egestion_{G|P} - uptake_{A_i|P} - flushing + inflow_P \tag{4}$$

Toxin production

$$\frac{dT}{dt} = production - decay - flushing \tag{5}$$

2.3 Model Description

The specific growth rate by the phytoplankton uses a Monod (1950) relationship based on nutrient availability of the form:

$$growth_A = A_i\left(MIN\left(maxA_i\left(\frac{R_N}{k_{A_i|N} + R_N}, \frac{R_P}{k_{A_i|P} + R_P}\right)\right)\right) \tag{6}$$

in units of mol C day^{-1} L^{-1}, and where A_i is the concentration of the phytoplankton species (mol C L^{-1}), maxA_i is the maximum specific growth rate of the species (day^{-1}), R_N is the ambient nitrogen concentration of resources available (μmol N L^{-1}), R_P is the ambient phosphorus concentration of resources available (μmol P L^{-1}), $k_{A_i|N}$ is the nitrogen half-saturation coefficient (mol N L^{-1}), and $k_{A_i|P}$ is the phosphorus half-saturation coefficient (mol P L^{-1}). Liebig's Law of the Minimum is applied to ensure the growth rate used is based on availability of the limiting nutrient (DeBaar, 1994).

The loss of phytoplankton to grazing is a function of the grazer population density and grazing rate, with grazing rate being a function of prey availability (i.e., phytoplankton concentration) and is expressed as:

$$grazing_{A_i} = G\left(\frac{A_i}{\sum A}\right)\left(dmax_G \frac{\sum A}{k_G + \sum A}\right) \tag{7}$$

with units of μmol C L^{-1} day^{-1} and where G is the zooplankton concentration (individuals L^{-1}), A_i is the algal concentration of a single phytoplankton species (mol C L^{-1}), $\sum A$ is the sum of both algal species (mol C L^{-1}), $dmax_G$ is the maximum specific grazing rate of the zooplankton (mol C $individual^{-1}$ day^{-1}), k_G is the half saturation coefficient for zooplankton grazing (mol C L^{-1}). In this mathematical equation, the phytoplankton are consumed by grazers without preference.

Phytoplankton mortality from toxin exposure, only applicable to the competing phytoplankton group (i=2), is a function of toxin production and the species' resistance to the toxin:

$$mortality_{A_2} = mTox_{A_2}\left(\frac{T}{kTox_{T|A_2} + T}\right)A_2 \tag{8}$$

with units of μmol C L^{-1} day^{-1} and where $mTox_{A_2}$ is the maximum mortality rate caused by the toxin (d^{-1}), $kTox_{T|A_2}$ is the concentration of toxin at which 50% of its cells die (μg-toxin L^{-1}), T is the ambient concentration of the toxin produced by *P. parvum* (μg-toxin L^{-1}), and A_2 is the concentration of the competing phytoplankton (μmol C L^{-1}). Without standards available for the toxic chemicals produced by *P. parvum*, development of a formal equation, or more accurately parameterizing the equation used here, is not possible. The equation used here assumes a saturating relationship, and was parameterized to fit empirical data associated with previous experiments addressing the toxic effects of *P. parvum* on other phytoplankton. Note, *P. parvum* is not affected by the toxin nor does it lose energy by its production.

The simulation of phytoplankton flushing losses, as well as zooplankton flushing losses, is discussed in a section further below.

Without a grazing preference, total assimilation (or population growth) by the zooplankton is a function of the grazing rate on all available prey and the grazers' static internal nutrient quotas (Nielsen, 1994). The ingestion of phytoplankton is the amount of each nutrient taken in by filtration and is of the form:

$$ingestion_{G|N} = \sum grazingA_i \frac{Qper_{A_i|N}}{Qper_{A_i|C}} \tag{9}$$

$$ingestion_{G|P} = \sum grazingA_i \frac{Qper_{A_i|P}}{Qper_{A_i|C}} \tag{10}$$

with units of mol N L^{-1} day^{-1} and mol P L^{-1} day^{-1} respectively, and where $grazingA_i$ is the total density of each phytoplankton group ingested (mol C L^{-1} day^{-1}), $Qper_{A_i|N}$ is the nitrogen quota (mol N $cell^{-1}$), $Qper_{A_i|C}$ is the carbon quota of the phytoplankton (mol C $cell^{-1}$), and $Qper_{A_i|P}$ is the phosphorus quota of the phytoplankton ((mol P $cell^{-1}$). Representing ingestion in this manner breaks the phytoplankton concentrations taken up by the grazers into total nitrogen and total phosphorus consumed. The assimilation rate, which equates to population growth, by the grazer population is a function of the grazer stoichiometry (static nitrogen and phosphorus content) and the N:P of the total prey ingested:

$$assimilation_G = MIN\left(\frac{ingestion_{G|N}}{Qper_{G|N}}, \frac{ingestion_{G|P}}{Qper_{G|P}}\right) \tag{11}$$

with units of grazer individuals L^{-1} day^{-1} (Roelke, 2000) and where $Qper_{G|N}$ is the static nitrogen content of the grazer (mol N individual^{-1}) and $Qper_{G|P}$ is the static phosphorus content of the grazer (mol P individual^{-1}), and other variables are the same as previously described. In this way, population growth of the grazer equates to the amount of the limiting nutrient ingested. The excess amount of non-limiting nutrient ingested by the grazer is immediately returned to the inorganic nutrient pool through the process of egestion (discussed further below).

Zooplankton per capita respiration is based on a basal rate and an activity constant simulating higher energy exertion when lower algal concentrations occur (Roelke, 2000):

$$respiratio\,n_G = aresp_G\left(\frac{grazing_{A_i}}{Qper_{G|C}}\right) + bresp_G G \tag{12}$$

with units of grazer individuals L^{-1} day^{-1} and where $aresp_G$ is a unitless activity coefficient, $Qper_{G|C}$ is the static carbon content of grazer individuals (mol C individual^{-1}), $bresp_G$ is the basal respiration rate (day^{-1}), and all other variables are the same as previously described. A two-part respiration function simulates lower metabolic activity when grazers are not feeding at higher rates (when prey densities are higher).

The toxin's effect on the grazer is akin to that of the phytoplankton:

$$mortality_G = mTox_G\left(\frac{T}{kTox_{T|G} + T}\right)G \tag{13}$$

with units of individuals L^{-1} day^{-1} and where $mTox_G$ is the maximum mortality rate of zooplankton caused by the toxin (d^{-1}), $kTox_{T|G}$ is the concentration of toxin at which 50% of the zooplankton die (μg-toxin L^{-1}), T is the concentration of toxic chemicals present (μg-toxin L^{-1}), and all other variables are the same as previously described. This mathematical equation results in the toxin inducing mortality of the grazers instead of deterring grazing activity. Again, standards are not available for the toxins produced by *P. parvum*. So, development of a formal equation, or more accurately parameterizing the equation used here, is not possible. As with the mortality term employed for phytoplankton, the equation used here assumes a saturating relationship, and was parameterized to fit empirical data associated with previous experiments addressing the toxic effects of *P. parvum* on zooplankton.

When any of the plankton groups experience a decrease in population, either through the lack of resource availability, competition, or exposure to toxic chemicals in the water, the nutrients comprised in the individual plankton cells or individual grazers are released back into the water in the form:

$$mortality_{A_i|N} = \sum \left(\left(growth_{A_i}^{t=\tau-1} - growth_{A_i}^{t=\tau} \right) + mortality_{A_2} \frac{Qper_{A_2|N}}{Qper_{A_2|C}} \right) \tag{14}$$

$$mortality_{G|N} = \sum \left(\left(assimilation_{G}^{t=\tau-1} - assimilation_{G}^{t=\tau} \right) + mortality_{G} \frac{Qper_{G|N}}{Qper_{G|C}} \right) \tag{15}$$

$$mortality_{A_i|P} = \sum \left(\left(growth_{A_i}^{t=\tau-1} - growth_{A_i}^{t=\tau} \right) + mortality_{A_2} \frac{Qper_{A_i|P}}{Qper_{A_i|C}} \right) \tag{16}$$

$$mortality_{G|P} = \sum \left(\left(assimilation_{G}^{t=\tau-1} - assimilation_{G}^{t=\tau} \right) + mortality_{G} \frac{Qper_{G|P}}{Qper_{G|C}} \right) \tag{17}$$

where Equations 14 and 15 have units of mol N L^{-1} day^{-1}, and Equations 16 and 17 have units of mol P L^{-1} day^{-1}, and where all variables are the same as previously described. The first parantheses in each equation is only valid when there is a decrease in the population; if not, the increase in population would be calculated twice. Releasing the nutrients back into the system in this way maintains mass conservation and allows the existing phytoplankton to intake the nutrients for further survival.

When the zooplankton respire, the excess resources return to the ambient supply in the following format:

$$respired_{G|N} = \sum \left(respiratio\ n_G Qper_{G|N} \right) \tag{18}$$

$$respired_{G|P} = \sum \left(respiratio\ n_G Qper_{G|P} \right) \tag{19}$$

with units of mol N L^{-1} day^{-1} and mol P L^{-1} day^{-1}, respectively, and with all variables the same as previously defined.

Excess nutrients consumed by the grazers, determined by the grazer's fixed stoichiometry and the N:P of the total ingested prey, are released back into the ambient nutrient supply (Nielsen, 1994) following:

$$egestion_{G|N} = ingestion_{G|N} - assimilation_G Qper_{G|N} \tag{20}$$

$$egestion_{G|P} = ingestion_{G|P} - assimilation_G Qper_{G|P} \quad (21)$$

with units of mol N L^{-1} day^{-1} and mol P L^{-1} day^{-1}, respectively, and where $ingestion_{G|N}$ is the total amount of nitrogen taken in by the grazers (mol N L^{-1} day^{-1}), $assimilation_G$ is the total assimilation of the grazer population (individuals L^{-1} day^{-1}), $Qper_{G|N}$ is the grazer static nitrogen content (mol N $individual^{-1}$), $ingestion_{G|P}$ is the total amount of phosphorus taken in by the grazers (mol P L^{-1} day^{-1}), and $Qper_{G|P}$ is the grazer static phosphorus content (mol P $individual^{-1}$). Note that following this notation, egestion of the nutrient limiting growth of the grazer will always be zero, with only the non-limiting nutrient being egested.

The uptake of nutrients by the phytoplankton species are calculated as:

$$uptake_{N|A} = \sum \left(growth_{A_i} \frac{Qper_{A_i|N}}{Qper_{A_i|C}} \right) \quad (22)$$

$$uptake_{P|A} = \sum \left(growth_{A_i} \frac{Qper_{A_i|P}}{Qper_{A_i|C}} \right) \quad (23)$$

with units of mol N L^{-1} day^{-1} and mol P L^{-1} day^{-1}, resepectively and where all variables remain the same as previously defined. The amount of uptake is in relation to the algae's growth and is taken out of the ambient supply, indicated by a decreasing variable in Equations 3 and 4, representing changes in the resource supplies.

The inflows entering the system, both pulsed and continuous, bring with them nutrient concentrations, affecting the existing nutrient concentrations of the form:

$$inflow_N = N_{source}(continuous + pulse) \tag{24}$$

$$inflow_P = P_{source}(continuous + pulse) \tag{25}$$

with units of mol N L^{-1} day^{-1} and mol P L^{-1} day^{-1}, resepectively and where N_{source} is the concentration of nitrogen entering the system (mol N L^{-1}), P_{source} is the concentration of phosphorus entering the system with the inflow (mol P L^{-1}), *continuous* is the chosen dilution rate used with a continuous inflow to the system (day^{-1}), and *pulse* is an intermittent rise in the dilution rate simulating a pulsed inflow to the system (day^{-1}). The *continuous* constant is found from daily hydraulic flushing rates at Lake Granbury and relating the Brazos River inflow rate to the volume of the lake, thereby cancelling out volumetric dimensions. The *pulse* constant includes a specified dilution rate occurring over a period of a certain number of days. Both variables, *continuous* and *pulse,* are chosen for the model and remain constant throughout the 30-day simulation. When the standard case is run, these variables equal 0, indicating no flow enters this closed system.

Toxin production is dependent on the growth rate and density of *P. parvum* and is of the form:

$$production = tox_A\left(1 - \mu rel_{A_1|C}\right)\frac{A_1}{Qper_{A_1|C}} \tag{26}$$

with units of g-toxin L^{-1} day^{-1}, and where tox_A is the maximum toxin production rate (g-toxin $cell^{-1}$ day^{-1}), $\mu rel_{A_1|R_j}$ is an unitless ratio of *P. parvum*'s nutrient-limited specific growth rate over its maximum specific growth rate to capture the alga's

decreased production of toxins with higher specific growth rates, A_1 is the concentration of *P. parvum* (mol C L^{-1}), and $Qper_{A_1|C}$ is the carbon-based cell quota of *P. parvum* (mol C $cell^{-1}$). The growth rate and density of *P. parvum* determines the rate of production. This toxin equation is designed to simulate *P. parvum*'s ability to increase chemical production when experiencing a low growth rate, reflecting stressed environment (Roelke et al., 2007; Graneli et al., 2008). Again, because standards are not available for the toxins produced by *P. parvum* development of a formal equation, or more accurately parameterizing the equation used here, is not possible. As with the mortality terms employed for phytoplankton and zooplankton, parameterization of this equation was based on a fit to empirical data associated with previous experiments addressing the toxic effects of *P. parvum* on other phytoplankton and zooplankton.

Toxin decay is governed by the toxin's half-life in an exponential decay function with the form:

$$decay = -kT \tag{27}$$

with units of g toxin L^{-1} day^{-1}, and where k is the toxin's first order decay coefficient (day^{-1}, Brooks, unpublished data) and T is the concentration of toxin (g toxin L^{-1}).

2.4 Calibration of the Model

Sampling and observations of Texas reservoirs plagued with *P. parvum* has led to a greater understanding of the alga's tendencies, including its vulnerability to flushing. Lakes Granbury and Possum Kingdom, both on the Brazos River system in Texas, have experienced recurring golden alga blooms and fish kills (Roelke et al., 2010c).

Mesocosm experiments lasting 28 days were conducted in Possum Kingdom to investigate the impact of nutrient additions as a *P. parvum* bloom deterrent, with samples taken every seven days (Roelke et al., 2007). Ten fixed stations located throughout the entirety of Lake Granbury, downstream of Possum Kingdom, have been sampled monthly by our research team for over five years. Both reservoirs experienced fish killing golden alga blooms during their respective experiments, spring 2005 in Possum Kingdom and spring 2007 in Lake Granbury, recording dynamics before, during, and after the bloom. Samples were collected and calculated in the same manner, resulting in duel records of nutrient concentrations (N and P), phytoplankton group dynamics, zooplankton group dynamics, *P. parvum* concentrations for each lake experiment, and environmental conditions of the systems including pH, temperature and salinity (Roelke et al., 2007; Roelke et al., 2010a). The hydrology of Lake Granbury was estimated as releases of the river into the lake (Grover et al., 2010; Roelke et al., 2010a). Toxicity of the water was determined through its LC_{50} values (Brooks et al., 2010).

Initial nitrogen, phosphorus, and phytoplankton concentrations were taken from enclosures not receiving any treatments measured at the start of the Possum Kingdom study. Estimated phytoplankton mortality rates from this study were used to calibrate the model. The modest zooplankton population changes observed in Lake Possum Kingdom prevented a useful estimated rate of change and therefore the initial zooplankton concentrations and estimated mortality rates were modeled after the Lake Granbury data. The model was simplified from the reported six phytoplankton groups and four zooplankton groups to 3 total plankton groups to maintain simplicity and

highlight responses from the toxin, though adding more plankton groups is feasible for future experiments and simulations. Without the ability to measure toxin concentrations in the water, toxin parameters do not have measurements for comparison.

2.5 Standard Case

A simulation, henceforth referred to as the standard case, depicts the domination of the community by *P. parvum*, the elimination of competitors, decline of grazers, and is used as the control case for experimental comparisons (Figure 2). Calculated in terms of mol C L^{-1} day^{-1}, the concentrations of phytoplankton are converted to chlorophyll-*a* concentrations for comparison with previously published research using a chlorophyll-a to carbon ratio of 50 (Riemann et al., 1982) and to present the data in a more tractable manner. The standard case is a 30-day simulation, and like the 28-day Lake Possum Kingdom experiments, shows the depletion of the competing phytoplankton and the grazers from the presence of the toxin. The model is not intended to reproduce exact dynamics seen in the data, but rather parallel mortality rates seen in both experiments. Similar to the Lake Possum Kingdom data, the competing phytoplankton, modeled after the diatom group, is present while *P. parvum* increases in density until it obtains an equilibrium density at which resources are insufficient to sustain further growth (Roelke et al., 2007). The model shows the zooplankton concentration present at the beginning of the bloom, but drops quickly while *P. parvum* is gaining dominance, and is removed until after the bloom conditions subsided, in similar growth patterns as observed in the Lake Granbury data (Roelke et al., 2010b). In both the observations and the modeled

data, the grazer populations are eliminated within ten days and the competing phytoplankton concentrations within twenty. Reducing the number of represented plankton groups prevents the exact population changes by eliminating other interactions and relationships not addressed in the model. The system becomes nitrogen limited after day 15 as *P. parvum* increases and reaches a concentration where the system is saturated. As *P. parvum* becomes the remaining alga, the nutrient levels affect the alga's cell demands requiring more nitrogen than phosphorus and then creating a nitrogen-limiting environment.

The zooplankton density initially spikes with an abundance of food available in the form of both phytoplankton groups and no toxin production. Within ten days the grazers are entirely eliminated. The competing phytoplankton remain in the system, are grazed upon until the grazers are removed, and then eliminated as well from the increasing toxin accumulation. While the competing phytoplankton are still present in the system, competition over the ambient nutrient causes *P. parvum*, with a slower maximum specific growth rate, to strain to obtain the necessary nutrients. The drop in *P. parvum* density at the start of the simulation, then its rapid increase to a saturating density, illustrates *P. parvum*'s ability to increase chemical production at slower growth

rates. The competing phytoplankton is a superior competitor in the absence of toxin with a higher growth rate compared with *P. parvum*, seen when the competing phytoplankton density exceeds that of *P. parvum* before substantial toxin production. The accumulation of toxin causes mortalities of both the zooplankton and the competing phytoplankton. The standard case is a closed system without any hydrological inputs.

The nutrient levels start at the concentrations noted at the beginning of the Lake Possum Kingdom experiment, differ during the simulation because *P. parvum* becomes the only species present in the system utilizing the nutrients in proportion to its internal demands. The Possum Kingdom enclosures included the other plankton groups that survived longer than the diatoms, drawing on the nutrient resources, resulting in different nutrient ratios than in the standard case. Though *P. parvum* has required more phosphorus than nitrogen at times, the biological values chosen in the standard case follow the Redfield ratio stating phytoplankton require more nitrogen than phosphorus for growth (Redfield, 1934).

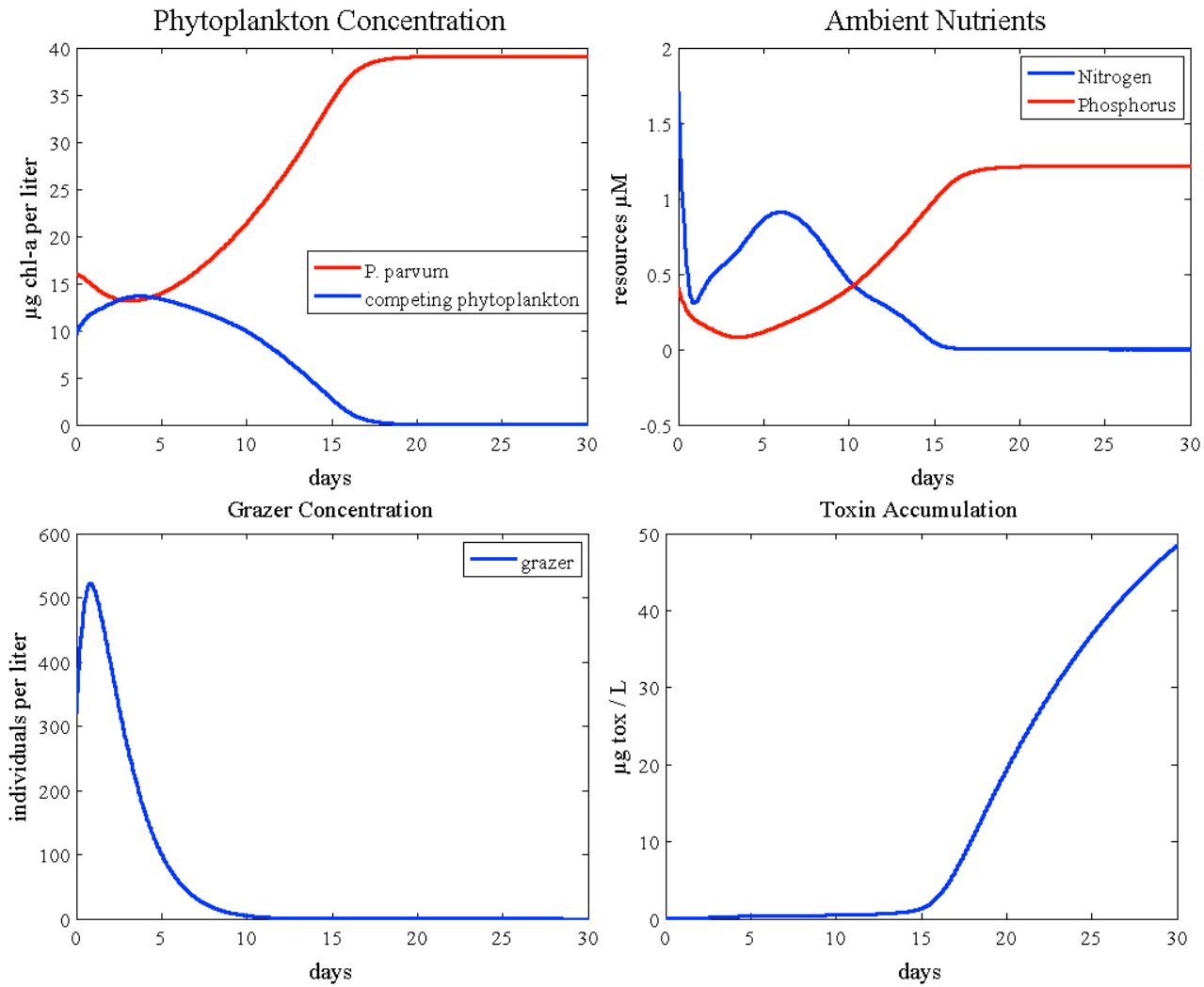

Figure 2. Simulations of the standard case: *Prymnesium parvum* eliminates the competing phytoplankton and grazer populations through the production of toxin

2.6 Sensitivity Analysis

A sensitivity analysis was performed on 24 parameters of the model comparing the cumulative output densities of the three plankton groups with the respective cumulative density of the standard case; the resulting differences are shown in Table 1. The cumulative density equation for each species equates to the sum of each plankton's biomass at days 0, 5, 10, 15, 20, 25, and 30, and is of the form:

$$\sum A_i = A_i^{t=0} + A_i^{t=5} + A_i^{t=10} + \ldots + A_i^{t=30} \tag{28}$$

$$\sum G = G^{t=0} + G^{t=5} + G^{t=10} + \ldots + G^{t=30} \tag{29}$$

where A_i is the phytoplankton density (μmol C L^{-1}) and G is the zooplankton density (individuals L^{-1}). This approach incorporates population density fluctuations throughout the simulation as using the final population density of the plankton (density at day 30) would not adequately account for population dynamics. The model was run with two manipulations of each parameter, a 20% increase and decrease, and the output cumulative population densities calculated. Differences in cumulative population densities between simulations were normalized against the change in parameter relative to the standard case, calculated using formulations of the form:

$$difference = \frac{(O_\Delta - O_{std})}{|P_\Delta - P_{std}|}\left(\frac{P_{std}}{O_{std}}\right) \tag{30}$$

where O_{Δ} is the resulting cumulative population density for the plankton species from the simulation with a changed parameter value, O_{std} is the cumulative population density for the plankton species from the standard case simulation, P_{Δ} is the new adjusted parameter value, and P_{std} is the parameter value used in the standard case. Using this relationship generates a normalized, dimensionless value accounting for the magnitude of change in the parameter as a function of the degree to which the parameter was changed (+ or – 20%). This relative difference equation varies slightly from other methods used to enumerate relative sensitivity (Haan and Skaggs, 2003) in that absolute value brackets are used in the denominator encasing the parameter values, P_{Δ} and P_{std}. This is accounted for in the way that the sensitivity analysis results are reported, where +20% and -20% variations in parameter values are demarcated. This approach also differs in that two sensitivities for the plankton response variables are reported for each parameter adjustment, one for the +20% change and another for the -20% change.

Table 1. Model parameters considered in the sensitivity analysis.

	Symbol	Units	Value	Sources
Prymnesium parvum				
Maximum specific growth rate	$\mu \max\ A_1$	day^{-1}	0.1	Baker et al., 2009
Nitrogen half saturation coefficient	$k_{A_1\|R_N}$	$mol\ N / L$	0.01	Errera et al., 2008 Baker, 2007
Phosphorus half saturation coefficient	$k_{A_1\|R_P}$	$mol\ P / L$	5.0E-3	Errera et al., 2008
Carbon cell quota	$Qper_{A_1\|C}$	$mol\ C / cell$	2.7E-06	Johansson and Graneli, 1999 Uronen et al., 2005
Nitrogen cellular content	$Qper_{A_1\|N}$	$mol\ N / cell$	2.4E-07	Johansson and Graneli, 1999 Uronen et al., 2005
Phosphorus cell quota	$Qper_{A_1\|P}$	$mol\ P / cell$	1.9E-09	Uronen et al., 2005
Competing Phytoplankton				
Maximum specific growth rate	$\mu \max\ A_2$	day^{-1}	0.57	Hamilton and Schladow, 1997 Tilman et al., 1982
Nitrogen half saturation coefficient	$k_{A_1\|R_N}$	$mol\ N / L$	0.1	Grover et al., 1999
Phosphorus half saturation coefficient	$k_{A_1\|R_P}$	$mol\ P / L$	0.001	Errera et al., 2008 Arhonditsis and Brett, 2005
Carbon cell quota	$Qper_{A_2\|C}$	$mol\ C / cell$	2.1E-06	Lynn et al., 2000 Popp et al., 1998
Nitrogen cell quota	$Qper_{A_2\|N}$	$mol\ N / cell$	3.0E-07	Lynn et al., 2000 Popp et al., 1998
Phosphorus cell quota	$Qper_{A_2\|P}$	$mol\ P / cell$	4.3E-08	Lynn et al., 2000 Popp et al., 1998
Toxin mortality rate	$mTox_{A_2}$	day^{-1}	1.0	
Toxin amount causing a 50% reduction in population	$kTox_{T\|A_2}$	$g\ toxin / L$	0.45	

Table 1. Continued.

	Symbol	Units	Value	Sources
Zooplankton population				
Maximum specific grazing rate	$d\max_G$	*mol C / individual day*$^{-1}$	0.045	Hansen and Bjornsen, 1997
Half saturation coefficient	k_G	*mol C / L*	6.67	Hessen and Bjerkeng, 1997
Carbon cell quota	$Qper_{G\|C}$	*mol C / individual*	0.046	Telesh et al., 1998 Rothhaupt, 1997 Anderson and Hessen, 1991
Nitrogen cell quota	$Qper_{G\|N}$	*mol N / individual*	0.003	Telesh et al., 1998 Rothhaupt, 1997
Phosphorus cell quota	$Qper_{G\|P}$	*mol P / individual*	1.1E-4	Telesh et al., 1998 Rothhaupt, 1997
Basal respiration rate	$bresp_G$	*day*$^{-1}$	0.05	Roelke, 2000
Active respiration constant	$aresp_G$	*n/a*	0.02	
Mortality rate from toxin	$mTox_G$	*day*$^{-1}$	2.35	
Toxin amount that causes a 50% reduction in growth	$kTox_{T\|G}$	*g toxin / L*	0.0145	
Toxin Coefficients				
Maximal toxin production rate	tox_A	*g toxin / cell day*$^{-1}$	1.0E-7	

2.7 Toxin Equations

Standards to measure *P. parvum*'s toxic chemical have yet to be developed (Baker et al., 2007, 2009; Valenti et al., 2010). The chemical production equation developed here was designed to include characteristics of *P. parvum* seen in toxic water. Toxin production increases with low densities and lower specific growth rates (Graneli and Johansson, 2003) and the standard case equation satisfies this condition.

Two other allelopathic relationships, from Martines et al. (2009) and Grover et al. (2010), were incorporated into the standard case to compare the resulting plankton dynamics against the standard case plankton densities. These published equations and their impact on the competing phytoplankton were used in place of the toxin's impact on the competing phytoplankton from the standard case equation; no changes were made to the grazers' reaction from the toxin to limit variation to only allelopathic reactions. The additional equations were run individually in the model with all other parameters held at the standard case values. The toxin production equations were simulated for 30-day simulation as in the standard case, and the resulting dynamics were compared against the standard case.

2.7.1 Martines et al. 2009

Developed for a similar model consisting of two phytoplankton, one producing a toxin killing the other, the equation from Martines et al (2009) is of the form:

$$\frac{dT}{dt} = \alpha\left(\mu \max A_1 - \mu A_1\left(R_j\right)\right)A_1 - KT \tag{31}$$

where α is a production constant (μg toxin cell^{-1}), μmaxA_1 is the maximum specific growth rate of *P. parvum* (day^{-1}), $\mu A_1(R_j)$ is the specific growth rate of *P. parvum* based on the limiting nutrient (day^{-1}), and A_1 is the density of *P. parvum* (μmol C L^{-1}). Toxin decay is of the first order where K is the decay rate constant (day^{-1}). Similar to the standard case, toxin production is related to the difference between the specific growth rate derived from limiting nutrients, and the maximum specific growth rate of *P. parvum*. This relationship allows the model to simulate an increase in toxin production when the specific growth rate is low.

In the standard case, competing phytoplankton density losses resulted from grazing and death from contact with the toxin. In this relationship, the competing phytoplankton are killed by two additional factors apart from grazing losses: a base mortality rate, m_{A_2} (day^{-1}), and a function relating the half saturation coefficient of the limiting nutrient and the plankton's growth rate that increases as toxin concentration increases. The mortality losses are defined as

$$m_{T|A_2} = \left(\frac{\mu max_{A_2}}{2k_{A_2|R_j}} \right) T + m_{A_2} \tag{32}$$

where μmax_{A_2} is the maximum specific growth rate of the competing phytoplankton (day^{-1}), $k_{A_2|R_j}$ is the competing phytoplankton's half saturation coefficient of the limiting nutrient (μmol N or P L^{-1}), and T is the concentration of the toxin (μg-toxin L^{-1}).

2.7.2 Grover et al., 2010

Originally used to model cyanotoxin production by cyanobacteria in a freshwater lake, the second allelopathic equation tested from Grover et al. (2010) depicts toxin production as proportional to the growth of *P. parvum* in the form:

$$\frac{dT}{dt} = \frac{A_1}{Qper_{A_1|R_C}} \mu_{A_1} \varepsilon_T - K_T T \tag{33}$$

where A_1 is the density of *P. parvum* (μmol C L^{-1}), $Qper_{A_1|R_C}$ is the carbon quota of *P. parvum*(μmol C cell^{-1}) , μ_{A_1} is the growth rate of *P. parvum* (day^{-1}), and ε_T is the toxin production coefficient (μg toxin cell^{-1}). Toxin decay is of the first order with K_T as the decay rate (day^{-1}) and T the concentration of toxin in the system (μg toxin L^{-1}). This equation does not depend on the difference from the maximum specific growth rate as the standard case does but has a linearly increasing function.

The competing phytoplankton are not killed by the toxin in contrast to the standard case, but their specific growth rate is impeded as the concentration of toxin increases using a Monod-like relationship preventing the phytoplankton from reaching their maximum specific growth rate despite nutrient availability

$$growth_{A_2} = \mu_{A_2|R_j} A_2 \left(\frac{k_T^I}{T + k_T^I} \right) \tag{34}$$

where $\mu_{A_2|R_j}$ is the specific growth rate of the competing phytoplankton determined by the limiting resource (day^{-1}), A_2 is the concentration of the competing phytoplankton (μmol C L^{-1}), k_T^I is a concentration of toxin that causes a 50% reduction in algal growth

rate (μg toxin L^{-1}). With this relationship, higher concentrations of toxin present will generate greater inhibition of the competing phytoplankton's growth.

2.8 Hydrology

The model is designed for the inclusion of hydrological flushing to test the effect of flow characteristics on bloom dynamics. The standard case was developed without any hydrological influences, but entirely closed systems are not common. To test the effects of hydrology on plankton dynamics in the standard case, three scenarios were investigated: a continuous inflow with changing inflow magnitude, pulsed inflows with changing pulsing periodicity, and combinations of these. Dilution rates were based on calculated hydraulic flushing rates found at Lake Granbury (Grover et al., 2010, Roelke et al., 2010), which were estimated using the rate of inflow into the reservoir from the Brazos River relative to the volume of the lake, resulting in a dilution rate without volumetric dimensions, which we now refer to as 'flushing':

$$flushing = \frac{inflow}{volume} \tag{35}$$

where *inflow* is the rate of inflow into Lake Granbury recorded from the USGS station at Dennis, TX (USGS Station 08090800), located just upstream of the lake (m^3 day^{-1}) and *volume* is the overall capacity of the reservoir (m^3).

Simulated pulsed inflows are defined as a specified dilution rate occurring over a period of a single day with varied intervals between events up to 15 days. The pulsing scenarios tested simulated pulses with intervals of 0, 3, 6, 9, 12, and 15 days. For these

simulations, instantaneous rates of flushing had distinctive magnitude, with pulsed inflows delivered using a sine function over a period of one day on the day that inflows occurred, and the magnitude of the pulse was a function of the interval period. To illustrate, during a simulation employing a 3-day pulsing interval., the magnitude of inflow was three-fold greater on the day that a pulse occurred compared to the continuous inflow simulation, but no inflow occurred on the other two days, which resulted in equal flushing over the duration of the simulations being compared.

The initial nutrient concentrations and the nutrient concentrations of source water in the simulation for the standard case were taken from the experimental data from Lake Possum Kingdom. Additional nutrient concentration scenarios were explored. Two simulations, each with varying pulsing and dilution rates, were run to test hydrological flushing effects with different source water composed of different nutrient concentrations. One nutrient concentration represents nutrient concentrations typical with the Brazos River. This concentration is a recorded nutrient concentration from the monthly sampling trips to Lake Granbury at a the station situated at the headwaters of the lake, located over the river channel and at times of high inflow into Lake Granbury, best represents nutrient levels typical of the river itself. The other nutrient concentration tested represents nutrient concentrations from bottom water and is from a station located at the base of Lake Granbury taken during winter months when *P. parvum* blooms are more common in Texas lakes.

3. RESULTS

3.1 Sensitivity Analysis

The sensitivity analysis results in Table 2 display the top 20 parameter adjustments (±20%) that generated the greatest deviation in the cumulative state variables relative to the standard case, where the state variables were *P. parvum*, competing phytoplankton, and grazers; and they were considered cumulative because values at time 0, 5, 10 … 30 were summed. The first 10 parameter adjustments listed caused the greatest increase in the designated cumulative state variables, and the last 10 parameter adjustments listed caused the greatest decrease in the designated cumulative state variables. The 'Relative Difference' values listed in the table, then, indicate the degree of change in the designated cumulative state variable divided by the 'Percent Variation', which is the degree of adjustment in a parameter value relative to the parameter's value in the standard case, i.e., ±20% (see Equation 20).

Each parameter adjustment and resulting relative difference in the designated state variable were graphed, and each resulted in a monotonic relationship (not shown). In other words, either the relationship was positive (meaning -20% parameter adjustment resulted in a decrease in the cumulative state variable and a +20% parameter adjustment resulted in an increase in the cumulative state variable), or decreasing (meaning -20% parameter adjustment resulted in an increase in the cumulative state variable and a +20% parameter adjustment resulted in a decrease in the cumulative state variable). There were no unimodal or concave relationships observed over the range of parameter space evaluated.

The parameter adjustments causing the greatest change in the state variables were not surprising. For example, the greatest relative population density changes were observed with increases in zooplankton. This stands to reason as the grazer population was eliminated in the standard case within ten days. So, parameter adjustments extending this persistence brought about large proportional changes. Similarly, the large decreases in the *P. parvum* density from parameter adjustments can be explained because of their dominance, or bloom behavior, in the standard case. Subsequently, parameter adjustments slowing the rate of bloom development or preventing the bloom state brought about large proportional changes.

Another trend involved an inverse relationship between density changes of the grazer and the competing phytoplankton populations compared to *P. parvum*'s density. When a population increase occurs in the density of *P. parvum*, the same parameter adjustment results in a decrease of both the competing phytoplankton and grazer densities, and vice versa. The other two plankton groups respond opposite of *P. parvum*'s density reaction to the parameter adjustment. Since *P. parvum* blooms in the standard case, any difference from this saturating density allows for the persistence of the other plankton groups.

Table 2. Sensitivity analysis results showing the most influential parameters in accumulated biomass density for all three plankton groups.

P. parvum Density Changes			Competing Phytoplankton Density Changes			Grazer Density Changes		
Parameter	Percent Variation	Relative Difference	Parameter	Percent Variation	Relative Difference	Parameter	Percent Variation	Relative Difference
$Qper_{A_1\|R_N}$	-20	0.80	$Qper_{A_2\|R_N}$	+20	3.88	$Qper_{A_2\|R_C}$	-20	16.20
$d\max_G$	-20	0.55	$mTox_G$	-20	3.39	$mTox_G$	-20	9.55
$Qper_{A_1\|R_C}$	+20	0.54	$Qper_{A_2\|R_C}$	-20	3.2	$Qper_{G\|R_N}$	-20	6.24
$Qper_{G\|R_N}$	+20	0.45	$Qper_{G\|R_N}$	-20	3.09	$Qper_{A_2\|R_N}$	+20	4.92
$mTox_G$	+20	0.41	$d\max_G$	+20	3.08	$d\max_G$	+20	3.15
$\mu\max A_1$	+20	0.30	$Qper_{A_1\|R_N}$	+20	1.63	$kTox_{T\|A_2}$	-20	2.45
$kTox_{T\|G}$	-20	0.17	$\mu\max A_1$	-20	1.21	$Qper_{A_1\|R_N}$	+20	2.09
$\mu\max A_2$	+20	0.17	$Qper_{A_1\|R_C}$	-20	1.04	$Qper_{A_1\|R_C}$	-20	1.80
tox_A	+20	0.13	tox_A	-20	0.65	$\mu\max A_2$	-20	0.62
$k_{A_1\|R_P}$	+20	0.11	$kTox_{T\|G}$	+20	0.55	$kTox_{T\|G}$	+20	0.47
tox_A	-20	-0.23	tox_A	+20	-0.41	tox_A	+20	-0.26
$\mu\max A_2$	-20	-0.24	$\mu\max A_2$	+20	-0.41	$kTox_{T\|G}$	-20	-0.35
$\mu\max A_1$	-20	-0.47	$kTox_{T\|G}$	-20	-0.47	$\mu\max A_2$	+20	-0.37
$Qper_{A_1\|R_C}$	-20	-0.87	$Qper_{A_1\|R_N}$	-20	-0.49	$Qper_{A_1\|R_C}$	+20	-0.49
$Qper_{A_1\|R_N}$	+20	-0.97	$Qper_{A_2\|R_C}$	+20	-0.71	$Qper_{A_2\|R_C}$	+20	-0.71
$Qper_{A_2\|R_N}$	+20	-1.51	$\mu\max A_1$	+20	-0.85	$Qper_{A_1\|R_N}$	-20	-0.73
$Qper_{A_2\|R_C}$	-20	-4.17	$Qper_{A_2\|R_N}$	-20	-1.03	$Qper_{A_2\|R_N}$	-20	-0.87
$mTox_G$	-20	-4.49	$Qper_{G\|R_N}$	+20	-1.07	$Qper_{G\|R_N}$	+20	-1.00
$Qper_{G\|R_N}$	-20	-4.59	$mTox_G$	+20	-1.14	$mTox_G$	+20	-1.09
$d\max_G$	+20	-4.60	$d\max_G$	-20	-1.62	$d\max_G$	-20	-1.10

Parameter adjustments related to zooplankton generated large density variations. Changes to the maximum specific grazing rate caused the greatest density decreases for all three plankton groups and is prominent in the density increases as well. Figure 3 shows the model output when the maximum specific grazing rate is increased by 20%, generating 3.08 and 3.15 relative density increases in the cumulative densities of the competing phytoplankton and zooplankton populations, respectively. The density of *P. parvum* experiences a decrease of 4.60 as compared with the standard case cumulative density and normalized as described in Equation 20. *P. parvum* does not generate any growth and is eliminated from the system with the competing phytoplankton as the grazer population reaches its peak density of over 1000 individuals and grazes down the concentration of the phytoplankton. The toxin does not accumulate throughout the simulation and without its presence, the competing phytoplankton reenters the system once the grazer population starves and leaves the system. The grazer population also reemerges at the end of the 30 days, responding to the now present food source after the competing phytoplankton density establishes itself as the only phytoplankton group.

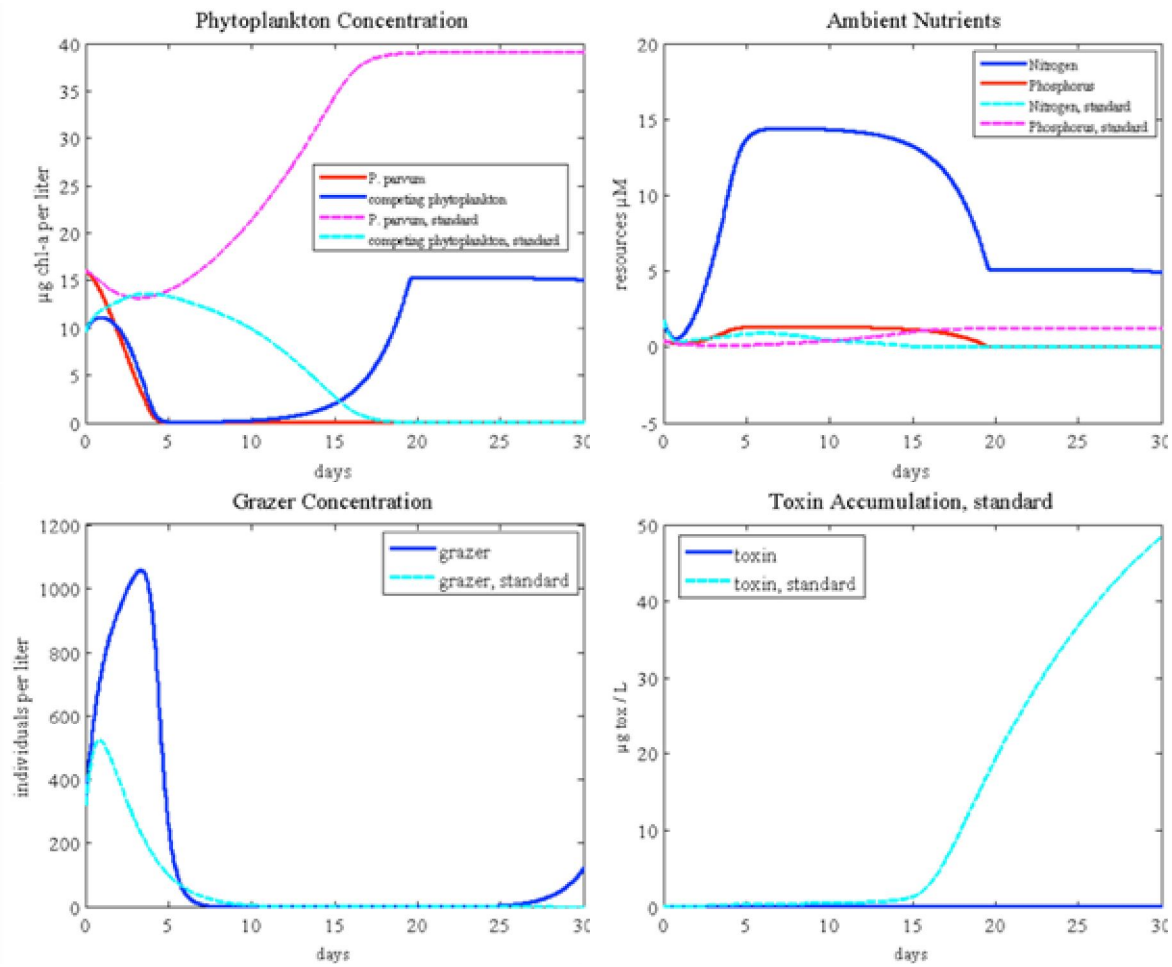

Figure 3. Model output when the maximum specific grazing rate is increased 20% compared with the standard case (dashed lines)

Grazer mortality rate differences also resulted in density fluctuations increasing grazer and competing phytoplankton densities with a 20% decrease, and increasing *P. parvum* density with an increase in the mortality rate. For example, when the specific mortality rate of the toxin on the grazer is increased by 20% (Figure 4), *P. parvum* reaches a saturating density faster than the standard case, generating the 0.41 relative cumulative density increase noted in Table 2. The grazer population does not reach the same peak density as in the standard case due to the increase in mortality rate by the toxin and is eliminated faster, a 1.09 relative decrease in its cumulative density. The competing phytoplankton obtain a similar peak density as compared to the standard case, but are removed from the system faster from the presence of the toxin, a 1.14 relative decrease in density. The toxin accumulates in the system faster as *P. parvum* approaches its saturating density.

Manipulations of the nutrient quota parameters for all three plankton groups account for almost half of all parameter adjustments listed in the sensitivity analysis results. Changes to these parameters equate to different proportions of nutrients being required by each plankton group for survival. Any variation of these parameters will

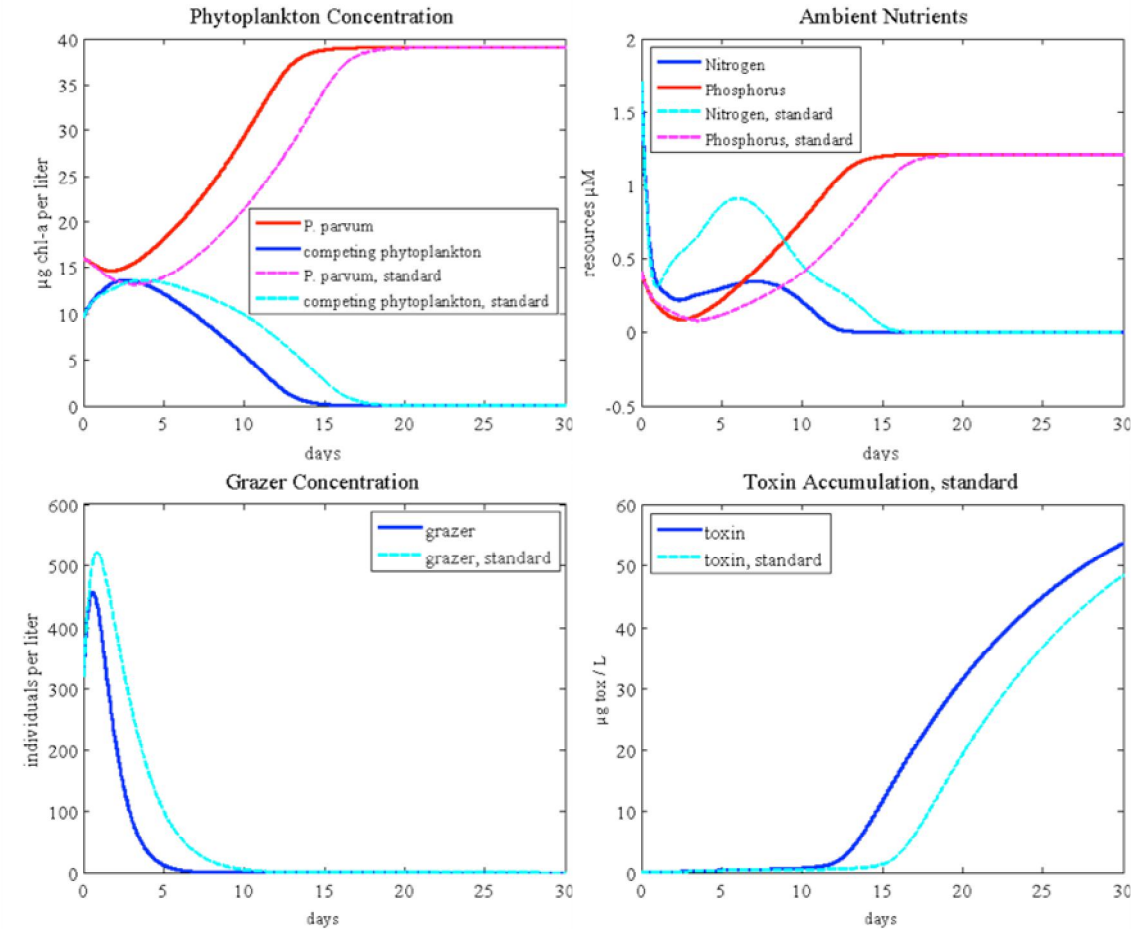

Figure 4. Model output when the parameter *mtoxG* is increased by 20% as compared with the standard case (dashed lines)

generate different proportions of the nutrients in each trophic level, leading to changes in the densities of the plankton groups. Altering the nutrient quotas of the phytoplankton redistributes the available nutrients among the lower trophic level and thus alters the concentration ingested by the grazer. Figure 5 shows the model output when the nitrogen cell quota of the competing phytoplankton is increased by 20%. This cell quota change benefits the competing phytoplankton and grazer populations, generating increases in their densities compared with the standard case. The competing phytoplankton maintain a presence in the system for almost the entire 30 days, a 3.88 relative increase in cumulative density. The zooplankton population also experiences an increased presence in the system, peaking at a density higher than that of the standard case and lasting nearly 10 days longer in the simulation. The density of *P. parvum* does not establish domination over the competing phytoplankton until day 15, ten days later than in the standard case. Noticeable toxin accumulation does not appear until after the competing phytoplankton population is removed and *P. parvum* is almost at its saturating density.

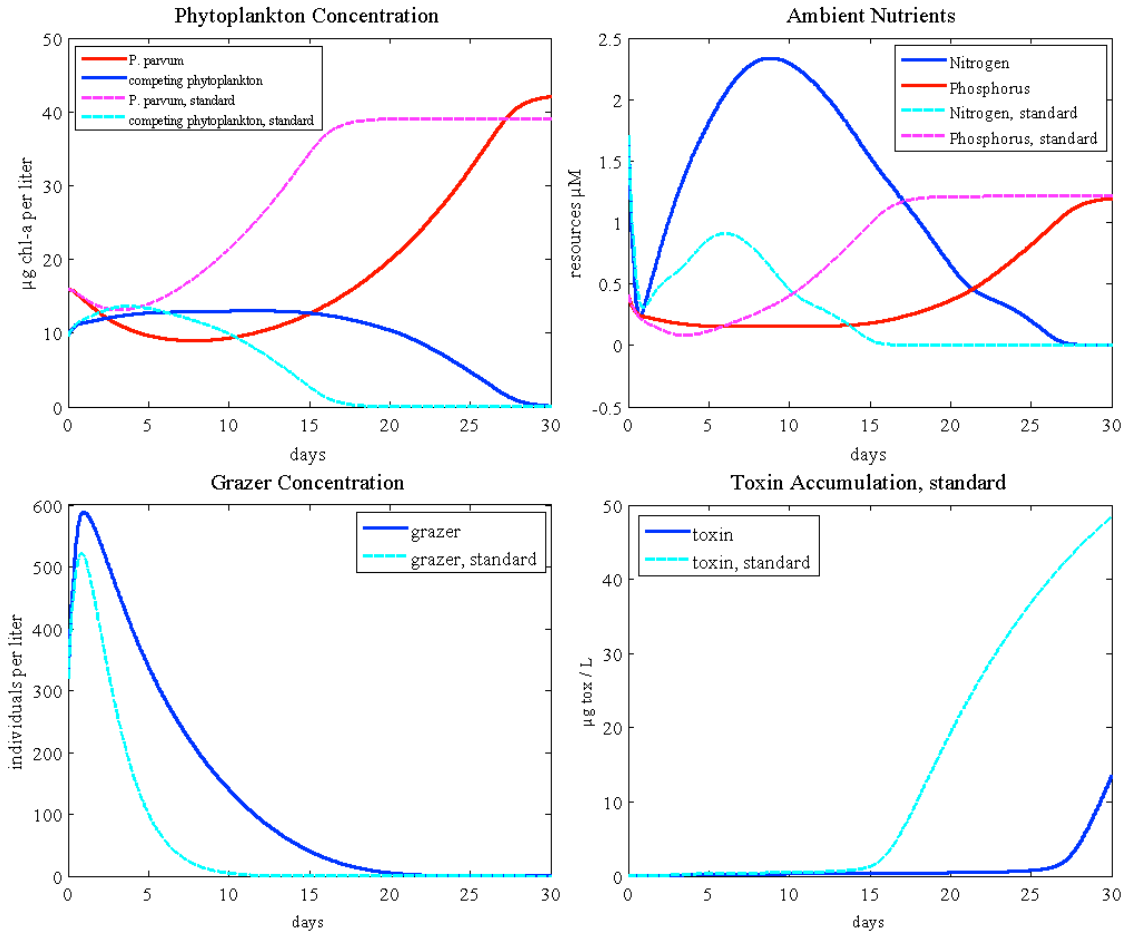

Figure 5. Model output when the nitrogen cell quota of the competing phytoplankton is increased by 20%

3.2 Toxin Equations

3.2.1 Martines et al. 2009

Inserting the Martines et al. (2009) allelopathy relationship into the model results in reduced competing phytoplankton and grazer concentrations as compared to the standard case (Figure 6). The zooplankton population does not spike as seen in the

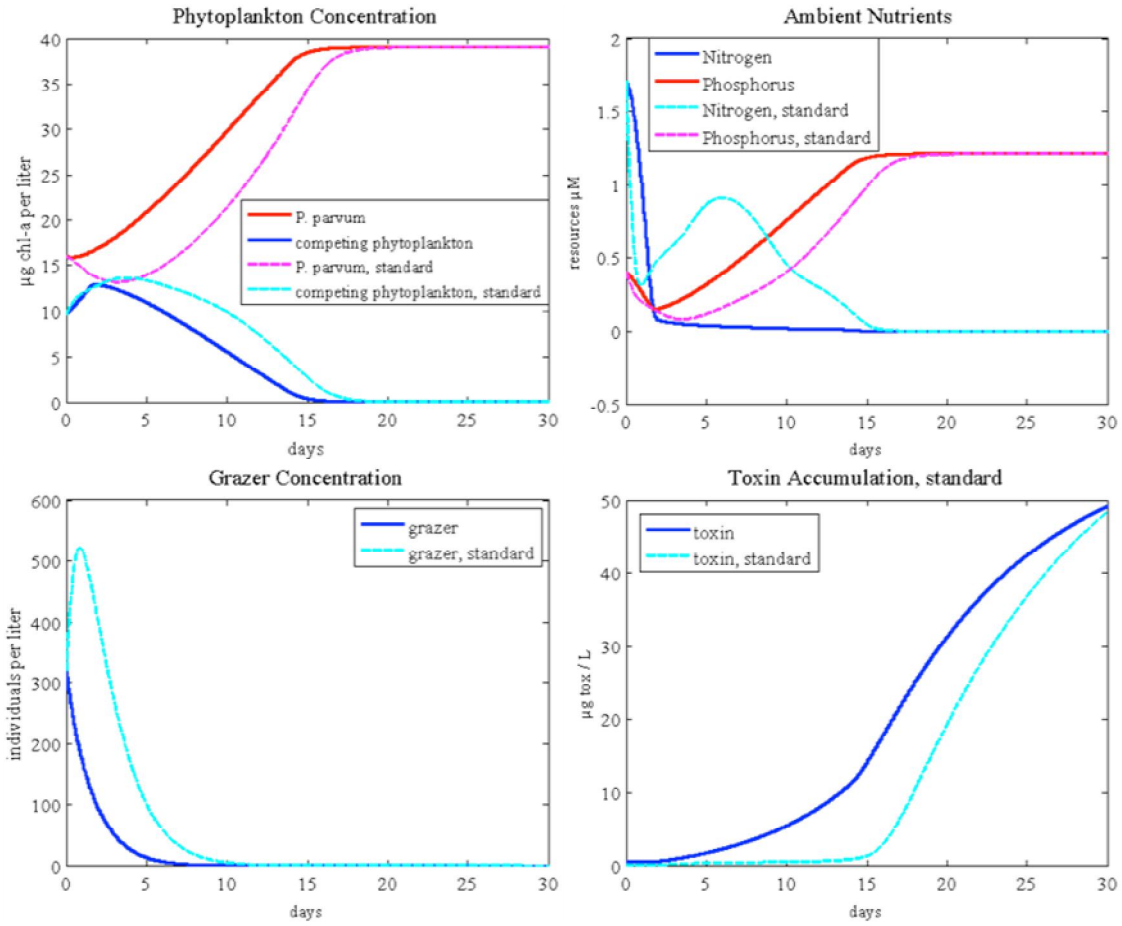

Figure 6. Model simulations using the Martines et al. (2009) allelopathic equations compared with the standard case (dashed line)

standard case, but is removed from the system at a quick rate, eliminated around day 7. The toxin's effect on the grazer was not altered from the standard case values emphasizing the toxin production rate is quicker. The competing phytoplankton's quicker demise results from the quicker toxin production rate as well, removed almost 5 days sooner than in the standard case. The concentrations of *P. parvum* and toxin both reach their highest possible density allowed for by the nutrients available faster than in the standard case (represented by the dashed line). The toxin accumulation is at a comparable rate to the standard case, though the Martines toxin production rate is quicker.

3.2.2 Grover et al.. 2010

Figure 7 shows the allelopathic equation from Grover et al. (2010) compared against the standard case (dashed lines). Instead of increasing its mortality rate, the competing phytoplankton's growth rate is inhibited in relation to the production of toxin.

With only stunted growth, the two phytoplankton species are capable of coexistence. Toxin production declines after the elimination of the zooplankton population and does not appear necessary to maintain *P. parvum*'s dominance of the system, suppressing the growth of the competing phytoplankton. The grazer population decreases from the spike in toxin production despite ample food sources available. Toxin concentrations do not last through the simulation, decaying after the spike.

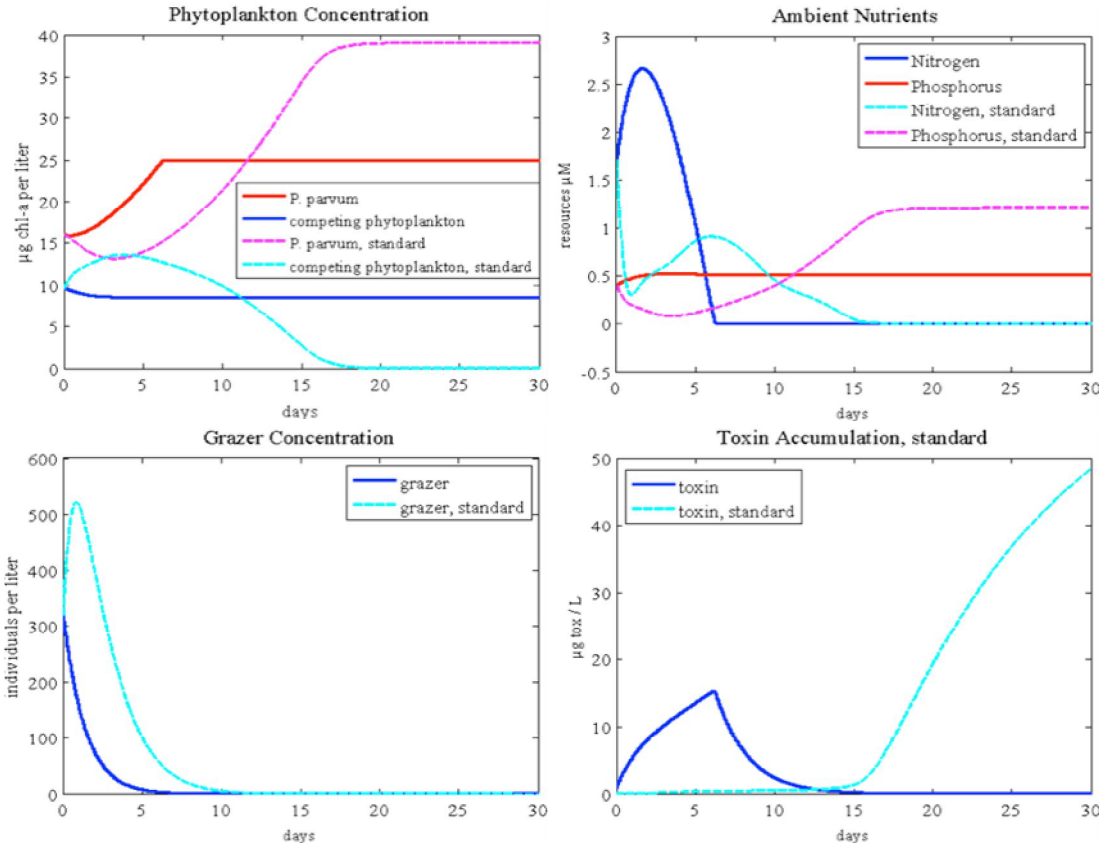

Figure 7. Model simulation comparing the toxin production equations of Grover et al (2010) and the standard case (dashed lines)

3.3 Hydrology

3.3.1 Magnitude of inflows

Inflows into the system reduces the density of *P. parvum* in a 30-day simulation. Figures 8 through 14 show model simulations with incrementally increasing dilution rates, 0.001/day to 0.65/day, typical of average daily inflow rates seen in Lake Granbury (Grover et al., 2010; Roelke et al., 2010). Neither phytoplankton species survives longer than five days with dilution rates higher than 0.65/day.

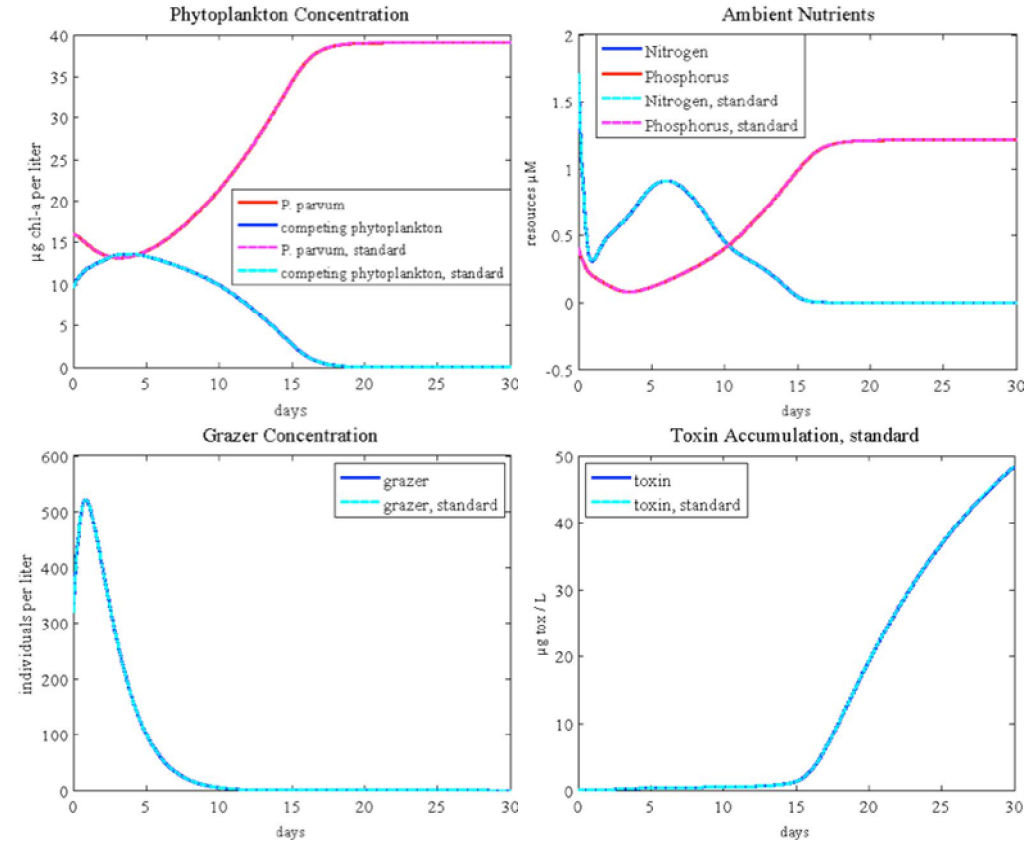

Figure 8. Model output with a 0.001/day dilution rate compared with the standard case without any dilution (dashed line)

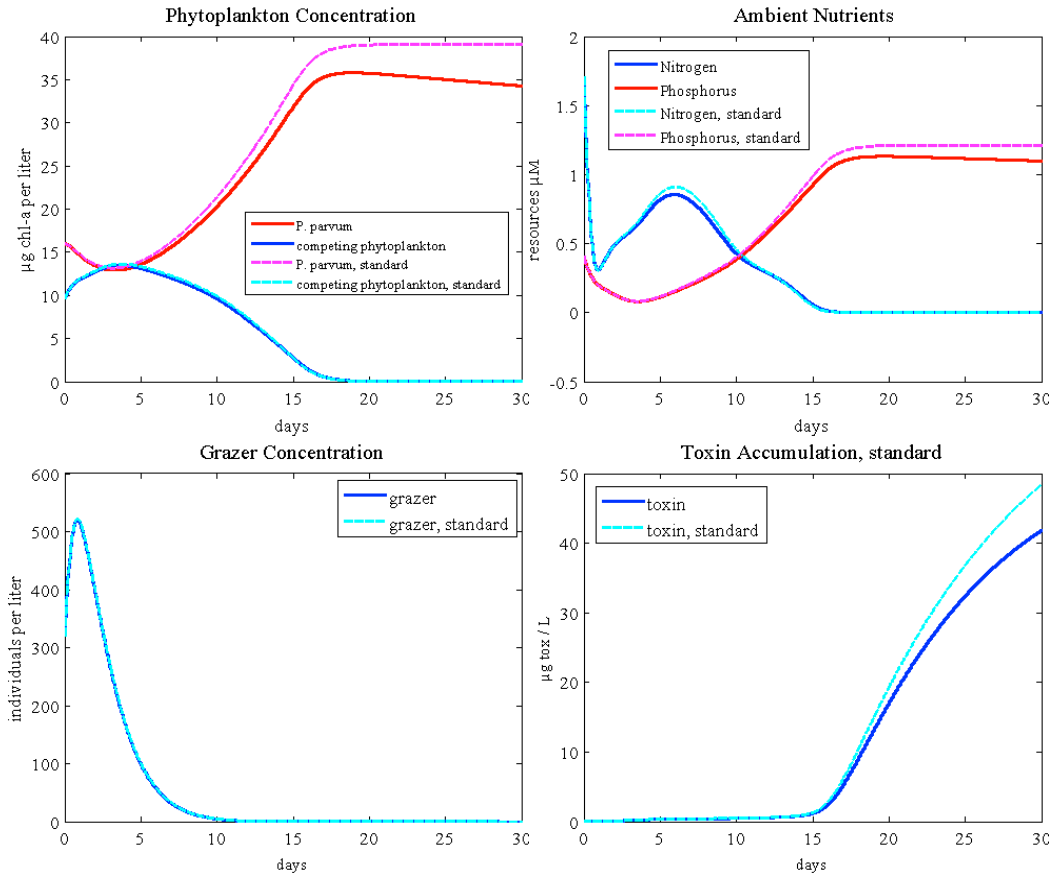

Figure 9. Model output with a 0.005/day dilution rate compared with the standard case without any dilution (dashed line)

With a dilution rate of 0.1/day, the competing phytoplankton remain in the system for the longest duration; at this dilution rate, *P. parvum* dominates the system still, but at an over 80% decrease in density (Figure 12). The grazers decrease slightly in density from the standard case (dashed line) until the phytoplankton groups are removed at which

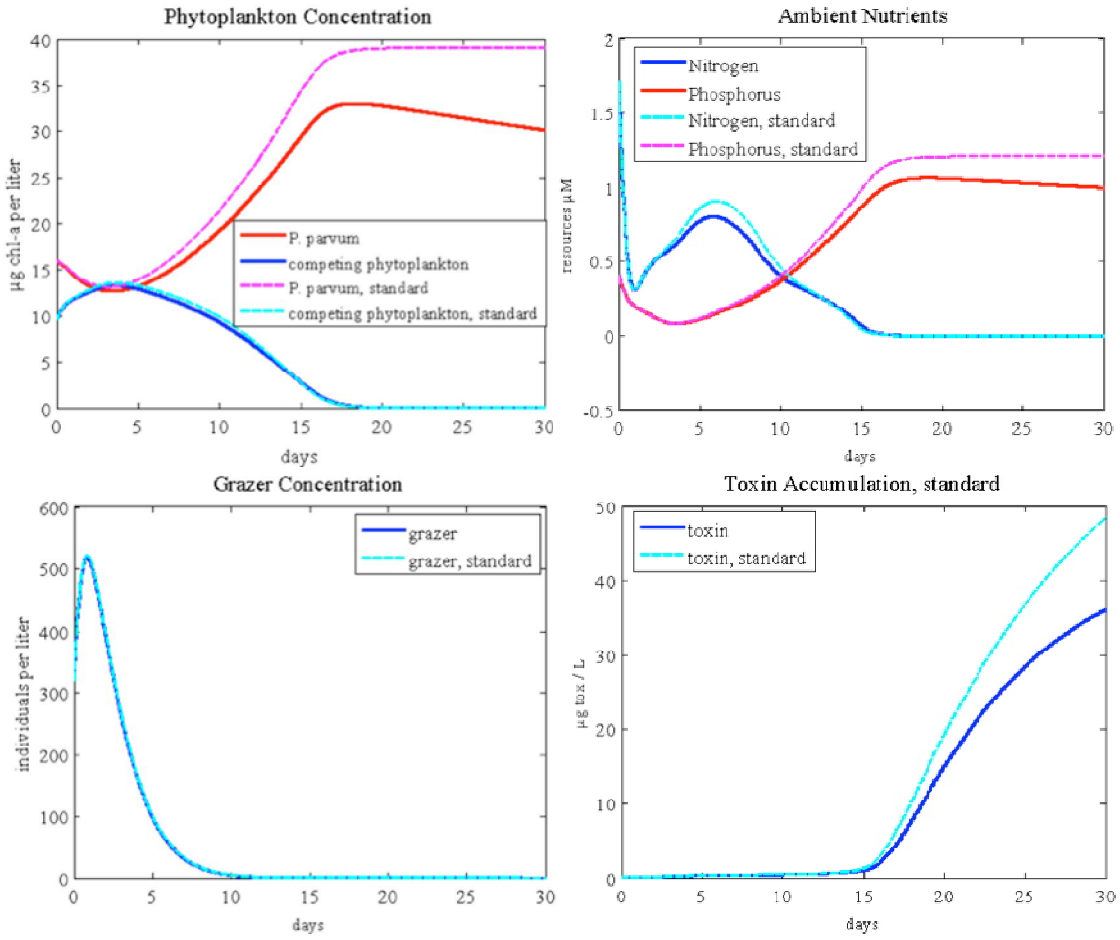

Figure 10. Model output with a 0.01/day dilution rate compared with the standard case without any dilution (dashed line)

point the grazer population is without a food source and does not reach the same peak density as in the standard case. Toxin accumulation decreases as dilution rates increase until no accumulation is seen (Figures 13 and 14).

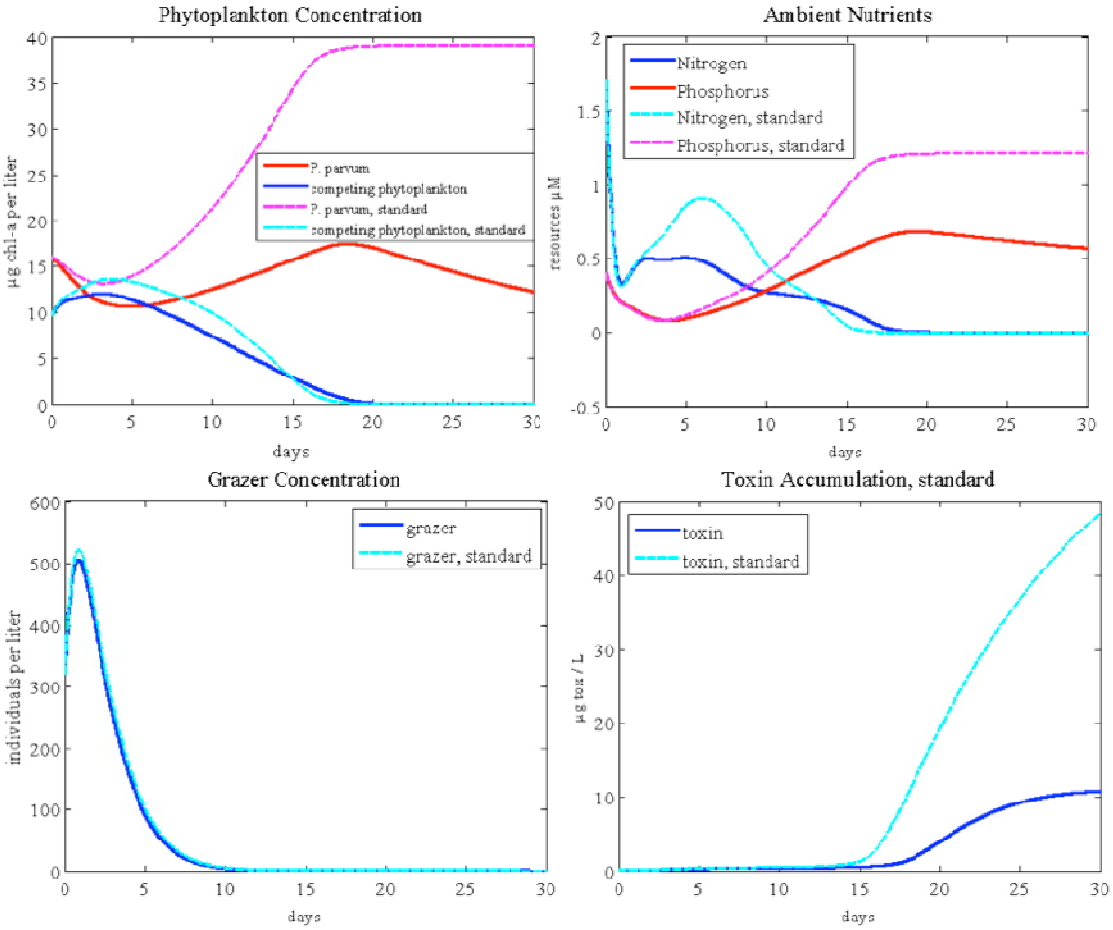

Figure 11. Model output with a 0.05/day dilution rate compared with the standard case without any dilution (dashed line)

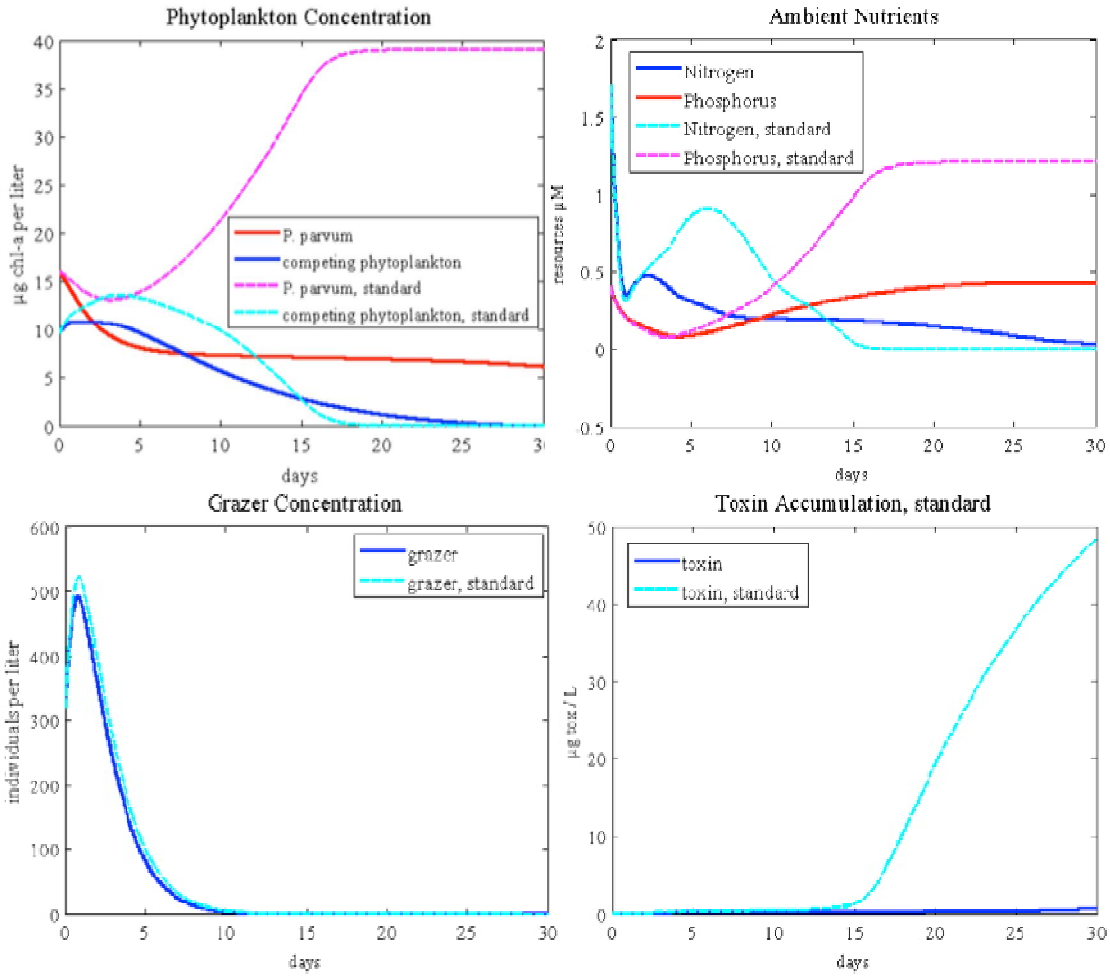

Figure 12. Model output with a 0.1/day dilution rate compared with the standard case without any dilution (dashed line)

Figure 13 shows the model output with a dilution rate of 0.3/day, a rate higher than the maximum specific growth rate of *P. parvum* but less than the maximum specific growth rate of the competing phytoplankton. The density of *P. parvum* does not spike nor maintain dominance in the system as in the standard case while the competing

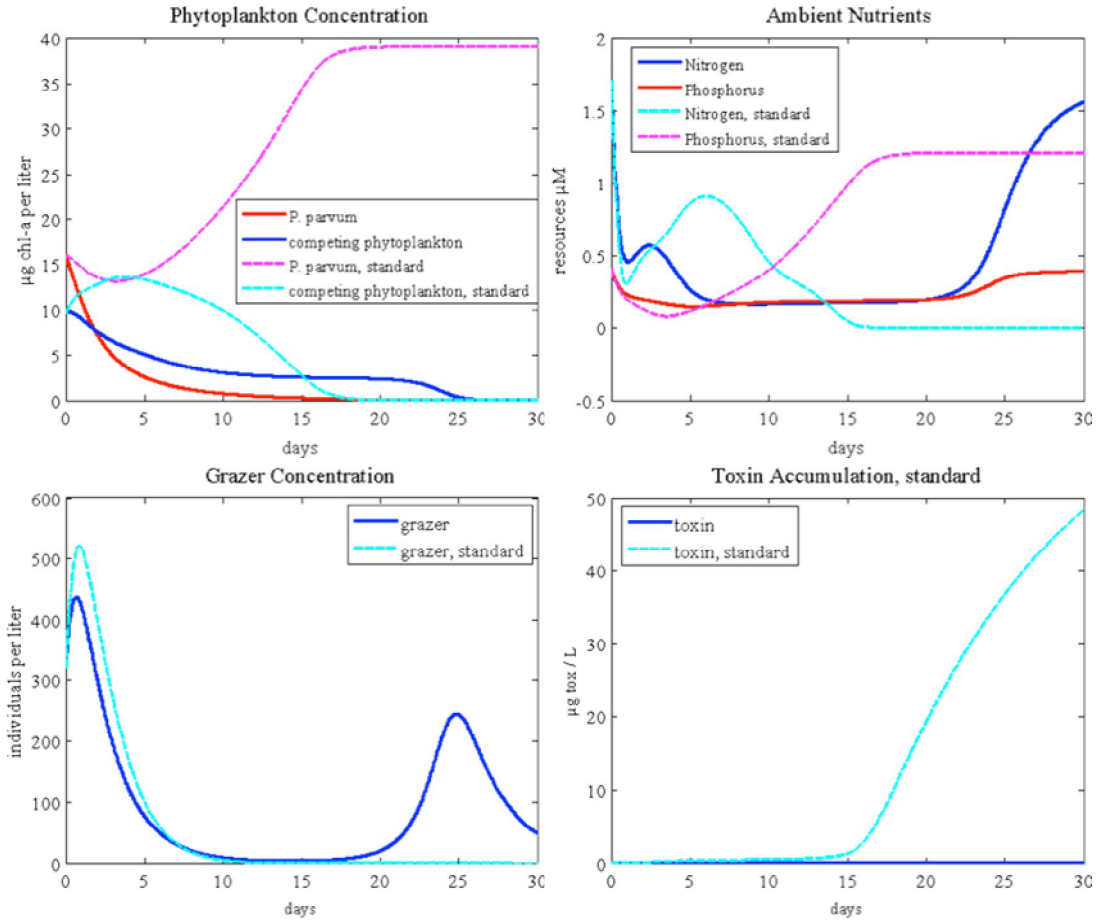

Figure 13. Model output with a 0.3/day dilution rate compared with the standard case without any dilution (dashed lines)

phytoplankton density persists until day 25 at which point the grazer population removes them. The competing phytoplankton do not reach a density higher than their initial concentration, but maintain a lower density throughout the majority of the system,

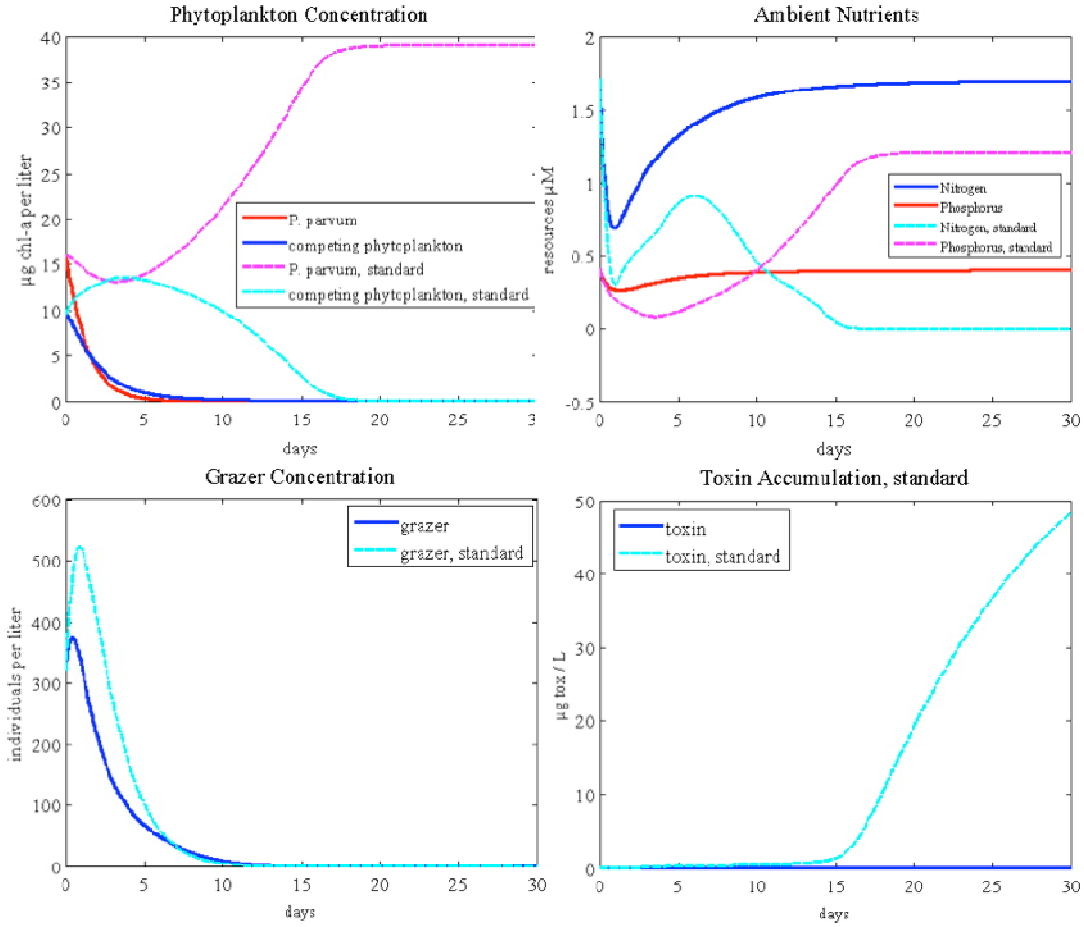

Figure 14. Model output with a 0.65/day dilution rate compared with the standard case without any dilution (dashed line)

showing its capability to outcompete *P. parvum* under continuous flow conditions. The grazer population initially spikes, and then is depleted from the system dilution, only to peak again at day 25, feeding upon the competing phytoplankton. There is little to no toxin production while *P. parvum* is still in the system. Figures 15 and 16 show continuous inflow conditions of large magnitude, 2.6/day and 16/day dilution rates,

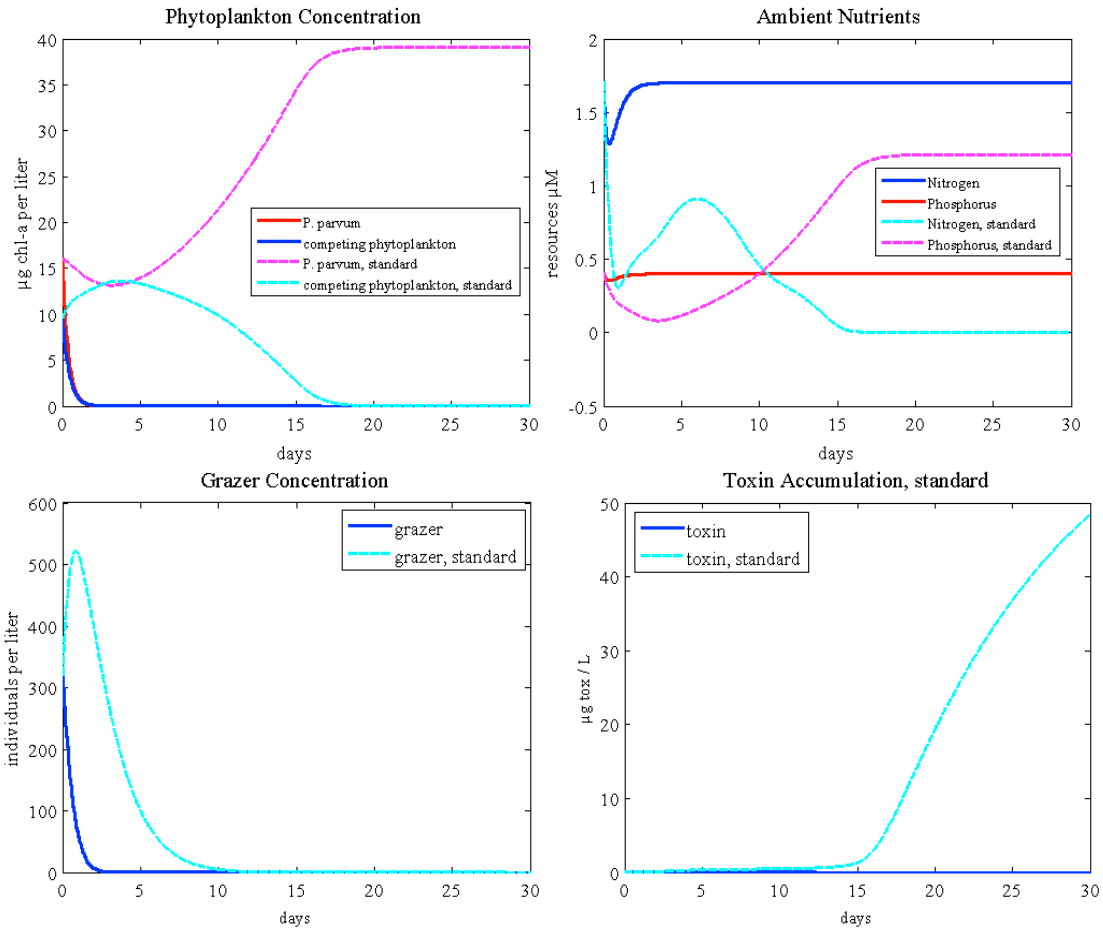

Figure 15. Model output with a 2.6/day dilution rate compared with the standard case without any dilution (dashed line)

respectively, representing conditions in Lake Granbury following heavy precipitation events. Very little plankton activity occurs as all three plankton species are removed quickly from the system. Toxin accumulation is hampered in these simulations from the lack of *P. parvum* density and therefore little if any accumulation is noticeable.

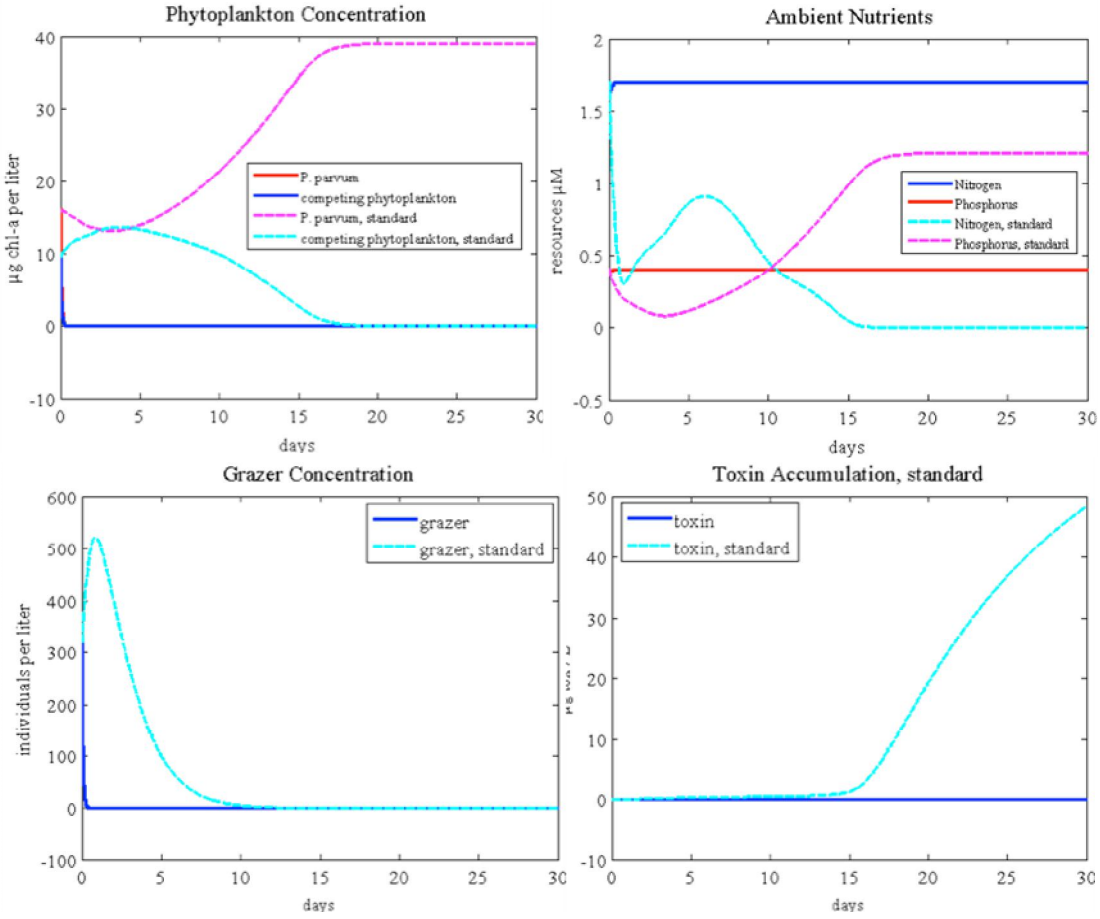

Figure 16. Model output with a 16/day dilution rate compared with the standard case without any dilution (dashed line)

3.3.2 Periodicity of inflows

The inclusion of pulsing inflows creates disturbances in the system, generating fluctuations in plankton densities. Figures 17-25 show population density changes resulting from the introduction of inflow pulse periodicity. Figure 17 shows a

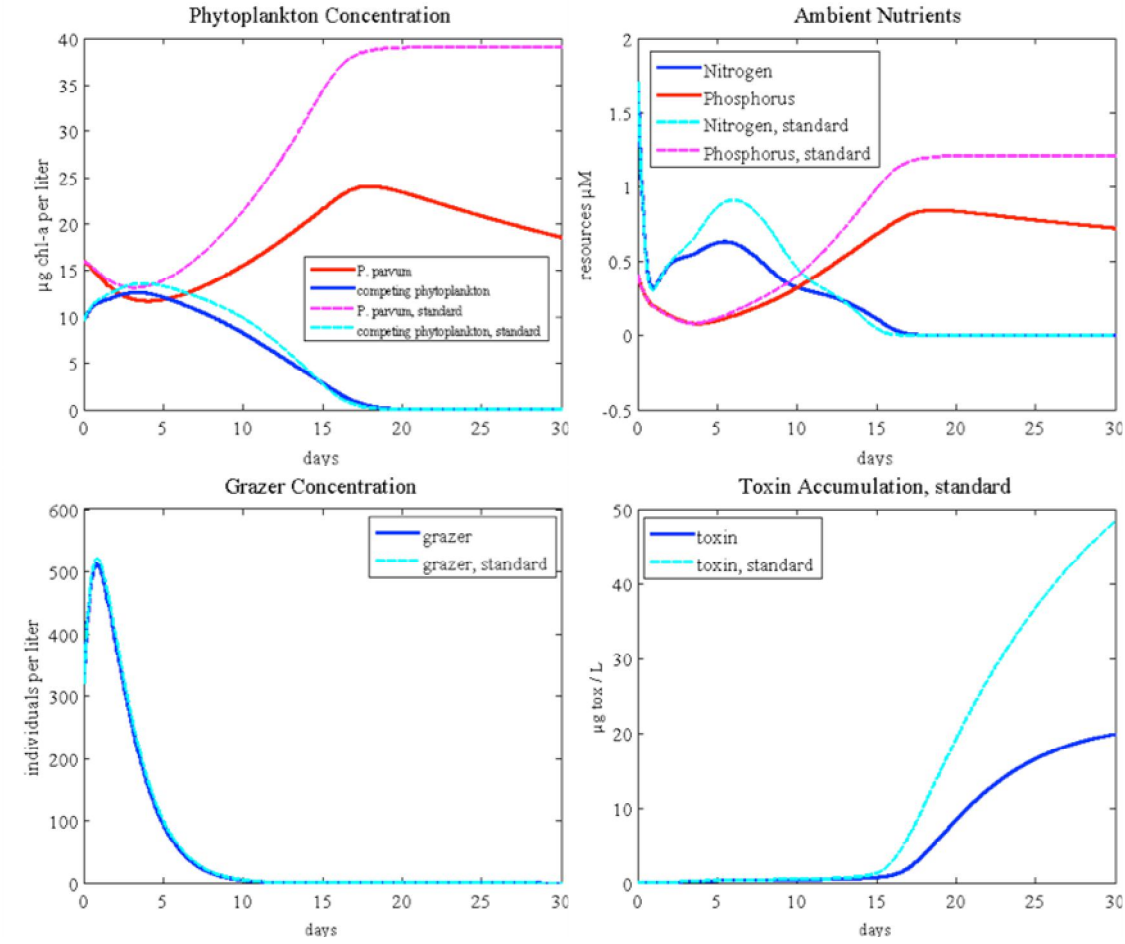

Figure 17. Model output with a 0-day pulse (continuous inflow) and a dilution rate of 0.03/day compared with the standard case (dashed line)

continuous inflow scenario with a dilution rate of 0.03/day, a typical daily dilution rate in wet conditions, not including very high inflow events, as reported in Grover et al. (2010) for Lake Granbury. Figures 18-22 show increases in periodicity in 3-day increments (Figure 18 has a 3-day pulse, Figure 19 a 6-day pulse, etc) with Figure 22 having a single pulsing event at day 15.

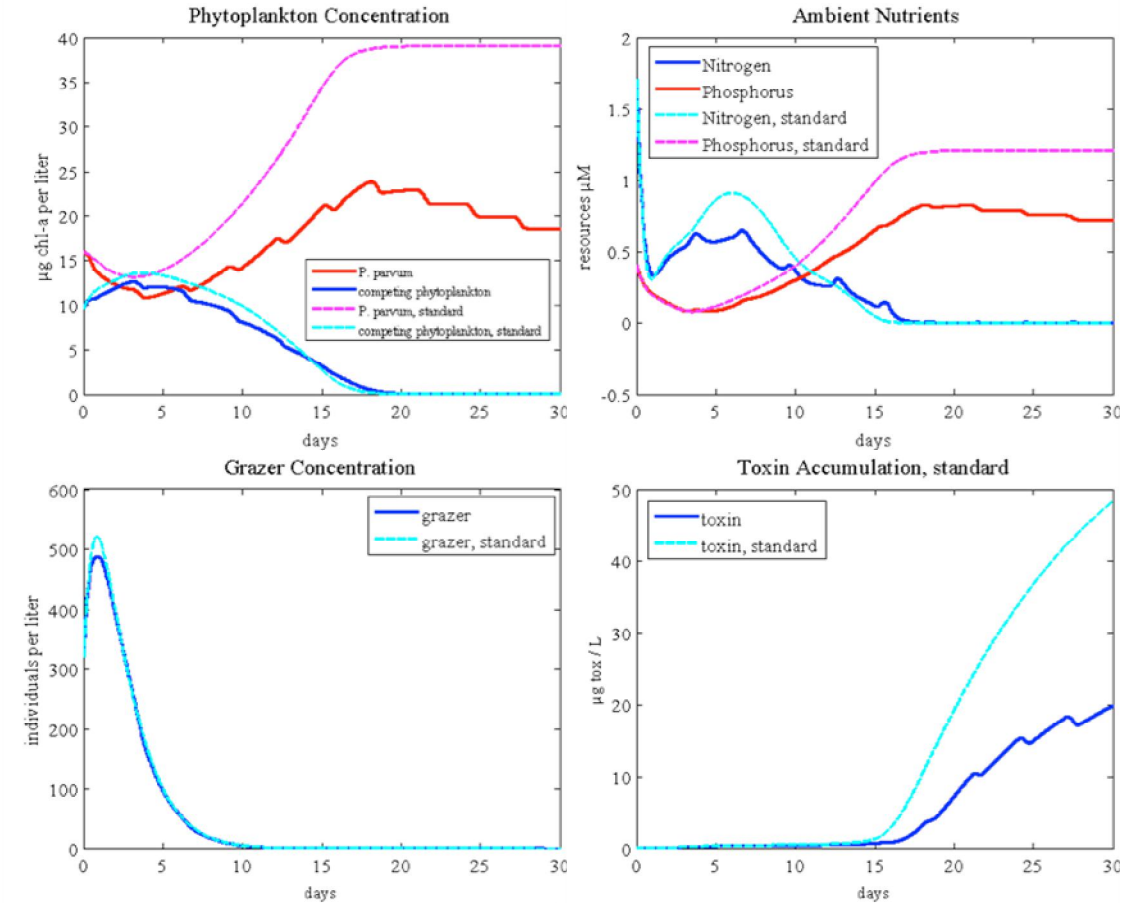

Figure 18. Model output with a 3-day pulse and a dilution rate of 0.03/day compared with the standard case (dashed line)

The simulation with a continuous flow provides expected results: the competing phytoplankton maintain a similar growth pattern as in the standard case but with a slightly reduced density, *P. parvum*'s density is greatly reduced, does not increase to reach a saturating density, snd grazer density does not change significantly from the

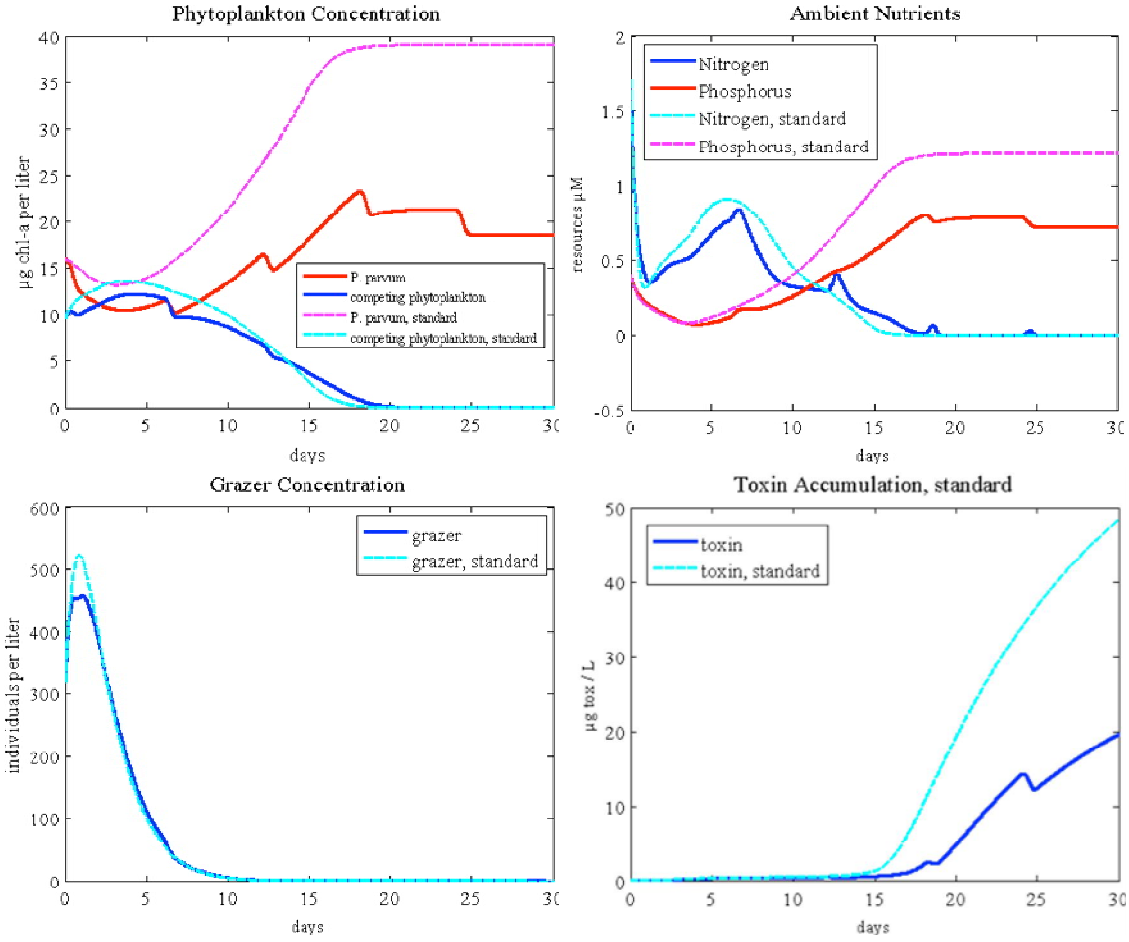

Figure 19. Model output with a 6-day pulse and a dilution rate of 0.03/day compared with the standard case (dashed line)

standard case. *P. parvum* does grow to a peak density of around 25 g-chlorophyll *a* then gradually declines while in the standard case, *P. parvum* increases to a saturating density of almost 40 g-chlorophyll *a*. With the reduction in the density of *P. parvum*, the toxin does not accumulate to the same concentration seen in the standard case.

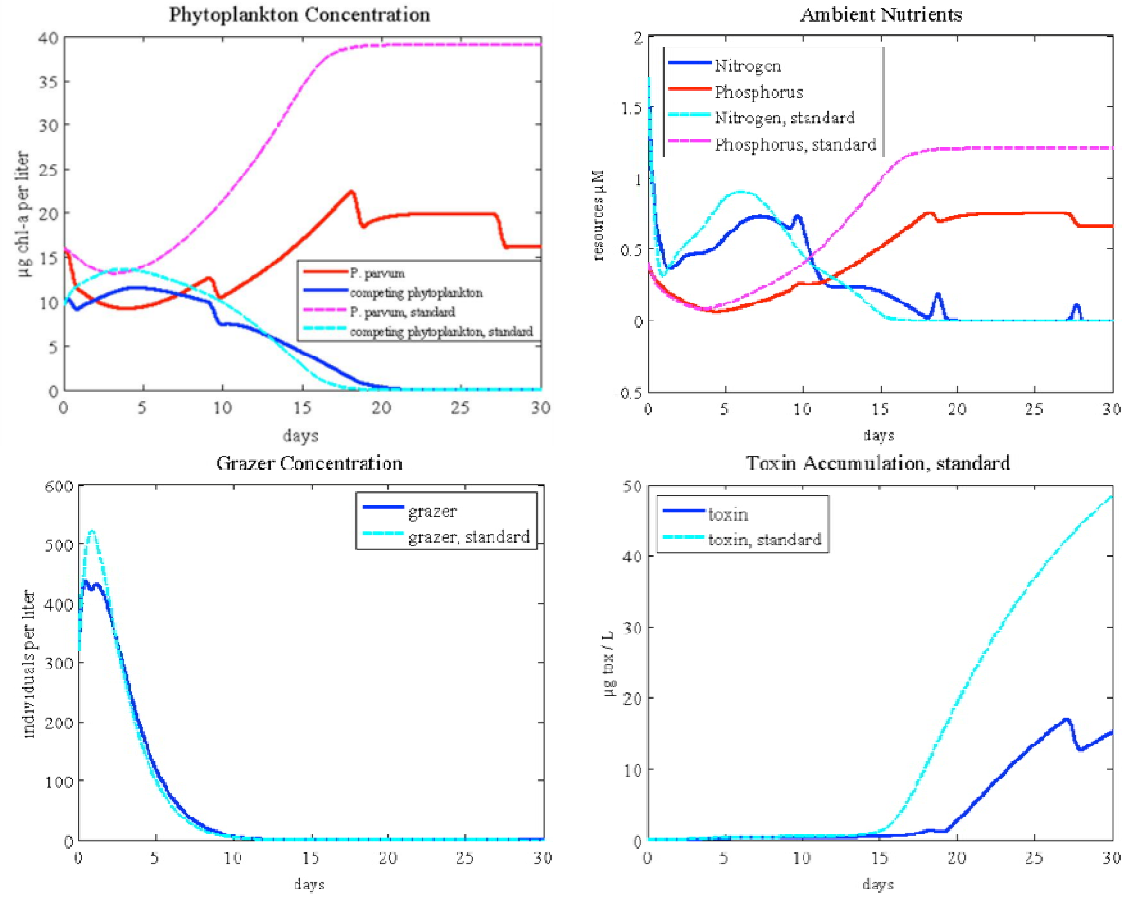

Figure 20. Model output with a 9-day pulse and a dilution rate of 0.03/day compared with the standard case (dashed line)

In all simulations testing pulsing events (Figures 18-22), *P. parvum* remains dominant at the end of the 30 day simulation though at various densities. *P. parvum* density does not reach a density higher than that of either the standard or continuous inflow simulation (Figure 17). The toxin accumulation is significantly lower, never reaching half of the standard case accumulation concentration but still prevents the

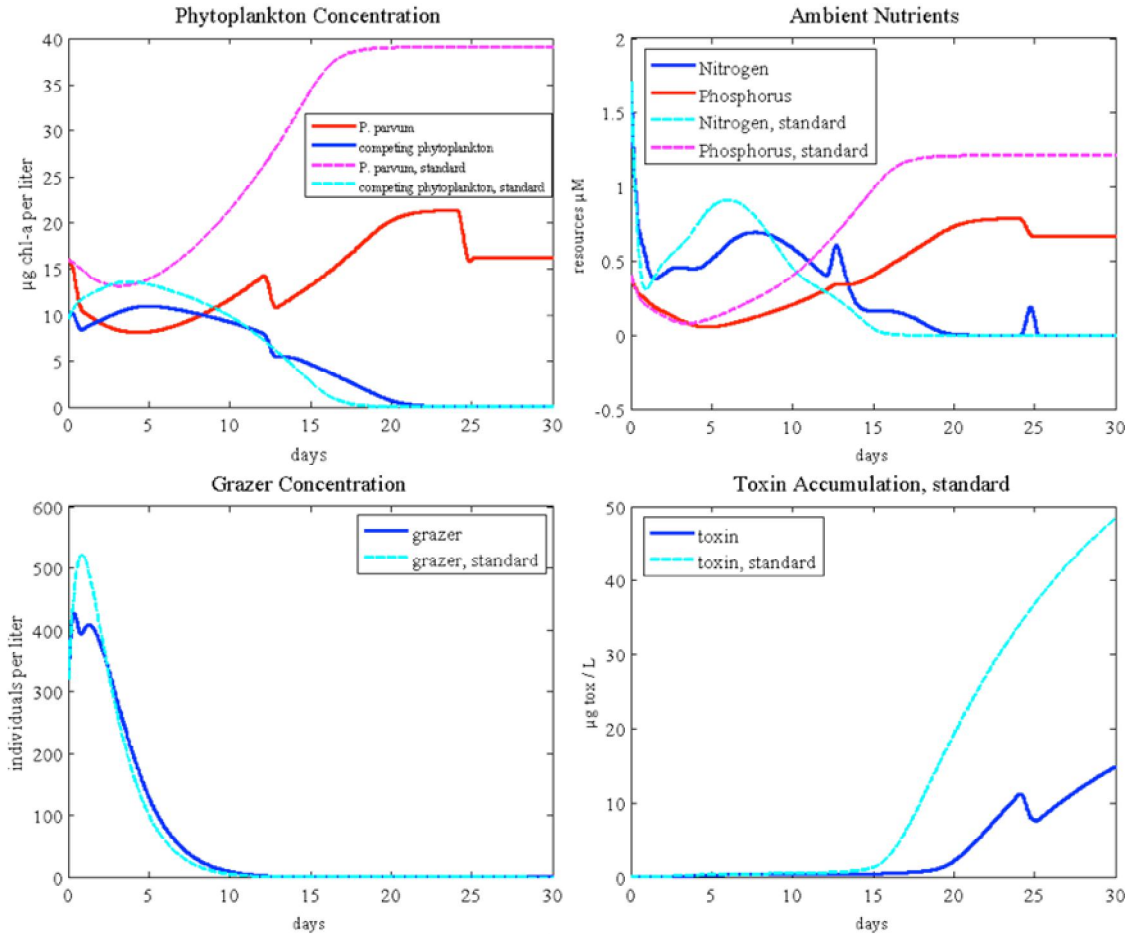

Figure 21. Model output with a 12-day pulse and a dilution rate of 0.03/day compared with the standard case (dashed line)

grazer population from increased feeding upon the phytoplankton. Grazer concentrations decrease slowly with the varied periodicities and remain similar in density to the standard case. The competing phytoplankton density peaks are not as high as in the standard case, and as pulses become less frequent, the competing phytoplankton experience a greater decrease in population density. Any inclusion of pulsing, however allows the competing phytoplankton to remain in the system longer.

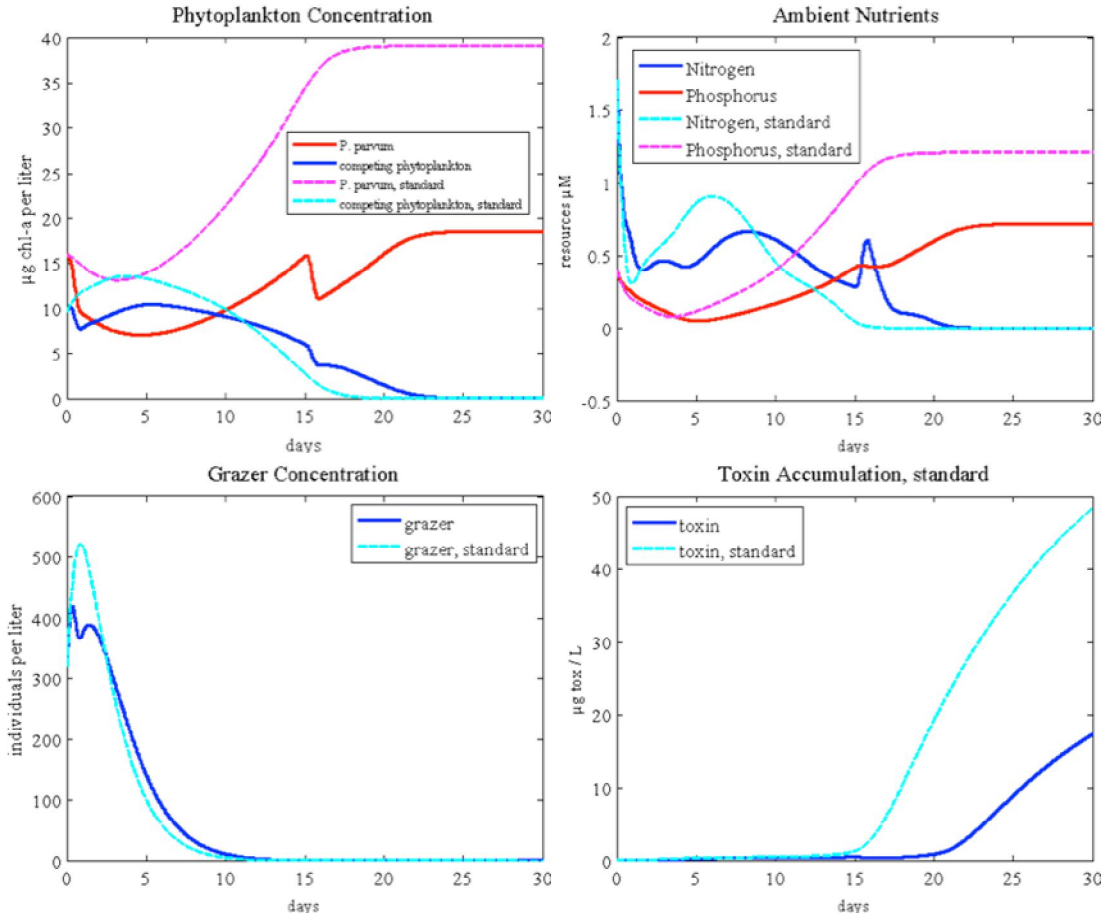

Figure 22. Model output with a 15-day pulse and a dilution rate of 0.03/day compared with the standard case (dashed line)

Testing the same pulsing periodicities at higher dilution rates generate greater density changes than with a lower dilution rate. Figures 23-28 illustrate pulsing periodicity but with a higher dilution rate of 0.09/day. This dilution rate remains lower than the maximum specific growth rates of *P. parvum* and the competing phytoplankton, but increases flow through the system.

Without a pulse and only a 0.09/day continuous inflow rate, both phytoplankton densities are decreased compared to the standard case (Figure 23). The density of *P.*

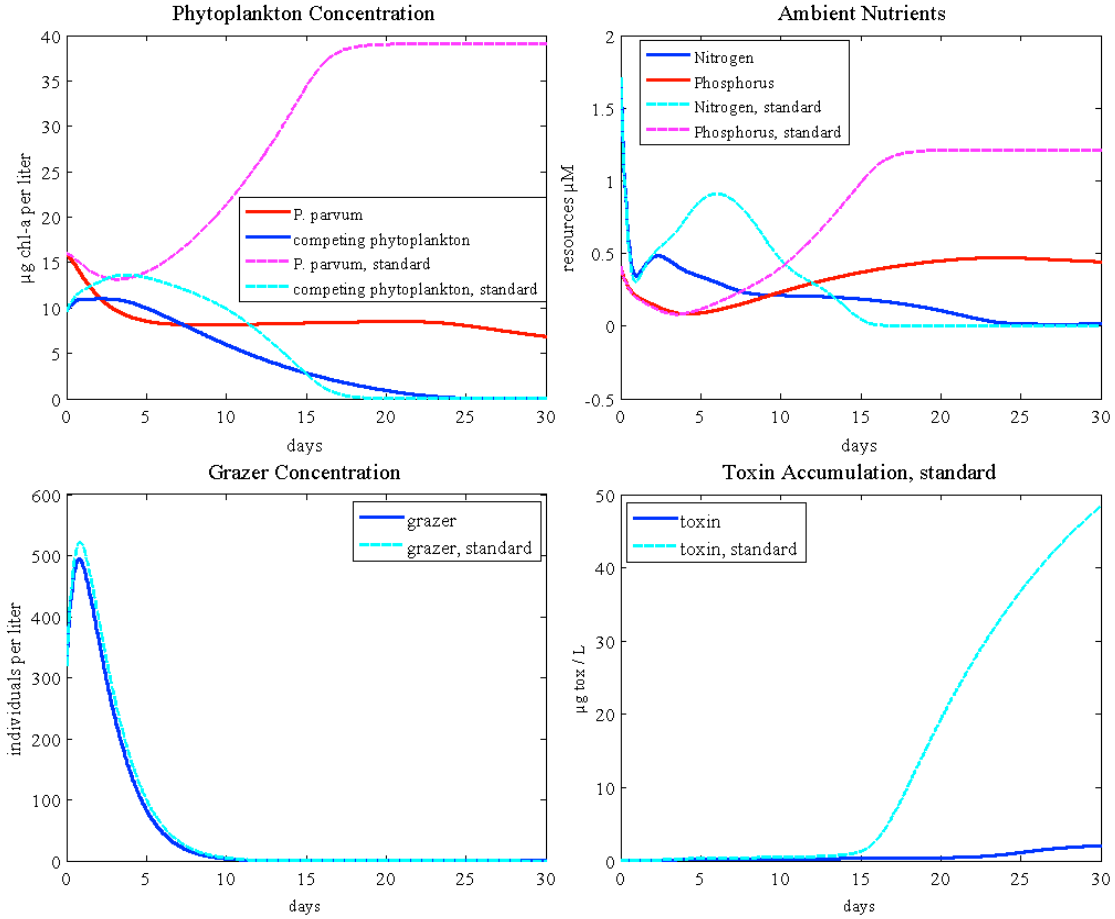

Figure 23. Model output with a 0-day pulse and a dilution rate of 0.09/day compared with the standard case (dashed line)

parvum does not reach a density higher than its initial value, but maintains a density slightly less than 10 g-chlorophyll *a* throughout most of the simulation, decreasing after day 25. Toxin accumulation is minimal and increases in concentration towards the end of the simulation after day 25 when *P. parvum* begins to decline in density. The competing phytoplankton experience only a slight increase in their density, peaking at day 5, then gradually decreases throughout the remainder of the simulation. The grazer population does not vary much from the standard case.

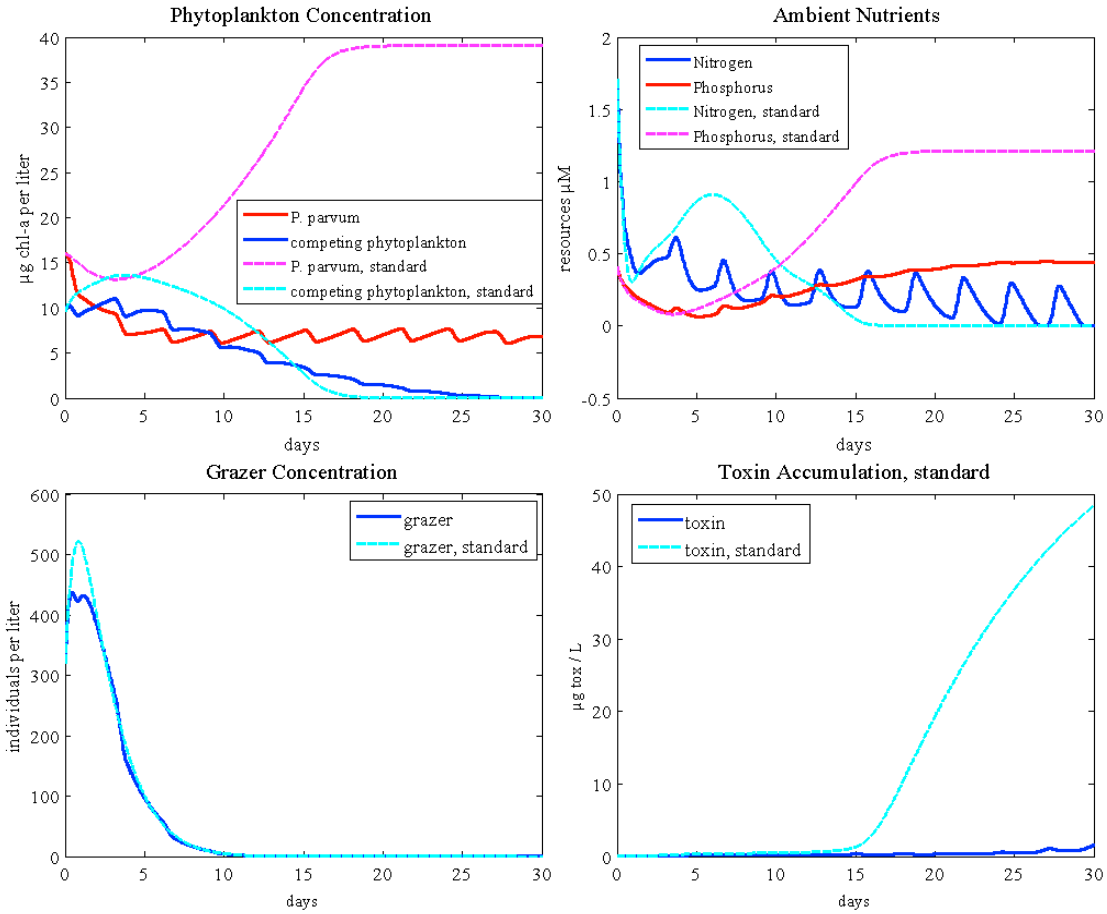

Figure 24. Model output with a 3-day pulse and a dilution rate of 0.09/day compared with the standard case (dashed line)

Adding pulses every third and sixth day (Figures 24 and 25) decreases the density of *P. parvum* but still maintains dominance in the system. In both simulations the toxin does not accumulate much and only does so after day 25. The competing phytoplankton densities lasts throughout the duration of both simulations. Zooplankton density peaks at the start of the simulation and declines until eliminated before day 15, but never reaches the same peak density as the standard case.

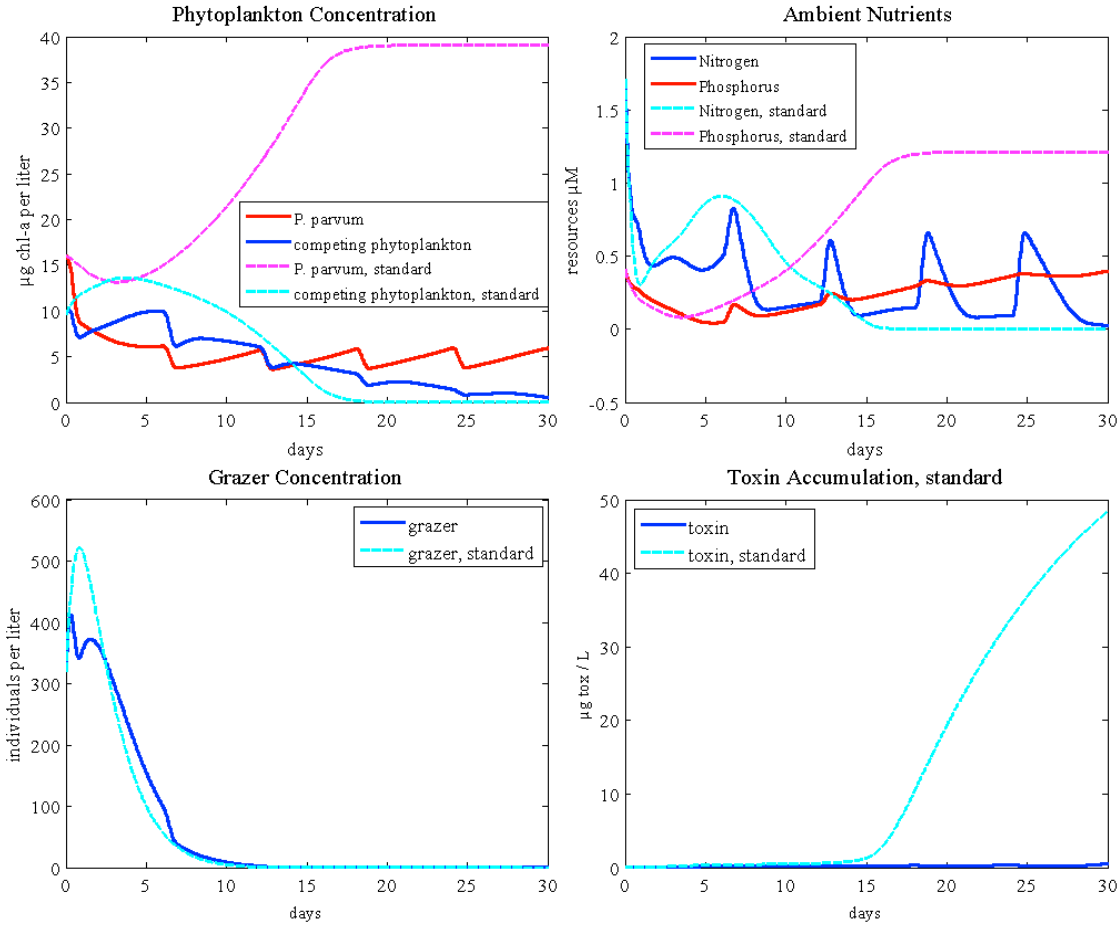

Figure 25. Model output with a 6-day pulse and a dilution rate of 0.09/day compared with the standard case (dashed line)

When the pulses occur every 9-days (Figure 26), the competing phytoplankton exceed the density of *P. parvum*. *P. parvum* density drops at the start of the simulation and sustains a low density throughout while the competing phytoplankton peak at day 10 and maintain dominance throughout the simulation. Grazer density does not peak as high as in the standard case, but remains in the system longer after peaking at day 4. Toxin accumulation is slight throughout the simulation.

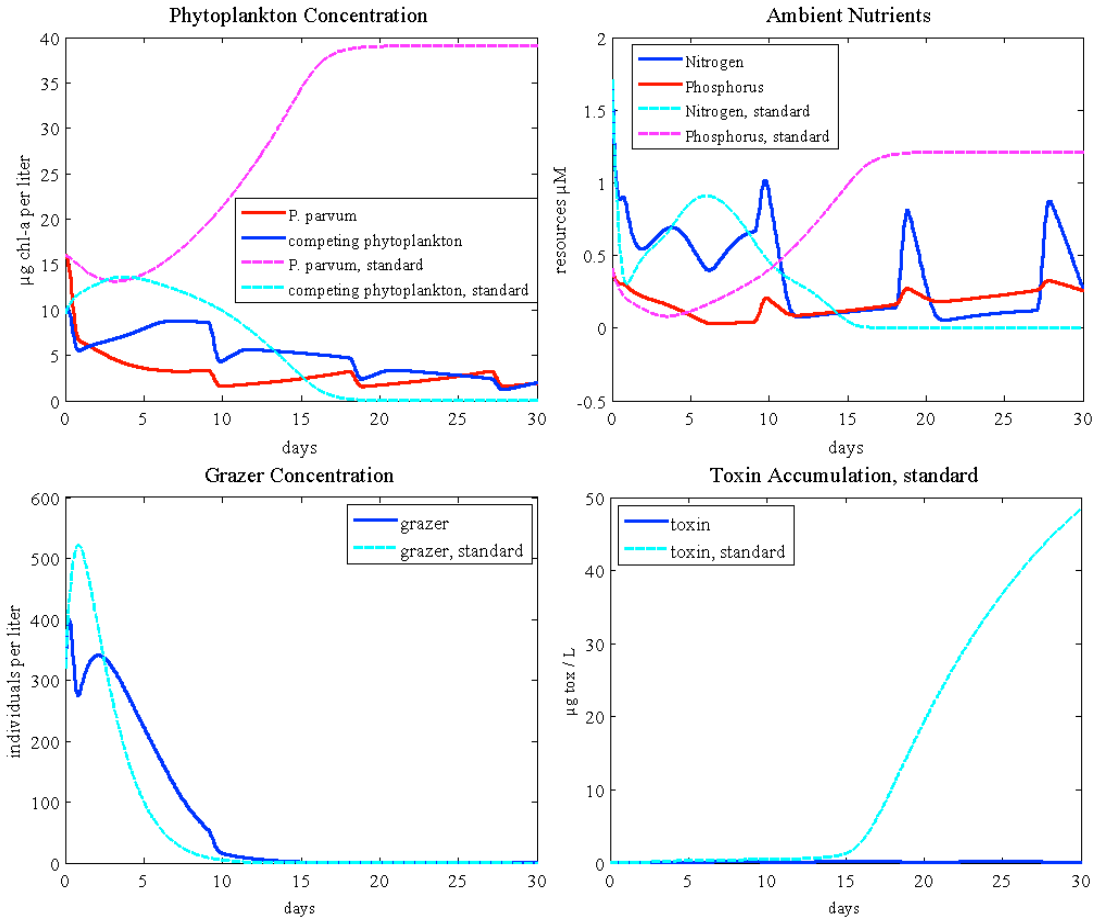

Figure 26. Model output with a 9-day pulse and a dilution rate of 0.09/day compared with the standard case (dashed line)

Pulses less frequent than every 9 days are shown in Figures 27 and 28, illustrating a 12-day pulse and a 15-day pulse, respectively. In both simulations, the density of *P. parvum* declines to near 0 at or before day 10 while the competing phytoplankton gain dominance. In Figure 27, the competing phytoplankton last throughout the simulation while with a single pulse at day 15 (Figure 28), the grazer population eliminates the phytoplankton community entirely. Zooplankton populations

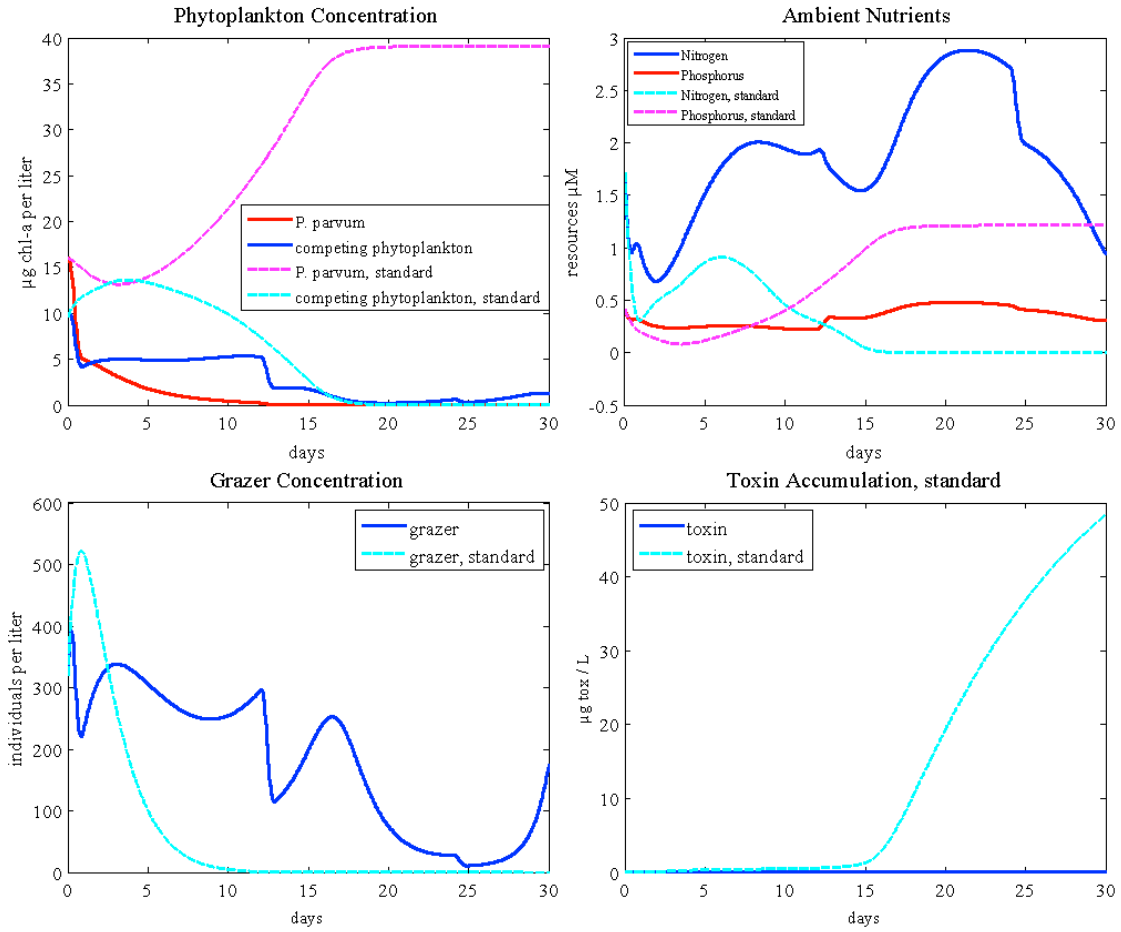

Figure 27. Model output with a 12-day pulse and a dilution rate of 0.09/day compared with the standard case (dashed line)

are significantly higher than in the standard case, present throughout the duration of the simulation due to the lack of toxin in the system. The grazer density responds to the pulsing events and the growth patterns of the phytoplankton resulting in more activity and density changes than in any previous simulation. Even while *P. parvum* is present in the system, the toxin does not accumulate to noticeable levels, allowing the grazers and the competing phytoplankton to remain in the system.

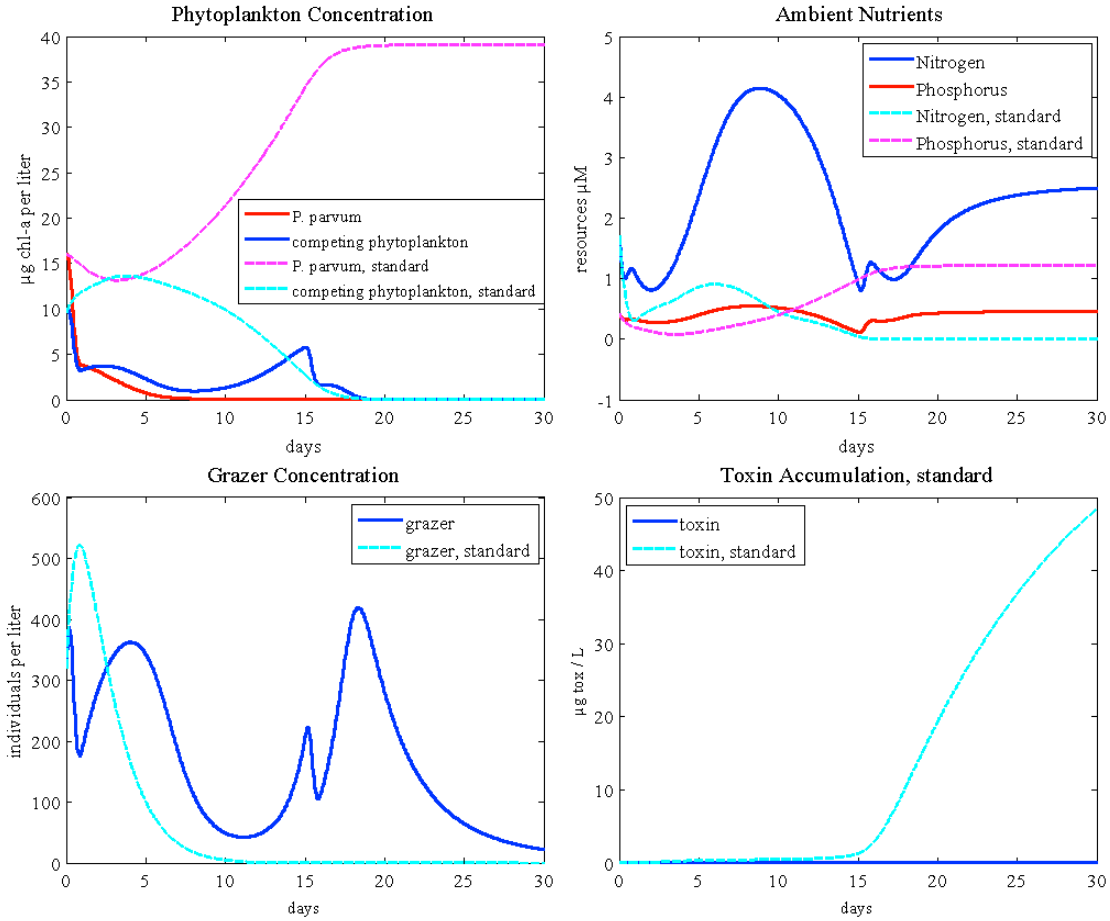

Figure 28. Model output with a 12-day pulse and a dilution rate of 0.09/day compared with the standard case (dashed line)

3.3.3 Combined frequency and magnitude of inflows

Combining pulsing and inflow magnitudes disrupts the system further. Figure 29 shows the resulting cumulative densities of the three plankton groups and the cumulative toxin concentration for simulations with both dilution rates and pulsing. Increases in both dilution rate and the time between pulses resulted in the lowest cumulative density of *P. parvum*. Varying the dilution rate appears to have a greater impact on golden alga's resulting cumulative density, causing a quicker decline in population density throughout the simulations. Accumulating toxin concentrations parallel the decreases seen in the density of *P. parvum*, decreasing at similar rates. This would be expected since toxin will not be produced without *P. parvum* being present. The density of *P. parvum* and toxin concentration are the most affected variables resulting from the hydrologic events, experiencing the greatest declines in concentrations.

The competing phytoplankton density remains relatively unchanged throughout most simulations of both pulsed inflows and varying dilution rates. When the dilution rates are high and more time is allowed between pulses, the competing phytoplankton experiences its greatest density followed by sharp declines in density at the maximum

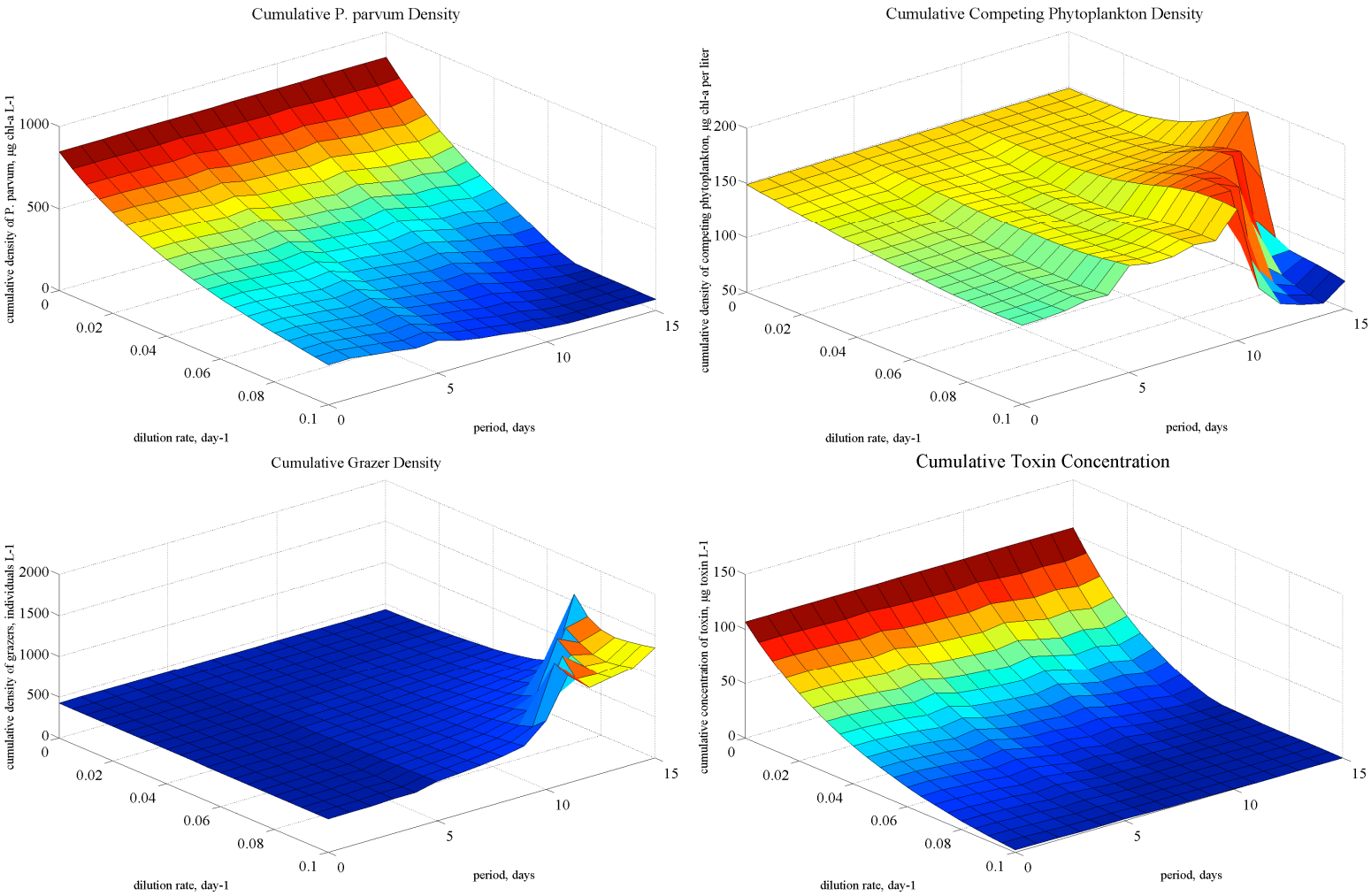

Figure 29. Plots varying the magnitude and periodicity of inflows using the standard case nutrient concentration

pulsing periodicity and dilution rate. This decline coincides with an increase in the grazer population and a sharp decline in *P. parvum* density. Before the spike, the grazer density remains low and unchanged throughout the majority of the simulations. With the removal of toxins from increased periodicity and dilution rates and a lack of production by the low-density *P. parvum*, the grazers experience an increase in population density, feeding on the competing phytoplankton and eliminating *P. parvum* concentrations. Figures 30 and 31 investigate further this region of low *P. parvum* density and the higher densities of the other two plankton groups. Figure 30 shows the model output with a 0.1/day dilution rate and a pulsing periodicity of 10 days compared against the standard case. The competing phytoplankton are dominant throughout the majority of the simulation, declining from the grazers' presence. Once *P. parvum* is removed from the system after day 10, the phytoplankton group does not reemerge in the system leading to neither toxin production nor accumulation. The grazer population does not exceed its initial density, but remains in the system until day 20, generating a higher density than seen in the standard case.

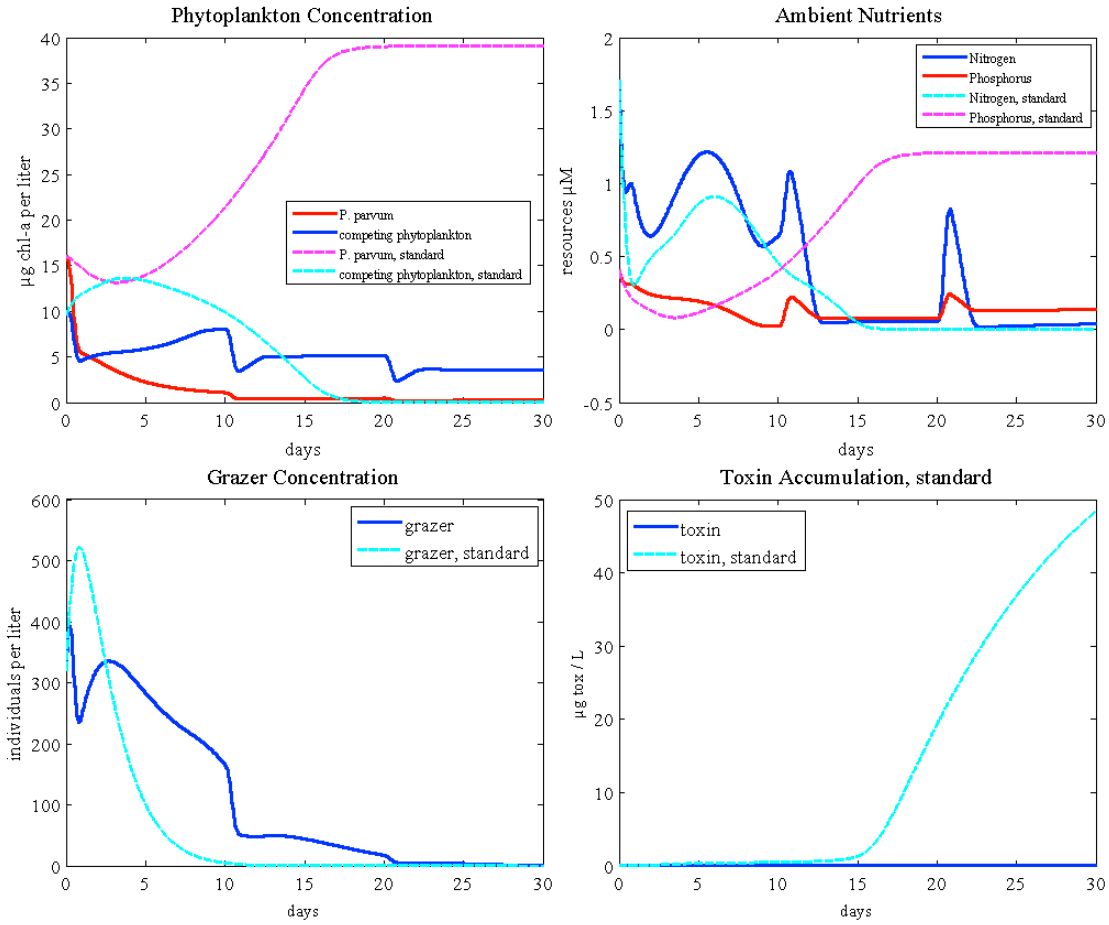

Figure 30. Model output with a 10-day pulse and a dilution rate of 0.1/day compared with the standard case (dashed line)

At the highest periodicity and inflow rate, grazer density experiences two density peaks after an initial spike while the two phytoplankton groups experience their greatest declines in density (Figure 31). The simulation shown has a periodicity of 15 days, meaning a single pulse occurs in the system at day 15, and corresponds with the bottom right-most section area seen in Figure 29 at a dilution rate of 0.1/day. In this simulation, the grazer density responds to the lack of *P. parvum* toxins, feeding on the competing phytoplankton until the food source is depleted by day 20. The competing phytoplankton maintain dominance of the system, but do not generate a high population density throughout the system. Toxin accumulation is low as *P. parvum* density is removed from the system by day 5.

The highest cumulative density of *P. parvum* is seen in simulations without any dilution or pulsing, the same cumulative density as in the standard case. This peak density exceeds the standard case densities of the other two plankton groups and allows for the greatest density decreases to be observed by this plankton. In other words, *P. parvum* density was highest in the standard case, and therefore has more density to lose with fluctuations in hydrology.

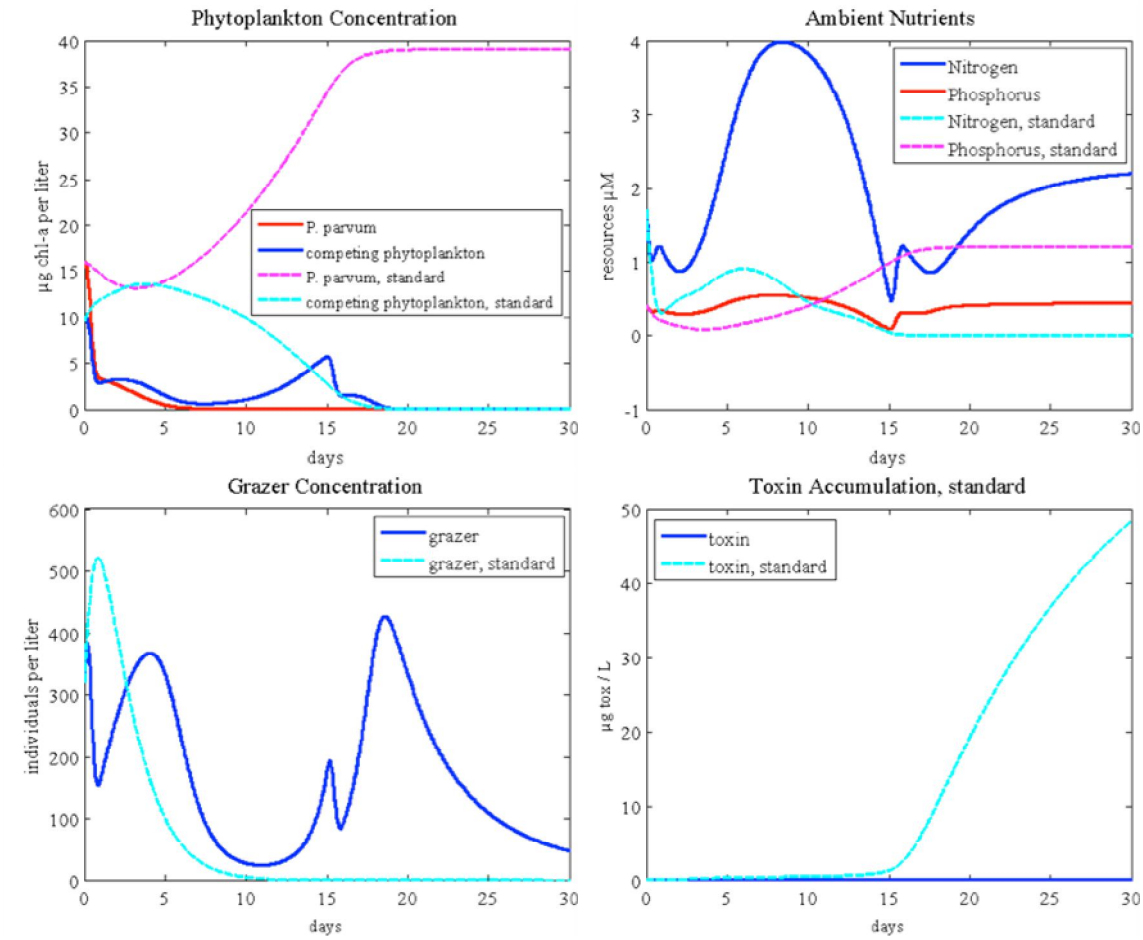

Figure 31. Model output with a 15-day pulse and a dilution rate of 0.1/day compared with the standard case (dashed line)

3.3.4 Nutrient influences

3.3.4.1 High river flow nutrient concentration

To test potential management strategies, pulsing and dilution rates were tested with different nutrient concentrations. Figure 32 shows the cumulative densities when varying periodicities and dilution rates using nutrient concentrations representative of high flow conditions of the Brazos River, entering Lake Granbury, 30.17μM N and 0.23μM P. This nutrient concentration was taken from a sampling station located at the top of the reservoir, above the deep river channel in Lake Granbury at the time of the high flushing event that eliminated the *P. parvum* bloom in April 2007. When compared to the standard case, the high-flow nutrient concentration produces lower densities in the grazers and competing phytoplankton and a much higher *P. parvum* density (Figure 33). *P. parvum* reaches a higher saturating density later in the simulation, almost three times as high as the standard case. The competing phytoplankton maintain presence in the system longer than in the standard case, but are removed shortly after day 25. Grazer

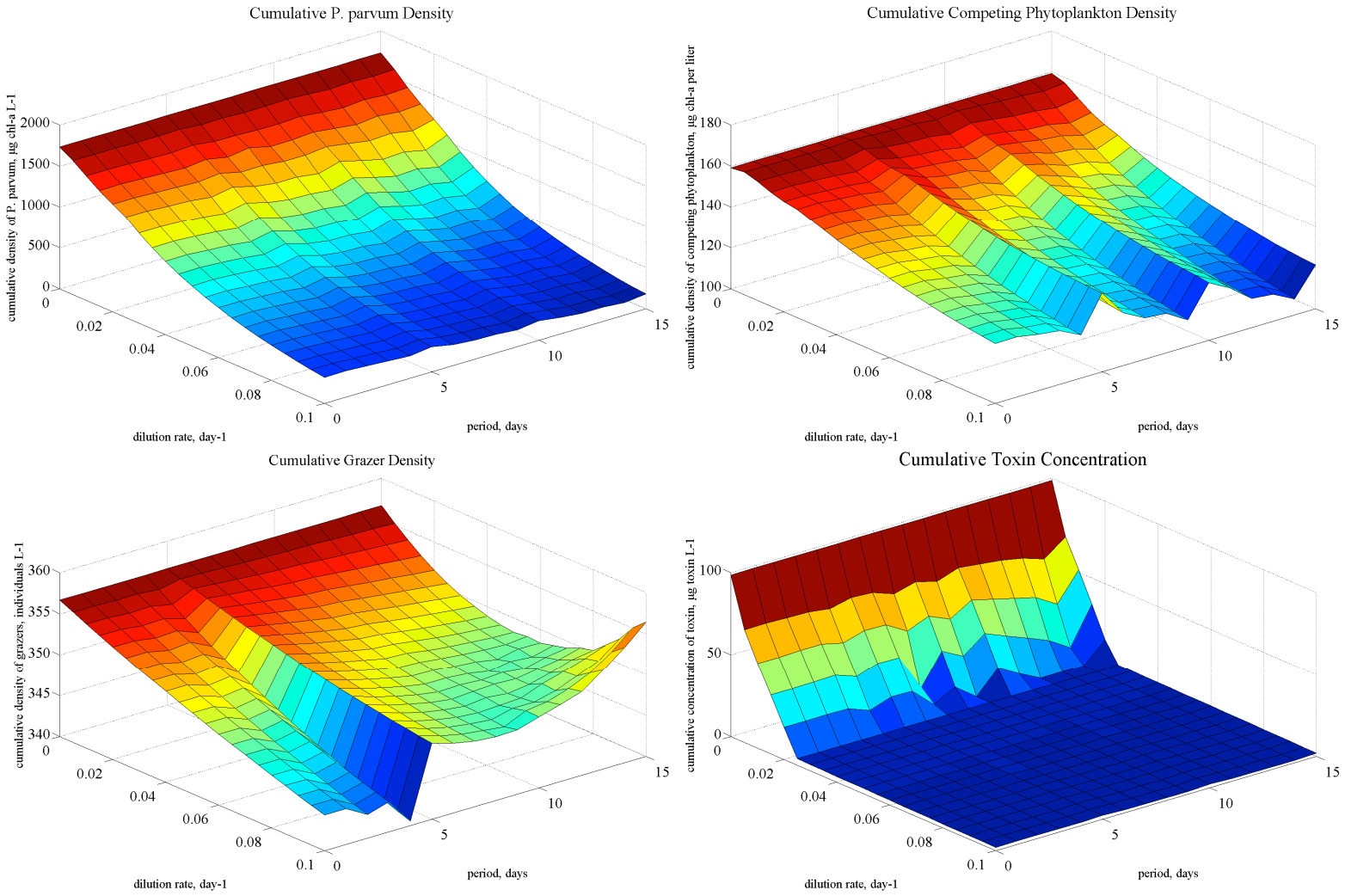

Figure 32. Model output varying periodicity and dilution rates and using a nutrient composition representative of high flow conditions of the Brazos River in April 2007

density mirrors that seen in the standard case, but at a lower peak and are removed quicker from the system. Toxin accumulation is slight until before day 25 when *P. parvum* reaches its peak density. At this point, the toxin concentration rises higher than seen in the standard case.

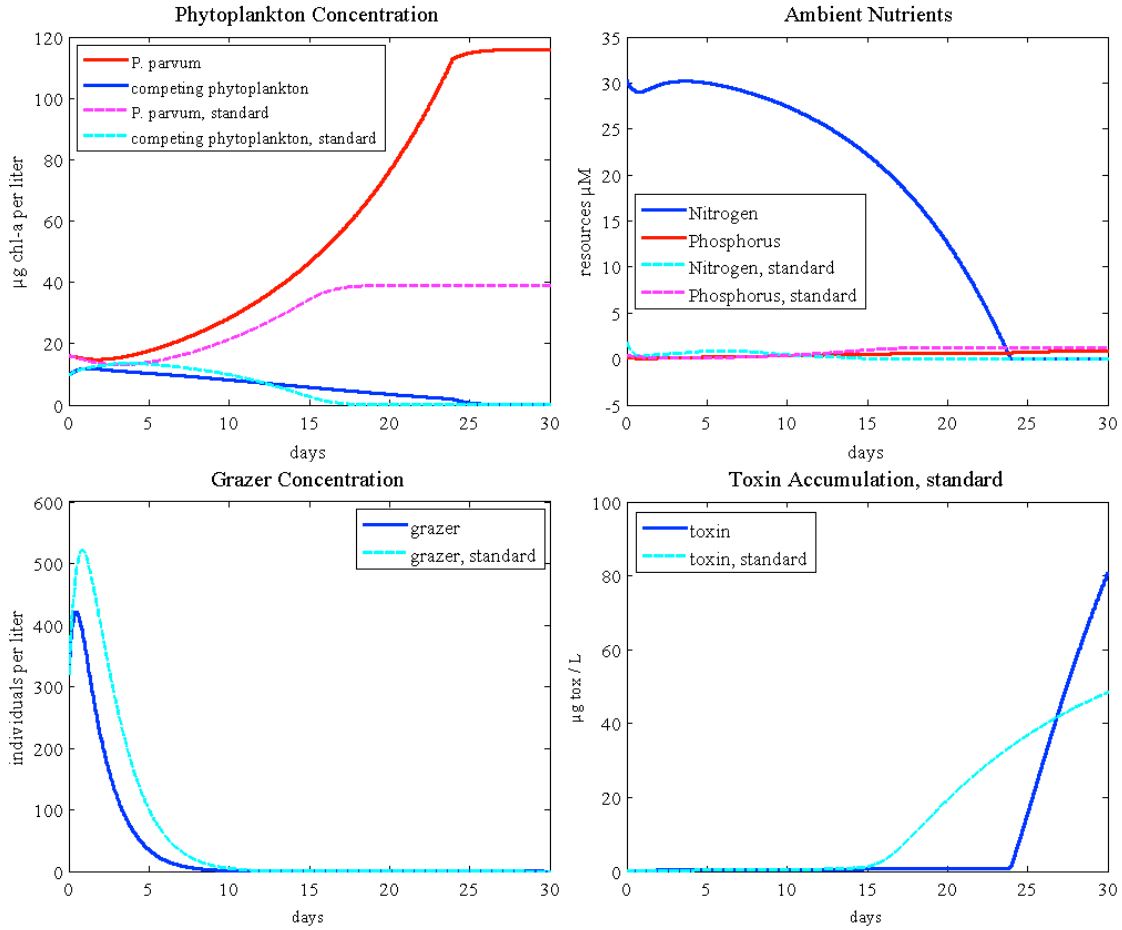

Figure 33. Model output comparing the nutrient concentration representative of high flow of the Brazos River with the standard case (dashed lines)

With the introduction of hydrological influences, both phytoplankton concentrations decline as the period and the dilution rates are increased (Figure 32). The cumulative density of *P. parvum* gradually declines, with more influence on the resulting density coming from changes in the dilution rate than changes in the periodicity. The competing phytoplankton density declines with the increased dilution, but experiences higher concentrations when pulsed every 5, 10, and15 days. These spikes in cumulative density are still lower than the standard case simulations. The grazer concentration declines throughout most of the simulations, but peaks with simulations run with a high period and dilution rate. With frequent pulses, or a low periodicity, the grazers experience more decline in density than with less frequent pulses. Pulses every 4 days resulted in the greatest declines of density. Toxin accumulation drops significantly as the dilution rate increases with low concentrations of toxin remaining in the system in simulations with dilution rates higher than 0.03/day. The lack of toxin accumulating in the system allows the grazers to feed upon the phytoplankton groups remaining in the system at a quick rate, increasing its density, as with the lower nutrient concentration.

The next two figures highlight simulations run with the high-flownutrient concentration from the Brazos River (Figures 34 and 35) compared with the same nutrient concentration with the inclusion of hydrological effects. Figure 34 illustrates model output when a 15-day pulse and a 0.1/day dilution rate are introduced. None of the three plankton groups exceed their initial densities. The grazer population lasts a similar amount of time as the simulation run without any hydrology but has a greater cumulative density, not experiencing the sharp decline at the start. This simulation

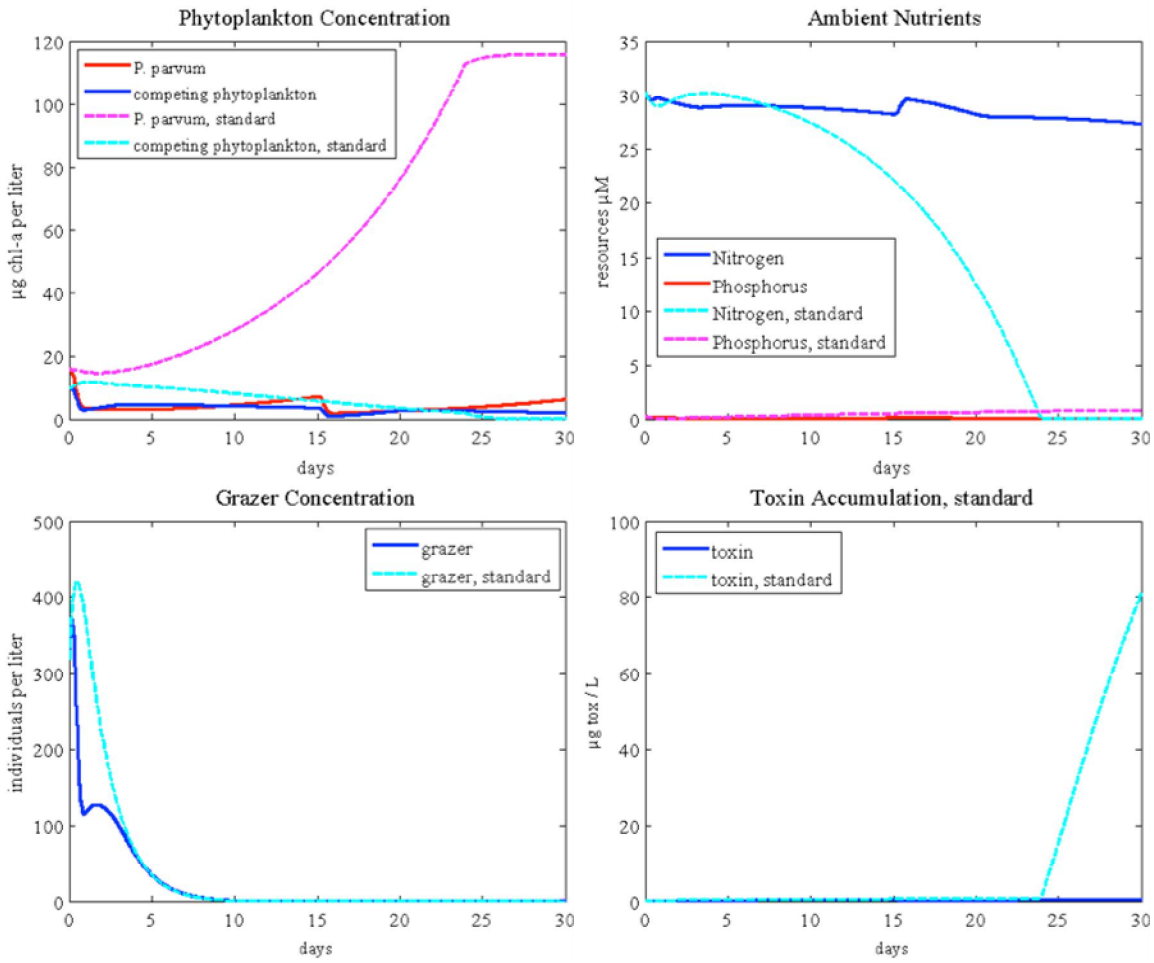

Figure 34. Model output comparing the standard nutrient concentration representing high flow of the Brazos River (dashed lines) with a simulation with a 15-day pulse and a 0.1/day dilution rate at the same nutrient concentration

illustrates the grazer density peak seen at the highest dilution rate and most infrequent pulsing strategy in Figure 32. The competing phytoplankton compete throughout the simulation with *P. parvum*, but are not dominant nor sustain a high density. There is little to no toxin accumulation despite *P. parvum* being dominant at the conclusion of the simulation. *P. parvum* density is low throughout the simulation, barely maintaining dominance over the competing phytoplankton.

Figure 35 shows the model simulation when the same nutrient concentration is run with a 5 day pulse and a 0.1/day dilution rate. This simulation represents the spike in the competing phytoplankton density and the increase in density by the grazers seen in Figure 32. The competing phytoplankton density sustains throughout the 30-day simulation but does not experience substantial growth. The density of *P. parvum* responds to the pulsing shown by the sudden drops in density, but maintains dominance of the system throughout the simulation. The grazer population declines suddenly and does not experience a large increase in density accumulation at the start of the simulation. Toxin does not accumulate through the simulation though it begins to accumulate at the end of the 30 days.

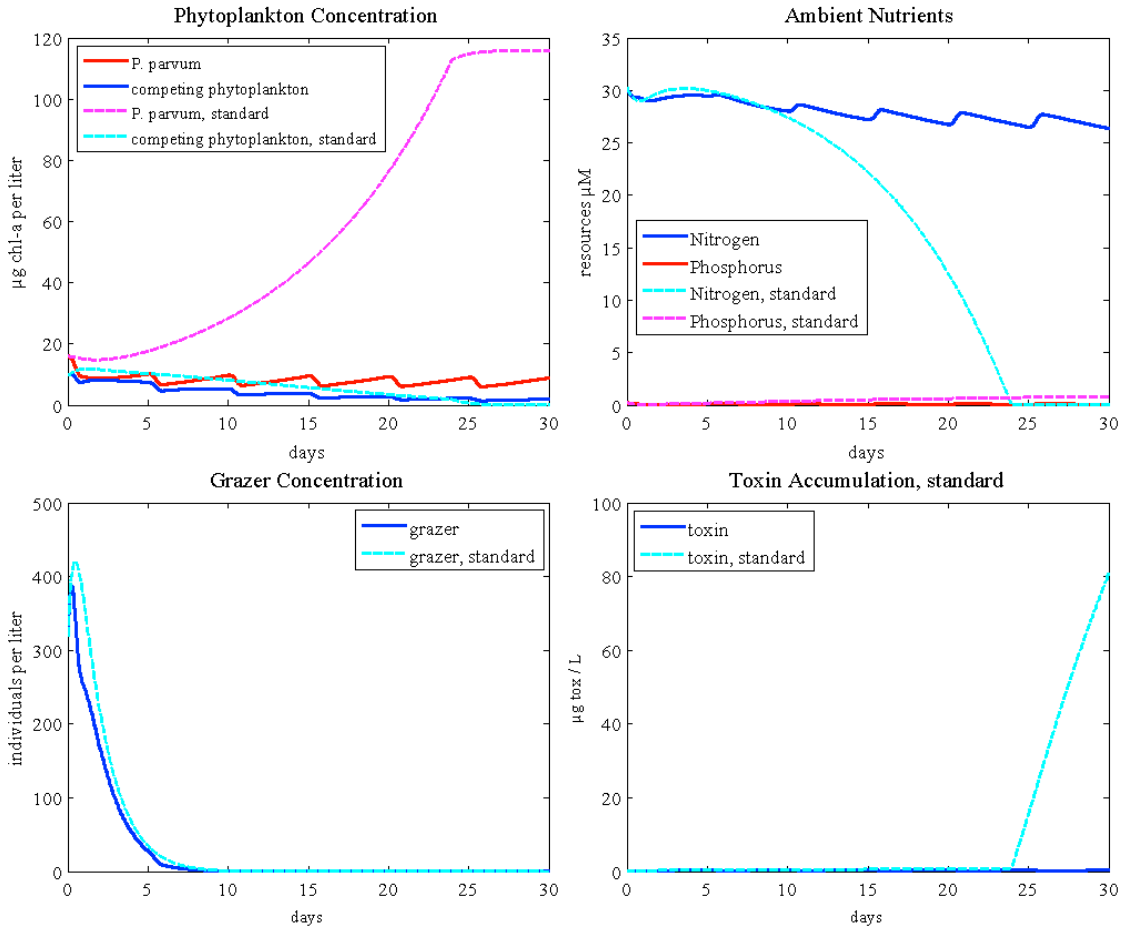

Figure 35. Model output comparing the standard nutrient concentration representing high flow of the Brazos River (dashed lines) with a simulation with a 5-day pulse and a 0.1/day dilution rate at the same nutrient concentration

3.3.4.2 Bottom source waters

As with the above explored nutrient concentration seen upstream of Lake Granbury, using bottom-water generates decreases in the density of *P. parvum.* Figure 36 shows the varying of periodicity and dilution rates using a nutrient composition lower than the high river flow concentration, representative of bottom waters of Lake Granbury, 13.97 μM N and 0.09 μM P. This nutrient composition is from a well-mixed, deep-water station at the bottom of Lake Granbury from January 2007.

As with the high river flow nutrient concentration, the cumulative density of *P. parvum* declines gradually as the period and dilution rates increase. The decrease is great however, a drop in density of over 2 magnitudes, and is the largest change in density compared with the other two plankton groups. The competing phytoplankton experience a greater decline in density when the dilution rate is increased than with less frequent pulsing events. The lowest phytoplankton densities occur with higher dilution rates and more time between pulses. Unlike simulations run using other nutrient

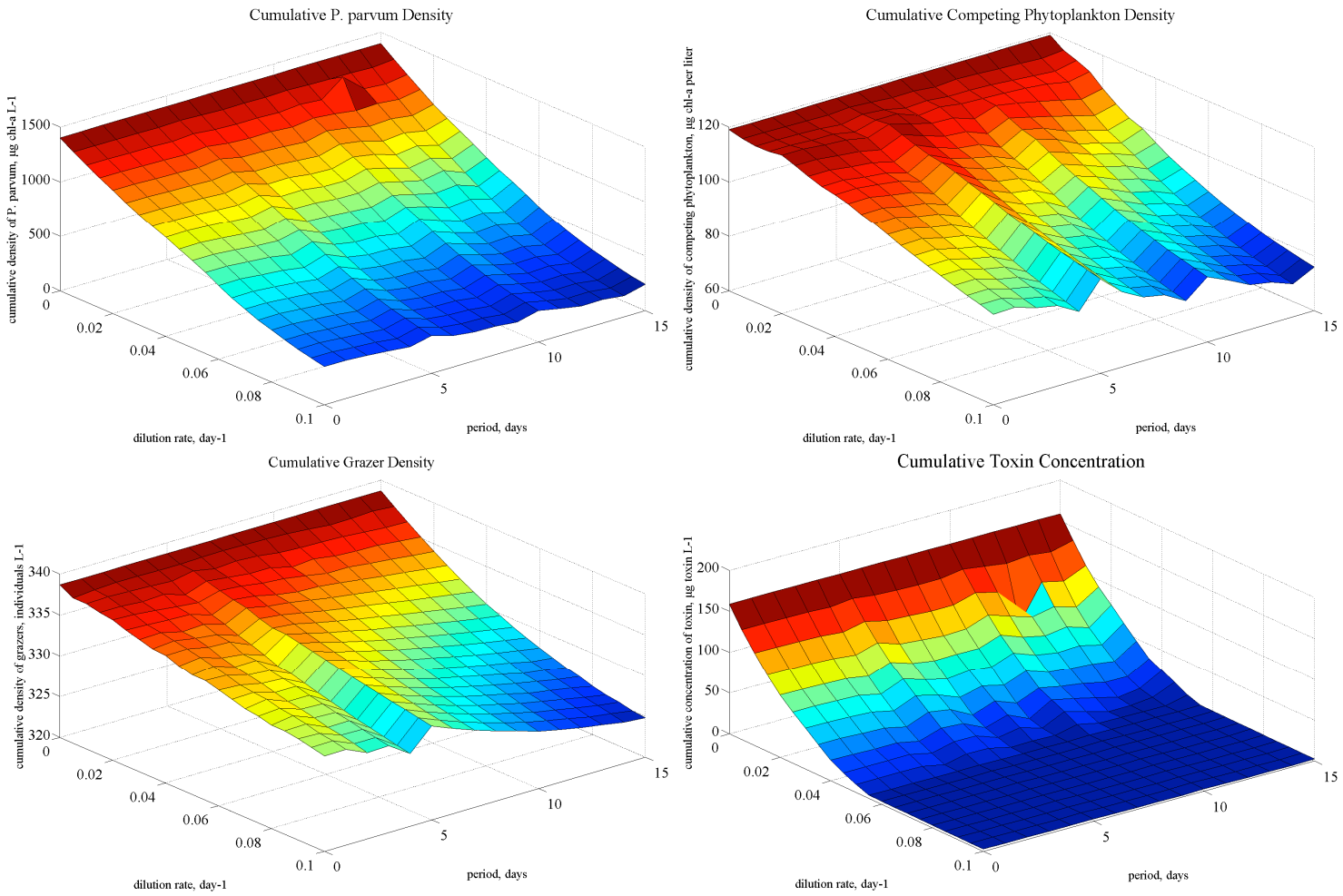

Figure 36. Model output when varying periodicity and dilution rates and using a nutrient composition representative of bottom waters of Lake Granbury

concentrations, the grazer density does not respond to the lack of toxin and does not increase in density throughout the simulations always resulting in densities lower than simulations without hydrological influences. The grazer population experiences its lowest density at the highest dilution rate and with the greatest amount of time between pulses. The toxin accumulates in the system but is quickly removed as the dilution rates increase. Little toxin is calculated for simulations containing dilution rates higher than 0.06/day.

Figure 37 shows the standard case simulation compared with the bottom-water nutrient concentration without any hydrological influences. The density of *P. parvum* greatly doubles the highest density capable of sustaining the alga population as seen in the standard case, maintaining dominance throughout the simulation. The competing phytoplankton are present in the system longer than in the standard case, but do not survive past day 20. Their density remains low and declining throughout. The grazers do not experience the spike in density seen with the standard case, but instead decline. Toxin accumulation occurs after *P. parvum* reaches its saturating density and exceeds the standard case concentration.

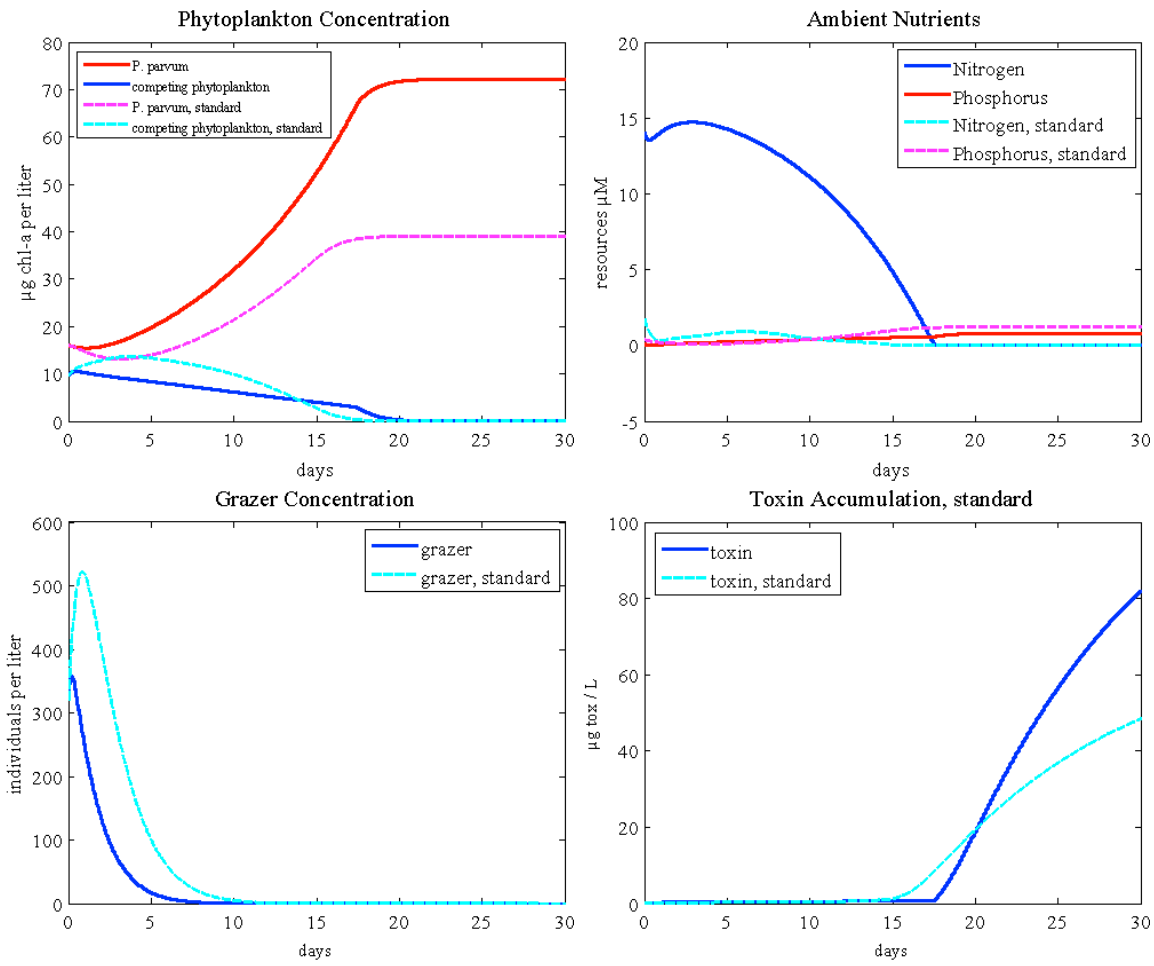

Figure 37. Model output comparing the nutrient concentration representative of bottom waters of Lake Granbury with the standard case (dashed lines)

Figure 38 shows the model output when the bottom water nutrient concentration experiences a 5-day pulse and a 0.1/day dilution rate. The density of *P. parvum* maintains domination throughout the simulation with a recurring pattern reacting to the pulses every 5 days. The competing phytoplankton are removed from the system after 25 days without experiencing densities higher than its initial condition. The grazer density is removed from the system quickly and the toxin does not noticeably accumulate.

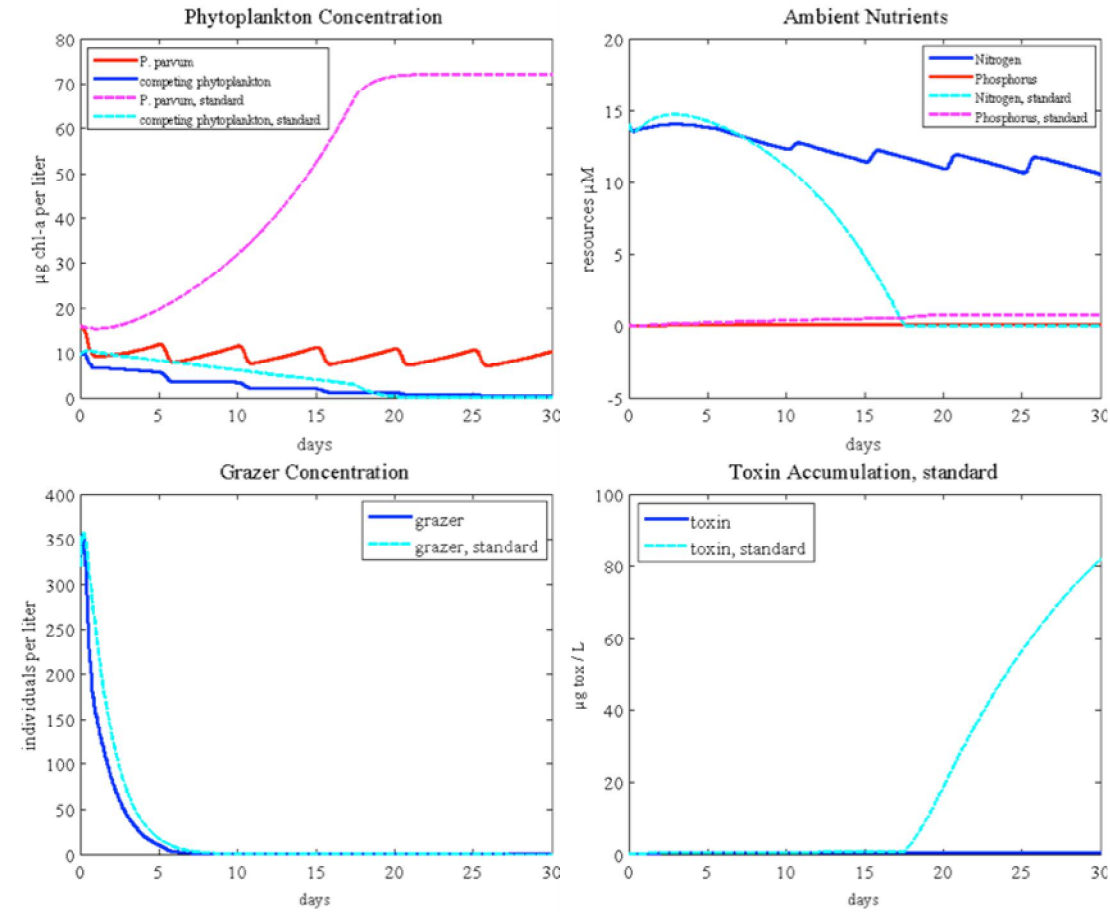

Figure 38. Model output comparing the standard nutrient concentration representing a bottom-water concentration of Lake Granbury (dashed lines) with a simulation with a 5-day pulse and a 0.1/day dilution rate at the same nutrient concentration

4. CONCLUSION

4.1 Sensitivity Analysis

Sensitivity analyses are robust tests that uncover the most influential parameters in simulation studies. The parameter adjustments identified as having high relative sensitivity for this model are valuable as their understanding will lead to further comprehension of the biotic interactions dictating *P. parvum* growth. Influential parameters are defined here as those parameters that, when manipulated, result in the greatest relative difference in the cumulative state variables. Accurate measurements of the parameters highlighted as influential will reduce error in predictive models and generate knowledge on the growth characteristics of *P. parvum* when faced with nutrient-depleted environments.

Changes to nutrient quotas were influential in density changes for all three plankton groups. By changing the cell quotas, ingestion rates of each nutrient by zooplankton are altered, changing their population dynamics, which then affects the model's top-down influence (Gasol et al., 1999; Sherr and Sherr, 2002). For example, changing the nutrient quotas of its prey (Figure 5), at least in regards to nitrogen, alters the population growth rate of grazers because more nitrogen is ingested per unit carbon (Equation 9) (Williams et al., 2008). Similarly, decreasing the carbon cell quota results in greater ingestion of nutrients per unit carbon (Monod, 1950). The resulting increased grazer density leads to an increased feeding rate on phytoplankton. Also, decreasing the nitrogen content of the grazer increases the effect of ingested nitrogen. In other words, the same amount of ingested nitrogen leads to more grazer individuals, which in turn

increases top-down control on phytoplankton (Hessen, 1992). With lower nutrient contents in the phytoplankton, the grazer may become nutrient-limited and not be capable of ingesting enough nutrients for survival.

Top-down control is also emphasized when adjusting the maximum specific grazing rate of the zooplankton. Increasing the maximum specific grazing rate allows the zooplankton to ingest the phytoplankton at such a rate all food sources are depleted from the system (Figure 3). A decrease in the maximum specific grazing rate prevents the zooplankton from ingesting enough nutrients for density growth before the toxin eliminates the group. The presence of a grazer is influential in determining the resulting densities of the two phytoplankton groups. Without a grazer present, the competing phytoplankton face their demise by the toxin accumulating in the system, allowing *P. parvum* to reach a system-saturating density. Knowing the grazer plays an important role in determining the presence of a bloom, accurate calculation of the grazer's maximum specific grazing rate will assist in predictive modeling of a potential *P. parvum* bloom. Just as the increased density of the grazers resulting from the changes in nutrient quotas increased the feeding rate, the increase in feeding rate of the grazers increases the grazer density (Williams, et al., 2008).

Altering the toxin's effect on the grazer population ($mTox_G$) influences the resulting densities of the two phytoplankton groups. Increasing the mortality rate from the toxin's presence, the zooplankton density decreases at a faster pace (Figure 4), the species dying at a faster rate from the toxin's presence. As shown previously, when the grazer presence is removed, the competing phytoplankton density is eliminated shortly

after from the toxin as well. The grazer species' presence prolongs competition between the two phytoplankton groups. Its quick removal decreases competiton, allowing *P. parvum* to overcome the competing phytoplankton. Decreasing the zooplankton mortality rate from the toxin delays the removal of the grazer from the system. The grazers and competing phytoplankton experience increases in density while *P. parvum* density decreases. These results indicate the grazer density is a buffer of sorts for the competing phytoplankton's susceptibility to the toxin. When the grazers are present, the competing phytoplankton are able to compete for longer durations of time with *P. parvum* while the absence of a zooplankton species, increases the mortality of the competing phytoplankton by the toxin.

4.2 Toxin Production Equations

Despite both toxin-production equations tested resulting in *P. parvum* densities reaching a saturating level, the toxin accumulation patterns varied. Without toxin standards, the concentration of toxin molecules in the water system is unable to be determined and modeling efforts are based on the conditions observed when waters are toxic (Brooks et al., 2010). Toxins produced by *P. parvum* may reach a saturating concentration, seen in the Martines et al. (2009) and standard case simulations, or a lower toxin concentration may be all that is needed to suppress competitors as with the Grover et al. (2010) equation. Standards to measure the toxin's concentrations are absolutely necessary to further research and knowledge of the prymnesins.

The components of a model related to *P. parvum* toxins have underpinning ecological mechanisms. That is, toxin related variables can be calculated and calibrated in experimental settings. The Martines et al. (2009) equation, when implemented, displays results comparable to the standard case resulting densities. One significant drawback is a dimensionality issue in the competing phytoplankton's mortality function (Equation 32). This function uses units uncommon with ecological parameters and are difficult to reproduce, thus without the ability to measure the parameters used in the model, the equation is not as robust a choice for modeling the toxic chemical production. The novel approach to toxic chemical production presented here contains fully mechanistic variables, apple to be accurately determined through experimentation. The Grover et al (2010) model inhibits the competing phytoplankton's growth rate allowing coexistence of the phytoplankton groups, a common feature seen in nature. Both the inhibition of growth and lysing of target cells are observed with *P. parvum* (Graneli and Hansen 2006), and successful coexistence between species groups during blooms has been noted (Fistarol et al., 2003). The toxin's ability to deter grazers aids both phytoplankton species relieving grazing pressures and releasing the nutrients from the now dead grazers back into the system (Roelke and Buyukates, 2001). The competing phytoplankton has a growth advantage with ample nutrients and lack of top-down control with the removal of the grazer density, yet is suppressed by the toxin's presence from reaching its maximum specific growth rate. The toxin's addition to the system shifts plankton assemblages away from the quicker growing algae and allows *P. parvum* to maintain dominance. This equation's parameters are feasible to reproduce with

laboratory experiments for verification and though does not include a mortality rate, does simulate *P. parvum*'s ability to prevent growth of more competitive phytoplankton to obtain dominance. The Grover et al.(2010) equation is strong due to its ability to allow the coexistence of the two phytoplankton species. This toxic chemical production equation does not include a mortality factor where the toxin-producing phytoplankton induces the death of the targeted species. A significant difference separating the Grover et al. (2010) function from the model's approach and the Martines et al. (2009) equation is the assumption that toxin production increases proportionally as the nutrient-limited growth rate increases as in the case with Grover et al. (2010) while the latter two assume decreases in the nutrient-limited growth rate generates an increase in toxin production. The growth strategies of *P. parvum* are assumed to follow the second reasoning. Including a similar function into the toxin-production equation presented here would strengthen the representation of *P. parvum* dynamics, incorporating the alga's ability to prosper alongside competing phytoplankton.

4.3 Hydrology

The inclusion of hydrological events to the standard case forces the plankton groups to respond. Without disruption, the standard case illustrates *P. parvum*'s ability to out compete against the faster-growing competing phytoplankton and eliminate the grazer population through the use of its toxins. When the system is pulsed and inflows are increased, the dominance of the system becomes dictated by growth characteristics of the plankton groups and the presence of toxic chemicals produced by *P. parvum*. The

combination of dilution rates and freshwater inflows supports the idea that hydrological events are viable management strategies to decrease the density of *P .parvum* (Roelke et al., 2010a).

The lowest and highest rates of dilution produce expected results in that lower dilution rates do not impact population densities much and the highest dilution rates eliminate the population densities quickly, while the intermediate ranges emphasize the growth characteristics of the phytoplankton. As witnessed in Figure 29 high rates of dilution without and with few pulsing events result in the suppression of all three plankton groups. Dilution rates below 0.1/day resulted in the dominance of *P. parvum*, however the competing phytoplankton consistently prolonged their presence in the system. This rate is important as it is the chosen maximum specific growth rate of *P. parvum* in this simulation. If alone in the system, rates higher than this would result in the elimination of *P. parvum* as a species cannot sustain a population with system dilutions higher than its maximum specific growth rate (Ketchum, 1954). In this same manner, rates higher than 0.57/day would remove the competing phytoplankton from the system from lack of ability to grow faster than the system receives inflows (Figure 14). This range of dilution values is important as it defines environmental conditions during which the competing phytoplankton has a survival advantage based on its faster maximum specific growth rate. As with the toxin standards, the accuracy of estimations of the competing phytoplankton's maximum specific growth rate increases in importance.

With the addition of pulsing events, the dilution rate is still an influential variable, however the same range of dilution rates does not result in the same model output. In other words, the competing phytoplankton has an advantage when the dilution rate exceeds the maximum specific growth rate of *P. parvum* when there are not pulsing events, but with the inclusion of pulses, the range of dilution rates through which the competing phytoplankton density exceeds that of *P. parvum* is not the same. The pulsing events create disturbances in the system as seen in nature. Pulsing at 0.03/day, a rate lower than both phytoplankton's maximum specific growth rates, does not disrupt the system enough for *P. parvum* to lose dominance. Despite the periodicity of the pulses, *P. parvum* retains a greater density with little changes in the model output (Figures 17-22).

Pulsing events at a higher dilution rate, one still lower than both maximum specific growth rates, 0.09/day, allows the competing phytoplankton to exceed *P. parvum*'s density (Figure 26 and 27). In these simulations, the competing phytoplankton out-competed *P. parvum* for the available resources and dominated the system when the pulses were less frequent. In the same way dilution rates greater than *P. paruvm*'s maximum specific growth rate eliminated the species, the combination of less frequent pulsing with a dilution rate close to its maximum specific growth rate, *P. parvum* cannot gain enough of a foothold in the system to overcome the density of the competing phytoplankton. The disruptions to the system favor the faster growing plankton as it can rebound quicker and establish itself, maintaining a density higher than *P. parvum* (Reynolds, 1984). Since static systems are infrequent in nature, understanding the

relationship between pulsing events and the dilution rate could generate management strategies with the knowledge that combinations of pulses and dilution rates can result in the decrease in the density of *P. parvum*.

The pulsing events are intended to represent natural flushing events experienced in river systems, delivering water with different nutrient compositions into systems previously undisturbed. Introducing new nutrient concentrations to the system alters the competition between the phytoplankton groups in the same way inflows will induce responsive growth rates amongst the phytoplankton (Schluter, 1998). Nutrient concentrations higher than the standard case impact density differences, generating higher overall *P. parvum* densities (Figures 34 and 38). The competing phytoplankton fared better in these simulations as well, lasting longer throughout the 30 days than in the standard case, and enduring relatively smaller decreases in density when compared to the density declines of *P. parvum*. These simulations support the notion that managing hydrological activity of the lake system could mitigate blooms through the disruption of plankton communities and developing increased species diversity (Buyukates and Roelke, 2005; Roelke et al., 2010a).

Grazer communities appeared to influence the phytoplankton competition, acting as a buffer between the phytoplankton and the perturbations to the system (Cottingham and Schindler, 2000). In this way, the zooplankton shielded the phytoplankton from the disturbance to the system, allowing the faster growth rates of the competing phytoplankton to supersede the growth of *P. parvum*. When the grazer population increased in cumulative density, the competing phytoplankton experienced increased

competition with *P. parvum* in most cases (Figure 29). Altering the population of grazers throughout the system alongside a hydrological regimen appears a management strategy to influence the growth and survival of the competing phytoplankton to out compete *P. parvum*.

The bottom-water nutrient concentration simulations provide useful information regarding the type of water necessary to agitate the system in such a way to alter the dominating species. Flushing an entire lake system to achieve dilution and pulsing effects noted in this research is highly improbable and unfeasible with large systems. However, displacing water plagued by populations of *P. parvum* with water from the bottom regions of a lake appear to generate similar results: greater declines in *P. parvum* density than competing phytoplankton, and a decline in the concentrations of toxin (Figure 37). Pumping water from lower depths or from other areas of the lake appears to introduce enough disruption to the system to be a successful mitigation strategy easily employed in terms of economics and feasibility. Targeting certain areas of a lake with water with a different nutrient concentration would alleviate the need to flush the entirety of a lake.

REFERENCES

Anderson, D.M.. 2009. Approaches to monitoring, control and management of harmful algal blooms (HABs). Ocean Coast. Manag. 52,342-347.

Anderson, D.M., Glibert, P.M., Burkholder,J.M., 2002. Harmful algal blooms and eutrophication: Nutrient sources, composition, and consequences. Estuar. Coast. 25,704-726.

Anderson, T., Hessen, D.O., 1991. Carbon, nitrogen, and phosphorus-content of fresh-water zooplankton. Limnol. and Ocean. 36,807-814.

Arhonditsis, G.B., Brett, M.T., 2005. Eutrophication model for Lake Washington (USA) Part I. Model description and sensitivity analysis. Ecol. Model. 187,140-178.

Baker, J.W., Grover, J.P., Brooks, B.W., Urena-Boeck, F., Roelke, D.L., Errera, R., et al., 2007. Growth and toxicity of *Prymnesium parvum* (Haptophyta) as a function of salinity, light, and temperature. J. of Phycol. 43,219-227.

Baker, J.W., Grover, J.P., Ramachandrannair, R., Black, C., Valenti, T.W., Brooks, B.W. et al., 2009. Growth at the edge of the niche: An experimental study of the harmful alga *Prymnesium parvum*. Limnol. Ocean. 54,1679-1687.

Barkoh, A., Smith, D.G., Southard, G.M., 2010. *Prymnesium parvum* control treatments for fish hatcheries. J Am. Water Resour. Assoc., 46,161-169.

Brooks, B.W., James, S.V., Valenti, T.W., Urena-Boeck, F., Serrano, C., et al., 2010. Comparative toxicity of *Prymnesium parvum* in inland waters. J Am. Water Resour. Assoc. 46,45-62.

Burkholder, J.M., 1998. Implications of harmful microalgae and heterotrophic dinoflagellates in management of sustainable marine fisheries. Ecol. Appl. 8,s37-62.

Buyukates, Y. and Roelke, D., 2005. Influence of pulsed inflows and nutrient loading on zooplankton and phytoplankton community structure and biomass in microcosm experiments using estuarine assemblages. Hydrobiol. 548,233-249.

Chicharo, L., Chicharo, M.A., Ben-Hamadou, R., 2006. Use of a hydrotechnical infrastructure (Alqueva Dam) to regulate planktonic assemblages in the Guadina estuary: Basis for sustainable water and ecosystems management. Estuar. Coast. Shelf Sci. 70,3-18.

Cottingham, K.L., and Schindler, D.E., 2000. Effects of grazer community structure on phytoplankton response to nutrient pulses. Ecol. 81,183-200.

DeBaar, H.J.W., 1994. Von Liebig's law of the minimum and plankton ecology (1899-1991). Prog. Oceanogr. 33,347-386.

Errera, R.M., Roelke, D.L., Kiesling, R.L., Brooks, B.W., Grover, J.P., Schwierzke, L., et al., 2008. Effect of imbalanced nutrients and immigration on *Prymnesium parvum* community dominance and toxicity: Results from in-lake microcosm experiments. Aquat. Microb. Ecol. 52,33-44.

Fehling, J. and Davidson, K., 2004. Growth and domoic acid production by *Pseudo-nitzschia seriata* (bacillariophyceae) under phosphate and silicate limitation. J. Phycol. 40,674-83.

Fistarol, G.O., Legrand, C., Graneli, E., 2003. Allelopathic effect of *Prymnesium parvum* on a natural plankton community. Mar. Ecol. Prog. Ser. 255,115-25.

Gasol, J.M., Zweifel, U.L., Peters, F., Fuhrman, J.A., Hagstrom, A., 1999. Significance of size and nucleic acid content heterogeneity as measured by flow cytometry in natural planktonic bacteria. Appl. Environ. Microbiol. 65,4475-4483.

Graneli, E. and Hansen, P.J., 2006. Allelopathy in harmful algae: A mechanism to compete for resources? In: Graneli, E and Turner, JT (Eds.). Ecology of Harmful Algae. Ecological Studies vol. 189. Berlin: Springer, p. 189-201.

Graneli, E. and Johansson, N., 2003. Increase in the production of allelopathic substances by *Prymnesium parvum* cells grown under N- or P-deficient conditions. Harmful Algae 2,135-45.

Graneli, E., Weberg, M., Salomon, P.S., 2008. Harmful algal blooms of allelopathic species: The role of eutrophication. Harmful Algae 8,94-102.

Graneli, E., and Salomon, P.S., 2010. Factors influencing allelopathy and toxicity in *Prymnesium parvum*. J. Am. Water Resour. Assoc. 46,108-20.

Gross, E.M., 2003. Allelopathy of aquatic autotrophs. Crit. Rev. in Plant Sci. 22,313-39.

Grover, J.P., Sterner, R.W., Robinson, J.L., 1999. Algal growth in warm temperate reservoirs: nutrient-dependent kinetics of individual taxa and seasonal patterns of dominance. Arch. Fur Hydrobiol. 145,1-23.

Grover, J.P., Baker, J.W., Roelke, D.L., Brooks, B.W., 2010. Current status of mathematical models for population dynamics of *Prymnesium parvum* in a Texas reservoir. J. Am. Water Resour. Assoc. 46,92-107.

Haan, P.K. and Skaggs, RW., 2003. Effect of parameter uncertainty on DRAINMOD predictions: I. Hydrology and yield. Transactions of the ASABE 46,1061-1067.

Hallegraeff, G.M., 1993. A review of harmful algal blooms and their apparent global increase. Phycol. 32,79-99.

Hamilton, D.P. and Schladow, S.G., 1997. Prediction of water quality in lakes and reservoirs: part II: model calibration, sensitivity analysis and application. Ecol Model. 96,111-123.

Hansen, P.J. and Bjornsen, P.K., 1997. Zooplankton grazing and growth: Scaling within the 2-2,000- m body size range. Limnol. Ocean. 42,687-704.

Heil, C.A. and Steidinger, K.A., 2009. Monitoring, management, and mitigation of *Karenia* blooms in the eastern Gulf of Mexico. Harmful Algae 8,611-7.

Hessen, D.O., 1992. Nutrient element limitation of zooplankton production. Amer. Nat. 140,799-814.

Hessen, D.O. and Bjerkeng, B., 1997. A model approach to planktonic stoichiometry and consumer-resource stability. Freshw. Biol. 38,447-71.

Hilton, J., O'Hare, M., Bowes, M.J., Jones, J.I., 2006. How green is my river? A new paradigm of eutrophication in rivers**.** Sci. Total Env. 365,66-83.

James, T.L. and De La Cruz, A., 1989. *Prymnesium parvum carter* (chrysophyceae) as a suspect of mass mortalities of fish and shellfish communities in western Texas. Tex. J. Sci. 41,429-30.

Johansson, N. and Graneli, E., 1999. Influence of different nutrient conditions on cell density, chemical composition and toxicity of *Prymnesium parvum* (haptophyta) in semi-continuous cultures. J. Exp. Mar. Biol. Ecol. 239,243-58.

Ketchum, B.H., 1954. Relation between circulation and planktonic populations in estuaries. Ecol. Soc. Am. 35,191-200.

Legrand, C., Rengefors, K., Fistarol, G.O., Graneli, E., 2003. Allelopathy in phytoplankton – biochemical., ecological and evolutionary aspects. Phycol. 42,406-19.

Lindholm, T., Ohman, P., Kurki-Hesmo, K., Kincaid, B., Meriluoto, J., 1999. Toxic algae and fish mortality in a brackish water lake in Angstrom Land, SW Finland. Hydrobiol. 397,109-20.

Lynn, S.G., Kilham, S.S., Kreeger, D.A., Interlandi, S.J., 2000. Effect of nutrient availability on the biochemical and elemental stoichiometry in the freshwater diatom *Stephanodiscus minutulus* (Bacillariophyceae). J. Phycol. 36,510-522.

Martines, I.P., Kojouharaov, H.V., Grover, J.P., 2009. A chemostat model of resource competition and allelopathy. Ecol. Model. 215,573-82.

Miller, C.J., Roelke, D.L., Davis, S.E., Li, H., Gable, G., 2008. The role of inflow magnitude and frequency on plankton communities from the Guadalupe Estuary, Texas, USA: Findings from microcosm experiments. Est. Coast. Shelf Sci. 80,67-73.

Monod, J., 1950. La technique de culture continue, theorie et applications. Ann. Inst. Pasteur (Paris) 23,137-50.

Nielsen, S.N., 1994. Modelling structural dynamical changes in a Danish shallow lake. Ecol. Model. 73,13-30.

Paerl, H.W., 1997. Coastal eutrophication and harmful algal blooms: Importance of atmospheric deposition and groundwater as “new” nitrogen and other nutrient sources. Limnol. Ocean. 42,1154-65.

Popp, B.N., Laws, E.A., Bidigare, R.R., Dore, J.E., Hanson, K.L., Wakeham,S.G., 1998. Effect of phytoplankton cell geometry on carbon isotopic fractionation. Geochimica et Cosmochimica Acta. 62,69-77.

Redfield, A.C., 1934. On the proportions of organic derivations in sea water and their relation to the composition of plankton. In: Daniel, RJ (Ed.). James Johnstone Memorial Volume. Liverpool: University Press of Liverpool pp.177-192.

Reynolds, C.S., 1984. The Ecology of Freshwater Phytoplankton. Cambridge University Press: New York, 384 pp.

Riemann, B., Sondergaard, M., Schierup, H.H., Bosselmann, S., Christensen, G., Hansen, J., et al., 1982. Carbom metabolism during a spring diatom bloom in eutrophic Lake Mosso. Int. Rev. Ges. Hydrobiol. 67,145-148.

Roelke, D.L., Eldridge, P.M., Cifuentes, L.A., 1999. A model of phytoplankton competition for liming and nonlimiting nutrients: Implications for development of estuarine and nearshore management schemes. Estuar. 22,92-104.

Roelke, D.L., 2000. Copepod food-quality threshold as a mechanism influencing phytoplankton succession and accumulation of biomass, and secondary

productivity: A modeling study with management implications. Ecol. Model. 134,245-74.

Roelke, D.L. and Buyukates, Y., 2001. The diversity of harmful algal bloom-triggering mechanisms and the complexity of bloom initiation. Hum. Ecol. Risk Assess. 7,1347-62.

Roelke, D.L., Errera, D.M., Kiesling, R., Brooks, B.W., Grover, J.P., Schwierzke, L., et al., 2007. Effects of nutrient enrichment on *Prymnesium parvum* population dynamics and toxicity: Results from field experiments, Lake Possum Kingdom, USA. Aquat. Microb. Ecol. 46,125-40.

Roelke, D.L., Gable, G.M., Valenti, T.W., Grover, J.P., Brooks, B.W., Pinckney, J.L., 2010a. Hydraulic flushing as a *Prymnesium parvum* bloom-terminating mechanism in a subtropical lake. Harmful Algae 9,323-32.

Roelke, D.L., Schwierzke, L., Brooks, B.W., Grover, J.P., Errera, R.M., Valenti, T.W., et al., 2010b. Factors influencing *Prymnesium parvum* population dynamics during bloom initiation: Results from in-lake mesocosm experiments. J. Am. Water Resour. Assoc. 46,76-91.

Roelke, D.L., Grover, J.P., Brooks, B.W., Glass, J., Buzan, D., Southard, G.M., et al., 2010c. A decade of fish-killing *Prymnesium parvum* blooms in Texas: Roles of inflow and salinity. J. Plankton Res. 33, 243-253.

Rothhaupt, K.O., 1997. Grazing and nutrient influences of *Daphnia* and *Eudiaptomus* on phytoplankton in laboratory microcosms. J. Plankton Res. 19,125-39.

Schluter, L., 1998. The influence of nutrient addition on growth rates of phytoplankton groups, and microzooplankton grazing rates in a mesocosm experiment. J. Exp. Mar. Biol. Ecol. 228,53-71.

Schwierzke, L., Roelke, D.L., Brooks, B.W., Grover, J.P., Valenti, T.W., 2010. *Prymnesium parvum* bloom termination: role of hydraulic dilution. J. Plankton Res. 33,309-317.

Sherr, E.B., and Sherr, B.F., 2002. Significance of predation by protists in aquatic mircrobial food webs. Ant Leeuwenhoek 81,293-308.

Shumway, S.E., Allen, S.M., Boersma, P.D., 2003. Marine birds and harmful algal blooms: sporadic victims or under-reported events? Harmful Algae 2,1-17.

Smayda, T.J., 1990. Novel and nuisance phytoplankton blooms in the sea: Evidence for a global epidemic. In: Graneli, E. (Ed.). Toxic Marine Phytoplankton. New York: Elsevier pp. 29-40.

Smayda, T.J., 1997. Harmful algal blooms: Their ecophysiology and general relevance to phytoplankton blooms in the sea. Limnol. Ocean. 42,1137-1153.

Smith, V.H., 2003. Eutrophication of freshwater and coastal marine ecosystems. Environ. Sci. Pollut. Res. Int. 10,126-30.

Sommer, U., 1984. The paradox of the plankton: Fluctuations of phosphorus availability maintain diversity of phytoplankton in flow-through cultures. Limnol. Oceanogr. 29,633-6.

Southard, G.M., Fries, L.T., Barkoh, A., 2010. *Prymnesium parvum*: The Texas experience. J. Am. Water Resour. Assoc. 46,14-23.

Telesh, I.V., Rahkola, M., Viljanen, M., 1998. Carbon content of some freshwater rotifers. Hydrobiol. 388,355-60.

The MathWorks, Inc., 2009. Matlab: the language of technical computing. The MathWorks, Inc., Natick, MA.

Tilman, D., Kilham, S.S., Kilham, P., 1982. Phytoplankton community ecology – the role of limiting nutrients. Ann. Rev. Ecol. and Syst. 13,349-372.

Uronen, P., Lehtinen, S., Legrand, C., Kuoppo, P., Tamminen, T., 2005. Haemolytic activity and allelopathy of the haptophyte *Prymnesium parvum* in nutrient-limited and balanced growth conditions. Mar. Ecol. Prog. Ser. 299,137-148.

Valenti, T.W., James, S.V., Lahousse, M.J., Schug, K.A., Roelke, D.L., Grover, J.P., et al., 2010. A mechanistic explanation of pH-dependent ambient aquatic toxicity of *Prymnesium parvum carter*. Toxicon. 55,990-998.

Verspagen, J.M., Passarge, J., Johnk, K.D., Visser, P.M., Peperzak, L., Boers, P., et al., 2006. Water management strategies against toxic *Microsystis* bloom in the Dutch delta. Ecol. Appl. 16,313-27.

Williams, C.J., Lavrentyev, P.J., Jochem, F.J., 2008. Bottom-up and top-down control of heterotrophic bacterioplankton growth in phosphorus-depleted subtropical estuary, Florida Bay, USA. Mar. Ecol. Prog. Ser. 372,7-18.

APPENDIX A

A.1 Standard Case

```
% This is the standard case.


% A Half Dozen Phytoplankton, a Handful of Grazers, Two
% Nutrients, and some awesome fun
% Programming by Natalie Hewitt
% This is the bloom scenario
%-------------------------------------------------------
-----
%-------------------------------------------------------
-----


clear all


global dinky1 N P umaxA dmaxG knA knG QperA QperG day1p
period mark pulsesize tD GNtoP BrespG ArespG PtoxA c mtoxA
ktoxA mtoxG ktoxG ktox


  % Sets the default font and axis size to Times New Roman
set(0,'defaultAxesFontName', 'Times New Roman');
set(0,'defaultAxesFontSize', 12);
```

```
set(0,'defaulttextFontSize', 18);
set(0,'defaultAxesFontSize', 14);
set(0,'defaultFigureColor','white')
%-------------------------------------------------------------
-----
% PARAMETER VALUES
%-------------------------------------------------------------
-----
%-------------------------------------------------------------
-----
% INITIAL CONDITIONS
%-------------------------------------------------------------
-----
dinky1 =0;
    % to get the delta t in the toxin accumulation

N   = 1.70;        % Nitrogen source, µM
P   = 0.40;        % Phosphorus source, µM

% Initial Algal concentration - taken from Roelke 2000
%     µg chl-a / L
Ain =   [ 016.0,  0.0,    0.0,    0.0,    9.75,    0.0];
%       parvum         chlorophytes      diatoms
```

```
%            euglenophytes     cryptophytes
%                                                cyanobacteria

%   convert into carbon to run the model
Ain = Ain.*(50/1)*(1/12);
        % µmol C / L

% Initial nutrient concentrations for nutrients, µM
Rin = [N, P];

% Initial grazer concentrations, from Roelke 2000
% individuals / L
Gin = [0.0,      321.2850,       0.00,       0.00];
%   protozoan     rotifer     copepods      nauplii

%-------------------------------------------------------------
-----
% GROWTH & GRAZING RATES
%-------------------------------------------------------------
-----
% Maximum specific growth rates for phytoplankton species
%   d-1
umaxA = [ 0.10, 1.8, 0.72, 0.57, 0.5, 0.67];
```

```
% Maximum specific grazing rate
    % µmol C / ind / day
dmaxG = [.11956622, 0.045, 1.224, 1.32];

%-------------------------------------------------------------
-----
% HALF SATURATION COEFFICIENTS
%-------------------------------------------------------------
-----
% Phytoplankton half saturation coefficients
    % µmol N / L and µmol P / L

knA = [0.01000  0.30000      0.29986    0.48530  0.10000
0.09281;   % N
       0.00500  0.32285      0.15000    0.16142  0.01000
0.05166];  % P

% Zooplankton half saturation coefficients
    %   µmol C / L
% knG = [3.83014,   0.208333,    7.916667,   .75601];
%   protozoan     rotifer     copepods      nauplii
knG = [3.164,   6.66667,    8.3259094,   14.25];
```

```
%-------------------------------------------------------------
-----
% CELL CONTENT
%-------------------------------------------------------------
-----
% Fixed cell contents phytoplankton
%  (µmol nutrient / cell)
QperA = [2.7330e-06    8.44e-6      5.2667e-6    6.8917e-6
2.07e-6      0.05e-6;
            % µmol carbon per cell
        0.2430e-06    1.079e-6     0.7357e-6    1.3286e-6
0.304e-6     0.0071e-6;
            % µmol nitrogen per cell
        0.0019400e-06  0.200e-6     0.0293e-6    0.0200e-6
0.0432e-6    0.002e-6];
            % µmol phosphorous per cell
%

QperG = [.93830142  0.04625         0.817305    0.25;
            % µmol carbon per individual
         0.630846   0.002744994     0.15039
0.057142857;
```

```
            % µmol nitrogen per individual
          0.045060   0.0001050424    0.02187     0.01832];
            % µmol phosphorus per individual

% grazer N:P ratio used in the limiting nutrient logic
statements
GNtoP(1,:) = QperG(2,:)./QperG(3,:);
GNtoC(1,:) = QperG(2,:)./QperG(1,:);    % N:C ratio of
grazers
GPtoC(1,:) = QperG(3,:)./QperG(1,:);    % P:C ratio of
grazers

% algae N:C and P:C ratios used in amounts ingested
ANtoC(1,:) = QperA(2,:)./QperA(1,:);
            % µmol N / µmol C
APtoC(1,:) = QperA(3,:)./QperA(1,:);
            % µmol P / µmol C

%-------------------------------------------------------------
-----
% RESPIRATION RATE
%-------------------------------------------------------------
-----
```

```
% Grazer Respiration Rate
    % basal grazer respiration rate
BrespG = [0.5      0.050     0.1195757  0.005];
% based on concentration of the grazer growth
    % d-1

ArespG = [0.2     0.02   0.35   0.2];
    % grazing respiration when actively ingesting
    % production dependent - unitless

%-------------------------------------------------------------
-----
% Toxin
%-------------------------------------------------------------
-----

Toxin = [ 00.0 ];
% µg tox / L

ktox = 0.0849    % day-1
    % 2.038668178/hr - the number above is multiplied by 24
to find /day
% used for the exponential decay of the toxins
```

```
% generated from knowledge that at 1 light intensity, the
half
% life of parvum is 0.34 hr
% using this, solved 0.5 = exp^(-kt) where t is 0.34hr


c = [  0.1 ];
    % fudge factor in the exponential of the toxin
production
    % allows for variability of control on the production
     of the % toxin

% µg tox / cell day -1
PtoxA = [  1.0e-7 ];
    % entirely made up this number
    % toxin production constant affecting the growth of
     % competing algae
    % allelopathic

% Phytoplankton effects from toxin
mtoxA = [0.0     0.45    0.45     0.45     1.0     0.45];
        % day -1
    % mortality rate of the toxin specific to each alga
```

```
ktoxA = [0.1e-25     0.25    0.25     0.25     0.45
0.25];
        % µg tox / L
        % amount of toxin that causes a 50% reduction in
algae density

% Grazer Toxin effects
mtoxG = [ 0.00250   2.35   0.550     0.00250 ];
    % day -1
    % mortality rate from the effect of the toxin specific
to each grazer

ktoxG = [ 0.25   0.01450     0.25     0.25 ];
    % µg tox / L
    % amount of toxin that causes a 50% reduction in grazer
concentration

%-------------------------------------------------------------
-----
%-------------------------------------------------------------
-----
% MODEL CONTROL
```

```
%-------------------------------------------------------------
-----
tD  = 0.0;      % Dilution rate, d-1
pulsesize   = 1;
    % percent of continuous flow that becomes episodic
period      = 0;
    % Period of pulsing (continuous = 0)
day1p       = 1;
    % Initial pulse = 1; No initial pulse = 0

%-------------------------------------------------------------
-----
% RUNNING THE MODEL
%-------------------------------------------------------------
-----

t0      = 0;    % time start
tfinal  = 30;  % time finish (days)
mark    = t0;
dinky   = 1.0;
zin     = [Ain, Rin, Gin, dinky, Toxin];
[t,z]   = ode45('standardCasefunc',t0,tfinal.,zin,1e-25);
% always the standard case
```

```
% [t2,z2] = ode45('standardCase2func',t0,tfinal.,zin,1e-
25);


%-------------------------------------------------------
-----
% conversions
%-------------------------------------------------------
-----
% convert algae back into chl-a
for i=1:6
    ChlA(:,i) = z(:,i)*12/50;
end


% keyboard
%-------------------------------------------------------
-----% PLOT THE MODEL OUTPUT
%-------------------------------------------------------
-----
figure
plot(t,z(:,7),'b',t,z(:,8),'r','LineWidth',2)
ylabel('resources µM','FontSize',16)
xlabel('days','FontSize',16)
title(' Ambient Nutrients','FontSize',20)
```

```
legend('Nitrogen','Phosphorus')

figure
plot(t,ChlA(:,1),'r',t,ChlA(:,5),'b','LineWidth',2)%,
t,ChlA(:,3),'k',t,ChlA(:,4),'c',
t,ChlA(:,5),'m',t,ChlA(:,6),'g')
legend('P. parvum','competing phytoplankton',2)
ylabel('µg chl-a per
liter','FontSize',16),xlabel('days','FontSize',16)
title('Phytoplankton Concentration','FontSize',20)

figure
plot(t,z(:,10),'b','LineWidth',2)%,t,z(:,11),'g',t,z(:,12),
'c')
xlabel('days','FontSize',16)
ylabel('individuals per liter','FontSize',16)
title('Grazer Concentration','FontSize',16)
legend('grazer','FontSize',10)

figure
plot(t,z(:,14),'LineWidth',2)
title('Toxin Accumulation','FontSize',16)
xlabel('days','FontSize',16)
```

```
ylabel('µg tox / L','FontSize',16)
```

A.2 Standard Case Function

```
% This is a function called by the routine, standard.m
% It contains the equations for the whole shindig.
% Programming adjusted and created by Natalie Hewitt
%-------------------------------------------------------------
-----
function zdot=standardCasefunc(t,z)

global dinky1 N P umaxA dmaxG knA knG QperA QperG day1p ...
period mark pulsesize tD BrespG ArespG PtoxA  c mtoxA ktoxA
... mtoxG ktoxG ktox

%-------------------------------------------------------------
-----
% INCOMING INFORMATION
%-------------------------------------------------------------
-----
A   = z(1:6)';      % Algae (µmol C / L)
R   = z(7:8)';      % Resources (nutrients); (µmol nutrient
/ L)
G   = z(9:12)';     % Grazers (individuals / liter)
```

```
T   = z(14)';       % Toxin (µg tox L-1)


%-------------------------------------------------------------
-----
% NUTRIENT PULSE
%-------------------------------------------------------------
-----
if period == 0
          % Continuous conditions
    D1 = tD;
     D2 = 0;
    else
          % Pulsing conditions
    D1 =(1-pulsesize)* tD;
     pulse = floor(t)/period - floor(floor(t)/period)==0;


          % On/Off switch
     D2 = pulsesize*tD*(2*period)*((1+cos(t*2*pi-
pi))/2)*pulse;
     if day1p == 0
        if t<period-1                          % No initial
pulse
               D2  = 0;
```

```
        end
    end
end



%-------------------------------------------------------------
-----
% ALGAE GROWTH RATE
%-------------------------------------------------------------
-----
for i=1:length(knA(1,:))
          % number of phytoplankton species (columns in K)
    for j=1:length(knA(:,1))
          % number of resources (rows of K)
        uA(j,i) = umaxA(i).*(R(j)./(knA(j,i)+R(j)));
                            % d-1
    end
end

uminA = min(uA);    % use Liebig's 'Law of Minimum'
    % d-1
urel = uminA(1)/umaxA(1);         % unitless
```

```
                        % used for toxin production
equation

%-------------------------------------------------------------
-----
% GRAZER GRAZING RATE
%-------------------------------------------------------------
-----
% Grazing Rate - based on the Monod function
grazC = dmaxG.*((sum(A))./(knG + sum(A)));
        % grazing rate based on the Monod equation using
the
        % half saturation coefficient in proportion to the
total
        % available carbon in the prey
    % µmol C / ind. / day
        % based on a Monod-relationship to relate the
        % "dependence of grazer activity on food quantity"
        % (Hansen and Bjornsen, 1997)

%-------------------------------------------------------------
-----
% amount of carbon from each phyto group ingested
```

```
for k=1:length(knG)
    for i=1:length(A)
        % µmol C / day / L
        ClossperA(k,i) = (A(i)/(sum(A)))*grazC(k)*G(k);
            % ClossperA is the carbon loss from ingestion
for
             % each species of algae

        % ClossperA is a 4x6 with grazer species in rows,
        algae % in columns
            % each value is the amount of carbon lost per
grazer
             % per species algae
    end
end

% total carbon lost from each algal species
ClostbyA = sum(ClossperA);
    % µmol C / day / L

%-------------------------------------------------------
-----
% Grazed amount by nutrient
```

```
%-------------------------------------------------------------
-----
% convert the ingestion losses of nutrients from carbon to
% nitrogen and phosphorus using the cell content ratio

for k=1:length(knG)
        % µmol N / day / L
    grazN(k,:) = ClossperA(k,:).*(QperA(2,:)./QperA(1,:));
        % using the cell content ratio QperA(C):QperA(N)
        % multiplied by the losses to find the nitrogen
lost in
        % proportion to the loss of carbon

    grazP(k,:) = ClossperA(k,:).*(QperA(3,:)./QperA(1,:));
        % µmol P / day / L
            % using published optimal N:P ratios, convert
the N
             % loss from ingestion
            % found above to phosphorus losses
end

% grazN and grazP are the total molar amounts lost from
% ingestion by the grazer species
```

```
%-------------------------------------------------------------
-----
% grazer ingestion
        % grazA sums the total nitrogen and phosphorus
losses
        % for each phyto species
grazA = [sum(grazN'); ...       % µmol N / day / L
         sum(grazP')];         % µmol P / day / L


%-------------------------------------------------------------
-----% GROWTH OF THE GRAZERS
%(sounds like a movie right?)
%-------------------------------------------------------------
-----


% total amounts of ingested nutrients per individual
TotalG = [grazA(1,:)./QperG(2,:);...
            % amount of nitrogen ingested per individual
                %  ind / L / day
          grazA(2,:)./QperG(3,:)];
            % amount of phosphorus ingested per individual
                % ind / L / day
```

```
RlimG = min(TotalG);
    % the minimum value in TotalG per grazer is the growth
rate
     % based on ingestion of nutrients
    % taking the minimum of TotalG will be the lower
ingested
    % nutrient and thus the limiting one

%-------------------------------------------------------
-----% GRAZER EGESTION
%-------------------------------------------------------
-----% Egestion of those nutrients not limiting

y1 = RlimG.*QperG(2,:);
y2 = RlimG.*QperG(3,:);

GegestR = grazA - [y1; y2];
        % from the total nitrogen and phosphorus ingested,
the
        % µmol nutrient d-1 L-1
```

```
%-------------------------------------------------------------
-----% GRAZER RESPIRATION
%-------------------------------------------------------------
-----
    % individuals L-1 d-1
Grespa = ArespG.*RlimG;
Grespb = BrespG.*G;
    % based on Roelke 2000 zooplankton respiration
    % BrespG is the basal respiration dependent on the
grazer
     % growth
    % ArespG is the active respiration rate when the food
     is
     % less abundant

Gresp = Grespa + Grespb;
    % GrespR is the total amount of respiration per
individual

% Grazer mortality
% Gmort = [0.005   0.905  0.0065   0.15];
```

```
%-------------------------------------------------------------
-----
% Toxin Production
%-------------------------------------------------------------
-----
% The production of toxins from P. parvum will have both an
% allelopathic term as well as inhibition of grazing
pressures

% use lim_res (found with algae growth rate) to determine
the
% limiting nutrient for growth of each algae
noP = A - [A(1) 0 0 0 0 0];
ToxLossA = mtoxA.*(T./(ktoxA + T)).*noP;
        % µmol C / L day-1

ToxLossG = mtoxG.*(T./(ktoxG + T)).*G;
        % ind / L day-1

%-------------------------------------------------------------
-----
% DIFFERENTIAL EQUATIONS
```

```
%-------------------------------------------------------------
-----

% total phytoplankton - µmol C / L / day
z1dot = A.*(uminA - D1 - D2 ) - ClostbyA - ToxLossA;

% first resource - µmol Nitrogen / L / day
z2dot = (D1 + D2)*(N - R(1)) - ...
sum(QperA(2,:).*uminA.*(A./QperA(1,:))) ...
    + sum(GegestR(1,:)) + sum(Gresp.*QperG(2,:)) + ...
sum(QperA(2,:).*ToxLossA./QperA(1,:))...
    + sum(ToxLossG.*QperG(2,:));

% second resource - µmol Phosphorous / L day-1
z3dot = (D1 + D2)*(P - R(2)) - ...
sum(QperA(3,:).*uminA.*(A./QperA(1,:))) + ...
    + sum(GegestR(2,:)) + sum(Gresp.*QperG(3,:)) + ...
sum(QperA(3,:).*ToxLossA./QperA(1,:))...
    + sum(ToxLossG.*QperG(3,:));

% total zooplankton - individuals / L / day
z4dot = G*( - D1 - D2 ) + RlimG - Gresp - ToxLossG;
z5dot = sin(25*t);
```

```
% toxin production - µg toxin / L day-1
z6dot = PtoxA.*(1-urel).*A(1)./QperA(1,1) - T*(D1 + D2) -
... T*ktox;

dinky1 = t;

%-------------------------------------------------------------
-----
% COUNTER (for impatient modelers)
%-------------------------------------------------------------
-----
if t>mark
format compact
  t
  mark=mark+10;
end
% This provides feedback to the monitor so impatient
modelers
% (like me) can check on the progress of the simulation

%-------------------------------------------------------------
-----
% OUTPUT
```

```
%-------------------------------------------------------------
-----

zdot=[z1dot,z2dot,z3dot,z4dot,z5dot,z6dot]';
```

VITA

Name	Natalie Case Hewitt
Address	Texas A&M University Department of Wildlife & Fisheries TAMU 2258 College Station, Texas 77843
Email Address	nhewitt@tamu.edu
Education	B.S. Applied Mathematics – Biology, Brown University, 2008 M.S. Water Management and Hydrological Science, Texas A&M University, 2011